

(NASA-CR-198413 IRD DROPOUT STUDY  
Final Report (Spectra Research  
Systems) 140 p

N93-16381

Unclas

G3/32 0136505

**IRD DROPOUT STUDY  
FINAL REPORT**

**AUGUST 1992**

**By  
SRS Technologies**

**Jeffrey S. Yalowitz  
Michael A. Schroer  
John E. Dickson, Jr.**

**Contract NAS8-39077**

**Prepared for  
National Aeronautics and Space Administration  
George C. Marshall Space Flight Center  
Marshall Space Flight Center, AL 35812**



**SYSTEMS TECHNOLOGY GROUP**

**990 EXPLORER BLVD., N.W.  
HUNTSVILLE, AL 35806**

**(205) 971-7000**

**IRD DROPOUT STUDY  
FINAL REPORT**

**AUGUST 1992**

**By  
SRS Technologies**

**Jeffrey S. Yalowitz  
Michael A. Schroer  
John E. Dickson, Jr.**

**Contract NAS8-39077**

**Prepared for  
National Aeronautics and Space Administration  
George C. Marshall Space Flight Center  
Marshall Space Flight Center, AL 35812**

**APPROVED BY:**



**Bruce E. Newman  
Vice President,  
BM/C<sup>3</sup>I Systems  
Directorate**

## FORWARD

This report was prepared by the Systems Technology Group of SRS Technologies for the National Aeronautics and Space Administration, Marshall Space Flight Center, under Contract NAS8-39077. The study was performed under technical direction of Ms. Jean Mann.

Ms. Mann, Mr. David Harris, Mr. Reggie Inman, and Mr. Bill Hopkins of the Communications Systems Branch, EB33, provided valuable encouragement and guidance through the study. In addition, Ms. Mann made arrangements for us to access computer databases and obtained records of early Shuttle flights. Mr. Inman provided important information on antenna characteristics and measurement methods through discussions and a tour of the MSFC antenna range. Mr. Hopkins provided details of ET range safety hardware and conducted IRD AGC characterization tests to support the study. We are grateful for their contributions.

## TABLE OF CONTENTS

SECTION	PAGE
1 INTRODUCTION .....	1
2 STUDY METHODOLOGY .....	3
2.1 Space Shuttle Range Safety System.....	3
2.2 Space Shuttle Flyout Profiles .....	5
2.3 Radio Transmission Fading Mechanisms .....	8
2.3.1 Terrain or Ocean-Surface Multipath.....	8
2.3.2 Atmospheric/Ionospheric Effects.....	10
2.3.3 Multipath Reflection and Diffraction From Shuttle Orbiter and ET Surface Features .....	13
2.5 Outline of the Study Tasks .....	16
3 SIMULATION AND ANALYSIS PROCEDURES .....	19
3.1 RF Propagation (Theoretical).....	20
3.2 Shuttle Dynamics.....	21
3.3 Receiver Characteristics .....	23
4 SIMULATION/ANALYSIS RESULTS .....	25
4.1 Terrain Multipath .....	25
4.2 Antenna Patterns.....	26
4.3 Trajectories/Attitudes.....	27
4.4 Atmospheric Effects.....	31
4.5 Plume Attenuation.....	32
4.6 Line-of-Sight Comparisons .....	34
5 CONCLUSIONS.....	36
6 APPLICATION OF METHODOLOGY TO FUTURE FLIGHTS.....	38
7 RECOMMENDATIONS .....	39
REFERENCES.....	40
APPENDICES.....	41

## LIST OF EXHIBITS

EXHIBIT	PAGE
2-1 Range Command/Control System Ground Station Parameters .....	5
2-2 Space Shuttle Altitude/Range Profile.....	7
2-3 Geometry of Terrain Multipath Fading .....	8
2-4 Plot of Received Signal Level Variations with Distance for a Ground-to-Air RF Link Experiencing Terrain Multipath Propagation .....	9
2-5 Signal Loss Due to Atmospheric Ducting of Radio Waves.....	10
2-6 Geometry of Tropospheric Multipath Propagation .....	11
2-7 Ionospheric Refraction Layers Defined by Free Electron Density Variations with Altitude .....	11
2-8 Multipath Propagation Caused by Refraction or Reflection in Condensed Exhaust Cloud .....	12
2-9 Gap in Signal Reception Caused by Refraction in Condensed Exhaust Cloud ...	12
2-10 Hypothetical Antenna Pattern or a Stub Antenna over a Complex Shape Conductive Surface .....	13
2-11 Multipath Propagation by Reflection and Diffraction at Vehicle Surfaces .....	14
2-12 Radar Beacon Range Equation.....	15
2-13 IRD Dropout Study Task Steps.....	17
3-1 Locus of Angles of Arrival on ET Antenna Pattern .....	22
3-2 Integrated Receiver/Decoder [11].....	23
3-3 Voltage vs. Signal Strength Plots From Two IRDs [11].....	24
4-1 Comparison of ET RSS Signal Strength Patterns .....	26
4-2 Yaw Look Angles vs. Shuttle Flight Time .....	27
4-3 Attitude Angles at Times of Deep Signal Fades.....	28
4-4 Record of ET Receiver AGC Voltages vs. Time After Launch (Transmission from Cape Canaveral).....	29
4-5 Calculation of Signal Strength Attenuation in the Diffraction Illuminated Zone .....	33
4-6 Line-of-Sight Range Between the Shuttle and the Visual Horizon at Selected Points During Fly-Out.....	35

## SECTION 1 INTRODUCTION

This final report describes work performed by SRS Technologies for the NASA Marshall Space Flight Center under Contract NAS8-39077, entitled "Integrated Receiver-Decoder Dropout Study". The purpose of the study was to determine causes of signal fading effects on ultra-high-frequency (UHF) range safety transmissions to the Space Shuttle during flyout. Of particular interest were deep fades observed at the External Tank (ET) Integrated Receiver-Decoder (IRD) during the flyout interval between solid rocket booster separation and ET separation. Analytical and simulation methods were employed in this study to assess observations captured in flight telemetry data records. Conclusions based on the study are presented in this report, and recommendations are given for future experimental validation of the results.

Episodes of extended signal fading have been observed during a number of Shuttle flights. These fading occurrences have been documented in telemetry records of UHF range safety system transmissions from ground transmitter sites to the ET range safety subsystem. The primary indication of the fading episodes is contained in the IRD automatic gain control (AGC) output signal, the amplitude of which is related to RF signal input to the receiver front end. Previous contract study efforts toward understanding of the fading effects have focused on modeling of plume plasma effects [1] and on compilation of case information to support comprehensive analysis [2]. The requirement for the present study includes consideration of various physical phenomena that could cause the signal dropouts seen in the telemetry records.

In this study, SRS analyzed data from Shuttle mission databases to identify fading occurrences and to compile associated flight trajectories and conditions. Concurrently, we reviewed information available on the Space Shuttle configurations and range safety equipment relevant to range safety RF transmissions. We then developed computer models of theoretical transmission characteristics, taking into account free space and terrain/ocean-surface multipath modes, atmospheric refraction, and antenna patterns (from scale-model testing, representing antenna losses and multipath effects of vehicle structures). The computer models were combined into an integrated simulation that accepts Shuttle trajectory and attitude as functions of time from the Shuttle mission database and produces graphical traces of theoretical signal transmission loss from ground site to ET IRD unit, along with traces of other parameters of interest. The software developed by SRS for this study also provides for display of IRD AGC voltage or received signal level taken from mission databases, on the same time scales as those of the simulation. Printouts

of signal arrival angles are also produced by the software. Statistical analyses and estimation of plume refraction modes were conducted independently of the integrated simulation effort.

Computer-aided studies were made of a number of Shuttle launches, and other launch histories were reviewed manually. Although terrain multipath and antenna-pattern-related signal variations were observed for some flight regimes, the theoretical effects predicted were not of sufficient magnitude or duration to produce the deep fades observed. However, a strong correlation was found between fade occurrences and Shuttle trajectory/attitude combinations that involve signal arrival angles from almost directly aft of the vehicle. This result and analytical findings have led to a conclusion that multipath propagation modes involving Shuttle structures and dual-antenna RF combining are likely to be at least contributing causes of the signal fading effects at aft signal arrival angles. These modes are characterized by rapid variation with arrival angle and are of greatest significance in aft arrival angles, where geometric line-of-sight is not available to either of the two ET antennas. The multipath effects implicated are likely to be of finer granularity in arrival angle than data available from previous scale-model antenna measurements and of most significance in an angular sector where fidelity of the antenna-range scale model was limited. Recommendations for further effort are directed toward obtaining finer-grained experimental data on antenna and structural multipath characteristics for more detailed correlation with mission data in this regime.

The methodology and software tools produced during this study can be applied directly to the analysis of IRD signal-strength data from future Shuttle flights. The procedures and support data to do so are described in this report.

Section 2 of this report describes the methodology used by SRS for the study. The analysis and simulation procedures are detailed in section 3. Results obtained from the application of these procedures to records in the Shuttle mission databases are discussed in Section 4. Section 5 presents the conclusions SRS has derived from the study. Procedures for application of the study results to future Shuttle launches are identified in Section 6. Section 7 provides recommendations for experiments to validate the conclusions.

## SECTION 2

### STUDY METHODOLOGY

During several Space Shuttle launches the 416.5 MHz range command/control transmitter (CCT) signal to the ET receiver has been observed to experience severe signal fading attenuation during powered flight. This attenuation occurs after SRB separation and usually before handover to a downrange tracking station. Prior to this study, no clear explanation had been developed for these drops in signal level.

Possible SSME exhaust plume plasma effects on IRD signal levels were investigated during previous studies. SRS has reviewed the methods used in this study and has compared them to rocket plume attenuation modeling results we and others have obtained in recent studies and experiments. We have interpreted the results of the plume study performed by Dr. Blaine Pearce to be that the SSME exhaust plume should only be a significant factor in signal attenuation if the level of contaminants in the plume exceeds a "specific" level. Although it is considered possible that the SSME fuel could contain contaminants from storage tank walls and engine component ablation, these sources are not considered probable sources of contamination in quantities sufficient to cause plume attenuation. Dr. Pearce's study did not eliminate refraction by water vapor in the SSME exhaust as a possible factor in RF propagation to ET antennas.

SRS has investigated several RF transmission phenomena which could possibly be the cause of the transient attenuation. The phenomena includes multipath propagation modes, antenna pattern effects, RSS hardware dynamic effects, atmospheric attenuation, and review of possible exhaust.

#### 2.1 Space Shuttle Range Safety System

Systems considered in the IRD dropout investigation included the on-board Range Safety System, particularly its ET portions, and the Range Command/Control System, which has a network of UHF radio transmitters at several sites selected to provide line-of-sight communications links for a variety of possible flyout trajectories flown at the Eastern Test Range. These systems together provide the capability to remotely activate a vehicle flight termination system (FTS) in the event that, while under powered flight, the vehicle fails in such a manner as to experience a malfunction turn which would cause the vehicle to violate established flight safety criteria. Generally, the criteria are manifested in impact limit lines (ILL), defining geographic areas to each



side of a vehicle's nominal flight path, and beyond which, intact vehicle impact or the debris impact from a failed vehicle will not be permitted.

An FTS consists of an antenna (or antennas), RF cabling, antenna couplers, receiver/decoders, power sources, Safe/Arm switches, detonators/boosters, and thrust termination ordnance. All components are redundant (antenna and the main termination ordnance mechanism may not be required to be redundant, depending on FTS design). The Eastern Space and Missile Center uses a UHF carrier (frequency of 416.5 MHz) for their Command and Control Transmitters (CCT) (destruct transmitters). A continuous wave (CW) transmission is provided from a time just prior to launch until the FTS is no longer required (Main Engine Cut Off (MECO) for the Space Shuttle). The CCT carrier "captures" the FTS receivers, keeping them locked to this CCT signal, a condition designed in part to prevent any spurious signal from activating the system. If it becomes necessary to terminate the flight, the carrier is modulated with a coded tone sequence, and then decoded by the vehicle Receiver decoder to activate the ordnance. The Space Shuttle system carries redundant FTS systems on each SRM, and a single system on the ET. The systems are cross-strapped so that activation of any one system activates all of them.

The FTS is monitored by the Range Safety Officer through the use of an S-Band telemetry downlink. On the vehicle, FTS receiver Automatic Gain Control (AGC) voltage is monitored and scaled to a zero-to-five volt value (5 vdc representing receiver saturation), and these data are transmitted via the telemetry stream to the Range Control Center, where they are displayed to the safety personnel on a CRT in the form of a bar graph. Observation of the display shows the Range Safety Officer whether, and to what level, the CCT has "control" of the FTS receiver, indicating when an alternative transmitter should be used.

Transmitter sites are located to provide adequate coverage for the various trajectories of vehicle launched on the Eastern Test Range. Current locations include Cape Canaveral Air Force Station (CCAFS), the Jonathan Dickinson site south of CCAFS, Wallops Flight Facility, the Bermuda Tracking Station, and the Antigua Tracking Station. If these locations are not compatible with the trajectory/geometry of a particular flight, portable CCT transmitters may be used to augment the fixed sites.

Received signal strength (measured as a function of the level of the receiver AGC voltage) is a function of the system hardware RF characteristics (transmitter power, antenna gains, system losses, etc.). The signal strength is also inversely proportional to the value of the square of the range between transmitter and receiver antennas. In addition, the aspect angle between the

transmitter and the FTS antennas is important. The UHF signal path is a line-of-site path requiring alternate transmitters be used as the vehicle goes "over the horizon" with respect to the affected site (changeover is generally accomplished as the antenna elevation angle decreases to three degrees, or if the telemetered AGC voltage decreases to 1.5 volts).

The Command/Control system transmitter power output levels vary from 600W to 10 kW. Antenna beamwidths range from omni-directional (0 dB gain) to 20 degrees (18 dB gain). The ground station antennas use left hand circular (LHC) polarization.[1] Exhibit 2-1 lists the respective ground station power and antenna characteristics.

Station	Power Output (W)	Antenna	
		Gain (dB)	Beamwidth (Degrees)
CCAFS	600	18	20
	10,000	0	Omni
Antigua	10,000	15	18x30
USNS Redstone	10,000	6	70
Bermuda	10,000	18	20
Wallops Island	600	18	20
Jonathan Dickinson	10,000	20	10

910411-855932-1527

### Exhibit 2-1 Range Command/Control System Ground Station Parameters

## 2.2 Space Shuttle Flyout Profiles

The Space Shuttle vehicle is launched with the orbiter's vertical stabilizer initially pointed south. At approximately seven seconds into flight, a roll maneuver is initiated to orient the orbiter center line

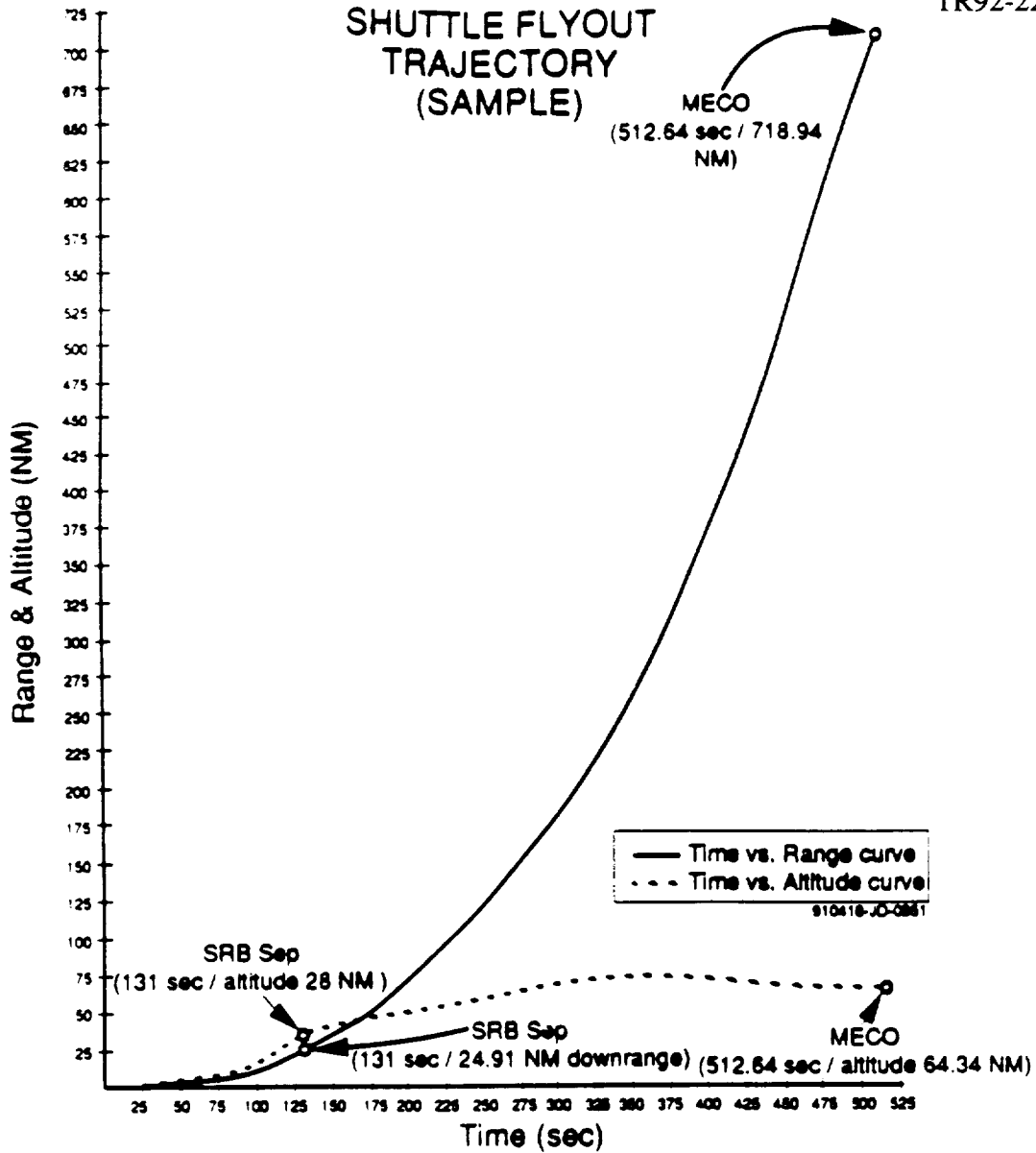
along the direction of the launch azimuth. The roll maneuver is generally complete at about 23 seconds after liftoff. After launch tower clearance (at approximately seven seconds into flight) the vehicle initiates a pitch-over (program down-range) maneuver which will result in the orbiter reaching a tail down attitude for the duration of the flight while under power from the Space Shuttle Main Engines (SSME). The vehicle pitch maneuver is complete at about 30 seconds.

Launch azimuth is a determining factor for the inclination of the orbit the vehicle is to achieve. These azimuths have ranged from about 037 degrees to 092 degrees, with resulting orbital inclinations of between 60 degrees (used with Spacelab missions) to about 28 degrees. The flyout azimuth is generally held fairly constant through MECO to conserve the energy that otherwise would be expended in accomplishing an orbital plane change during this phase of flight.

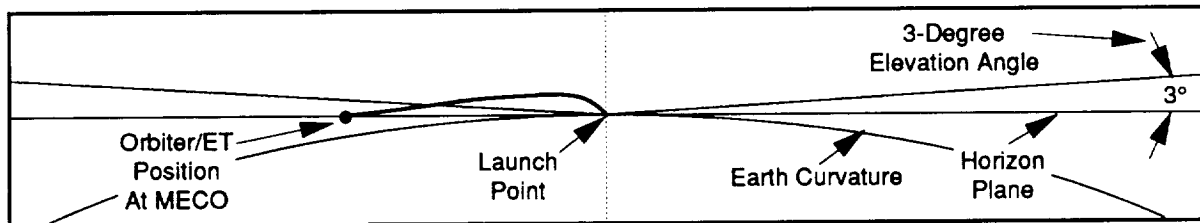
The launch azimuth is important in the analysis of the FTS receiver/decoder signal strength because it will determine which of several available CCTs will be employed to provide coverage for the flight until MECO. For instance, the higher inclination flights of the Shuttle project a ground track which essentially parallels the East coast of the US. Initial coverage for this (and all other) flights in this direction is from the Cape Canaveral Air Force Station command facilities or the Jonathan Dickinson site south of KSC on the Florida coast. The last available fixed site coverage for this azimuth comes from the transmitter facilities at the Wallops Island Flight Facility. Lower inclination flights may use command facilities located on Bermuda, Antigua, or both, after passing over the UHF radio horizon from the Cape.

During the flight, and prior to MECO, the Eastern Test Range safety officers monitor the telemetered receiver signal strengths (as a function of receiver AGC voltage) and the elevation of the transmitter tracking antennas (although capability exists to use an omni-directional antenna in the event of a tracking antenna failure). If the signal strength begins to fall, or if the transmitter antenna elevation decreases to about three degrees, a transmitter at an alternate location is brought up. Transmitter site switching is automated, based on these parameters, although the range safety officers can manually override the automatic system.

Exhibit 2-2a shows the vehicle altitude/range profile for a typical flight from liftoff to MECO. The flyout profile indicated by this graph shows the vehicle initially gaining altitude at the expense of range, then, as the velocity vector tends toward the horizontal, begins increasing the range at a high rate while remaining at a relatively constant altitude. As the flight progresses, earth curvature will block line-of-site contact between the Cape transmitter and the vehicle, as indicated by Exhibit 2-2b.



(a) Altitude and Downrange Distances vs. Time (Example Trajectory)



(b) Effects of Earth Curvature

**Exhibit 2-2 Space Shuttle Altitude/Range Profile**

The Wallops Flight Facility is located approximately 600 nautical miles (nm) or approximately 1110 km from the Cape. The distance to Bermuda is approximately 800 nm (1480

km) and the distance to Antigua, approximately 1300 nm (2400 km). All of these stations should have aspect angles to the vehicle which are large enough that plume attenuation would not be a significant factor. However, the specific flight trajectories and attitude of the vehicle must be considered in a definitive determination of aspect angle.

### 2.3 Radio Transmission Fading Mechanisms

In addition to potential failures in the RF hardware or misalignment of directional antennas, several phenomena can reduce Command/Control link signal strength at the vehicle. Absorption, reflection, or refraction of radio waves can occur through a number of mechanisms, resulting in signal attenuation or multipath signal phase effects. We considered the following four mechanisms to be of possible significance to the IRD dropout: 1) rocket exhaust plume attenuation, 2) terrain (or ocean surface) multipath fading, 3) atmospheric/ionospheric effects, and, 4) vehicle structures and on-board receive-system elements. These phenomena are discussed briefly in the following subsections.

#### 2.3.1 Terrain or Ocean-Surface Multipath

This effect is pronounced in communications links where at least one terminal is airborne. For ground-air links where the ground terminal uses a narrow beam antenna, terrain multipath is not significant at high look angles. However, when the look angle decreases to the elevation where the beam illuminates the surface, deep fades can occur. The higher the reflectivity of the surface, and the smoother it is, the greater the effect. Salt water, particularly at quiet sea state, which is a typical Shuttle launch condition, is probably the worst case.

Exhibit 2-3 illustrates the geometry of terrain multipath fading on a propagation path between a UHF ground transmitting station and a Space Shuttle vehicle in flight.

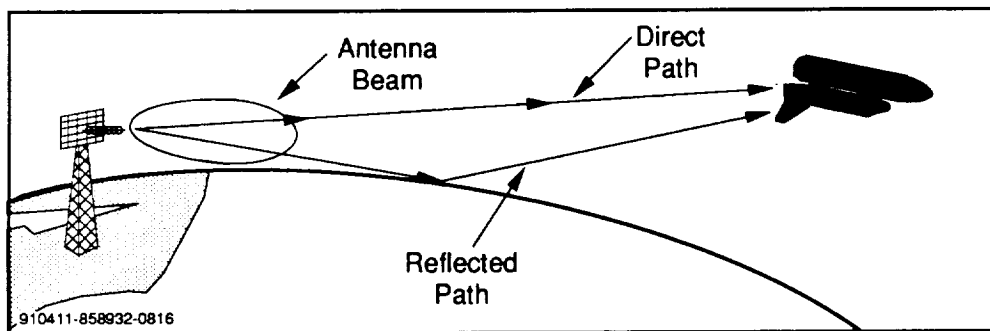
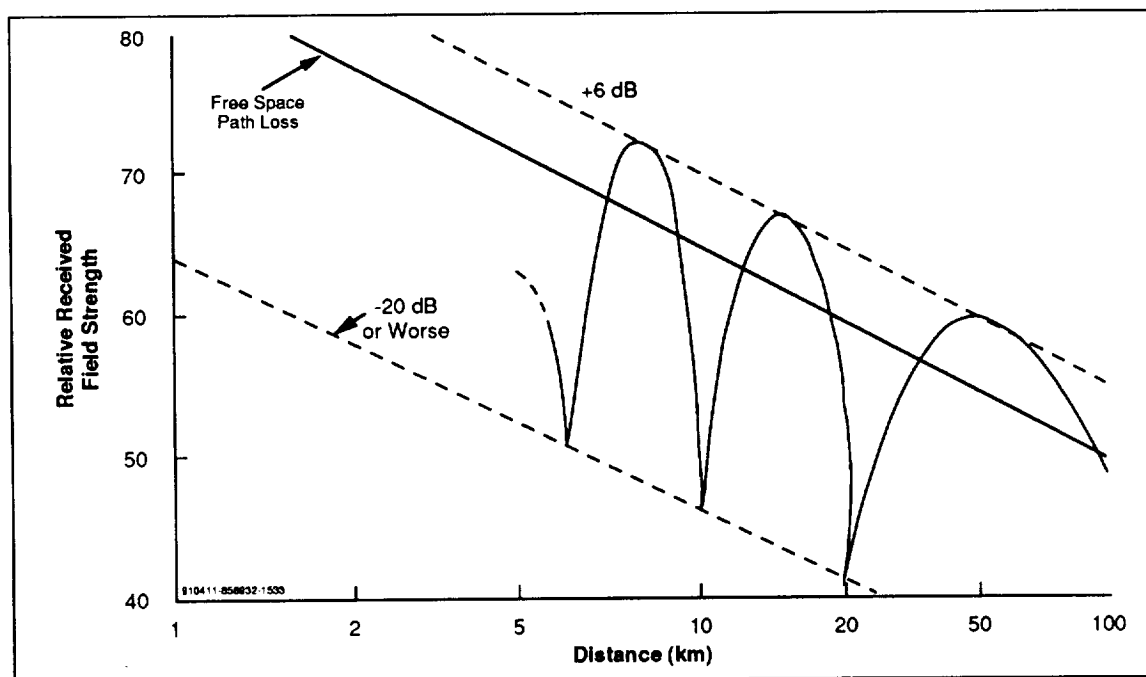


Exhibit 2-3 Geometry of Terrain Multipath Fading

Exhibit 2-4, adapted from John Griffith, Radio Wave Propagation and Antennas [6], plots the form of received signal level variations with distance for a link between a ground terminal with elevated antenna and an airborne terminal. Note the deep nulls spaced at roughly equal distances. Signal level variations of this form can occur for a given link as the airborne terminal flies away from the ground terminal.



**Exhibit 2-4 Plot of Received Signal Level Variations with Distance for a Ground-to-Air RF Link Experiencing Terrain Multipath Propagation**

Terrain multipath fading depths depend on the polarization of the signals, as well as on surface conductivity and antenna patterns. Because the actual (composite) receiver-antenna signal level is dependent on direct and reflected phase angles (i.e., direct and reflected path lengths), exact mathematical characterization requires a tape measure. However, the approximate terminal locations for signal nulls and the relative depths of nulls can be predicted analytically. At low angle of incidence of a reflected vertically polarized signal (e.g., below Brewster's angle) which is expected for Shuttle positions near MECO, reflection can be highly efficient and thus cause either strong reinforcement or strong cancellation.[7]

Observed fading instances can be fit to analytic models through correlation of the signal strength (AGC) measurements with flight path geometries and knowledge of command transmitter locations and antenna heights.

### 2.3.2 Atmospheric/Ionospheric Effects

The atmospheric regimes through which the Shuttle passes in the upper stratosphere and ionosphere are not well characterized, particularly with regard to granularity or patchiness of features that cause refraction and reflection of radio waves. Standard atmosphere profile models assume that refractivity does not change much horizontally, but such assumptions may not be valid for the Shuttle in flight downrange before MECO. Several factors can be expected to cause variations of significant magnitude, if they occur:

**Ducting in the Atmosphere** - Temperature inversions in the troposphere or stratosphere can cause ducting of signals, creating "holes" in field strength in certain regions, as illustrated by Exhibit 2-5.

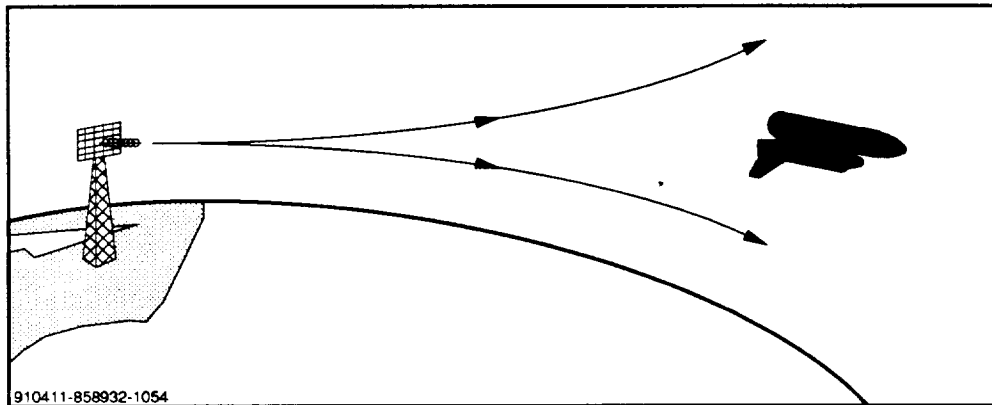


**Exhibit 2-5 Signal Loss Due To Atmospheric Ducting of Radio Waves**

**Air Density Boundaries** - Regions or blobs of air of differing density in the troposphere can cause refraction if boundary surfaces are not perpendicular to the signal ray path. This phenomenon can cause multipath propagation fading, as illustrated by Exhibit 2-6. Alternatively, it can create "shadow" zones with severely attenuated signal strength. Multipath propagation by this effect is quite common in terrestrial microwave relay of common carrier signals, requiring diversity reception techniques in many such links.[8] This effect is used for troposcatter over-the-horizon communications, where communications link designers count on refraction from density change surfaces.[6]

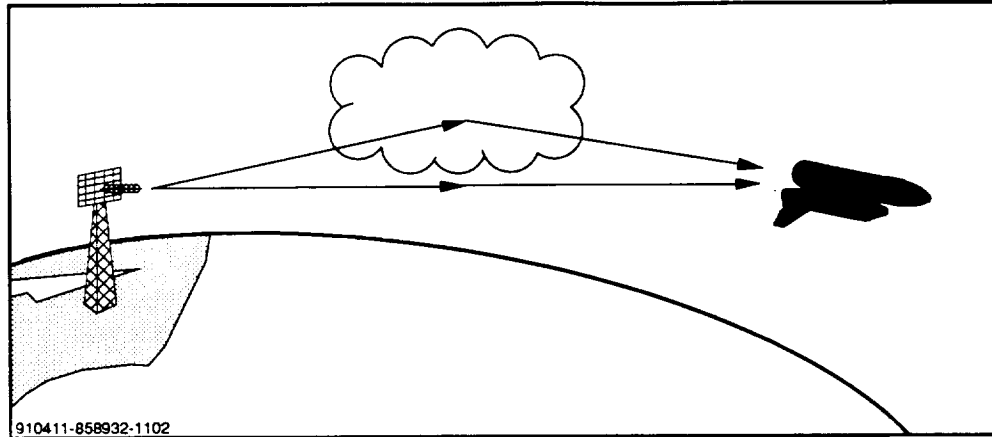


**Exhibit 2-6 Geometry of Tropospheric Multipath Propagation**

**Ionospheric Effects** - Prior to MECO, the Space Shuttle passes through/into three well-known altitudes of ionospheric electron-density boundaries - the D, E, and F, layers. Exhibit 2-7 shows the electron-density boundaries that define these layers. These ionospheric effects are notoriously irregular, both in times of existence and patchiness.[6,9] HF sky-wave propagation is dependent on them. VHF ionospheric scatter communications has been used in the past. UHF Satcom communications are sometimes subject to ionospheric scintillation fading.[10] The combination of Shuttle altitude, geographical position, and command link frequency are not common, so studies of relevant ionospheric effects were not available prior to this study to reject or admit the possibility of ionospheric scattering or multipath fading causing IRD dropouts.

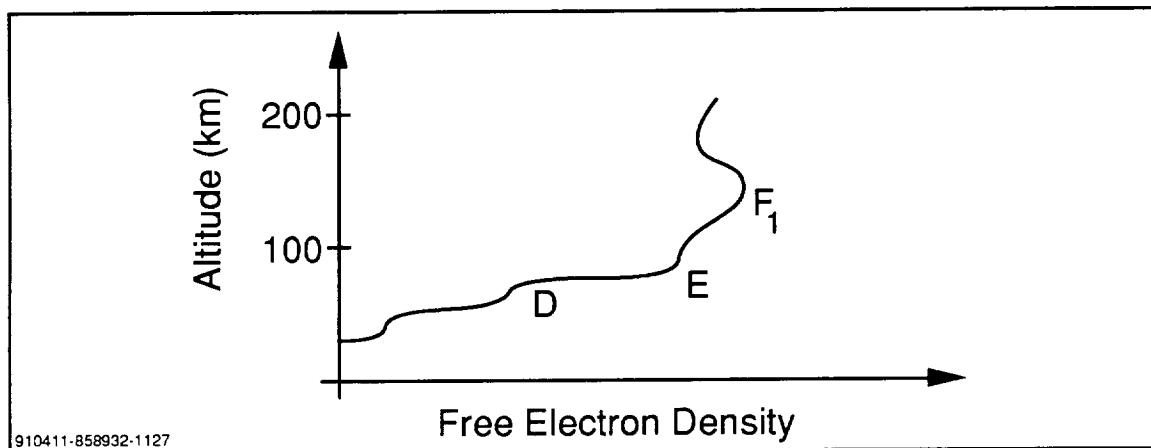


**Exhibit 2-7 Ionospheric Refraction Layers Defined by Free Electron Density Variations with Altitude**



**SSME Exhaust Cloud Effects** - The Shuttle main engine exhaust can cause an effect on refractivity similar to that of tropospheric refraction discussed above, by in effect creating a massive "cloud" of water vapor. This "cloud" certainly has the potential to support atmospheric multipath propagation. It can also refract signals away from or toward individual Shuttle antennas given certain geometries. Exhibit 2-8 and 2-9 illustrate these effects.

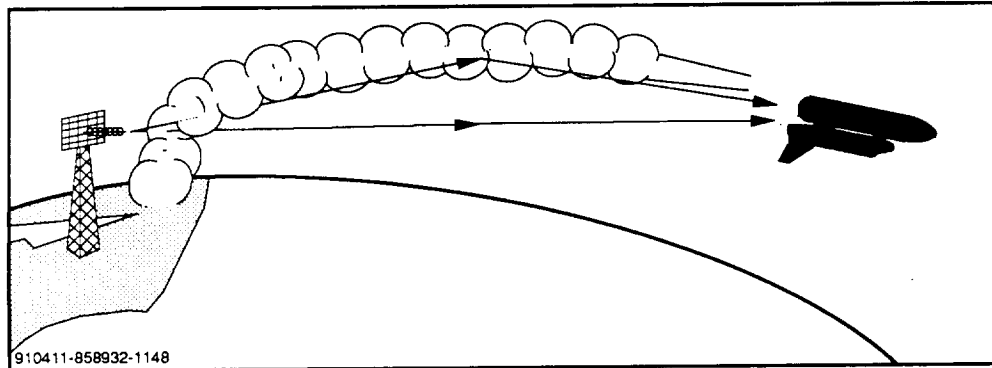


**Exhibit 2-8 Multipath Propagation Caused by Refraction or Reflection in Condensed Exhaust Cloud**

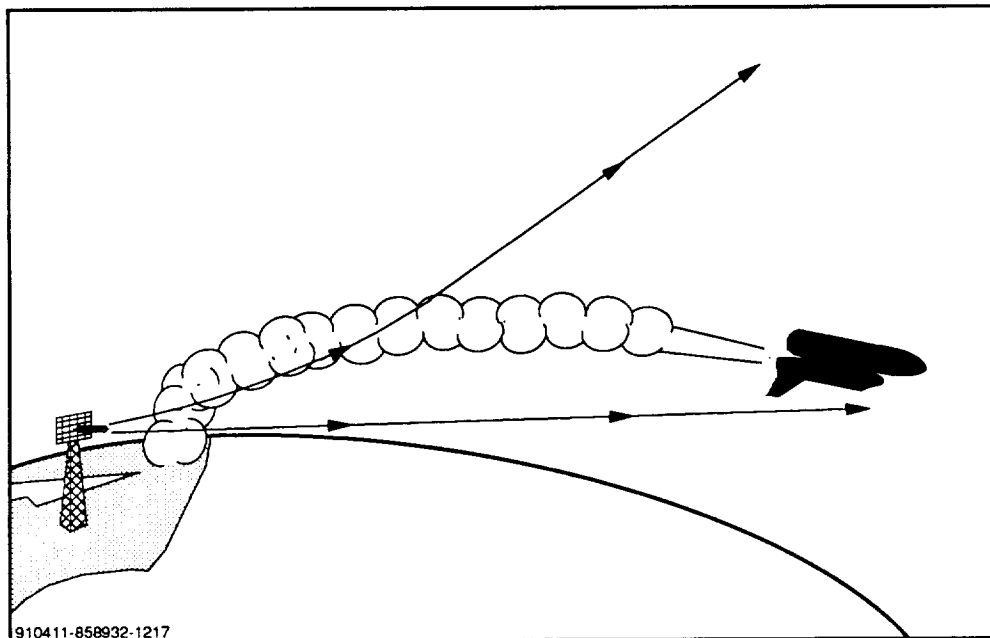


**Exhibit 2-9 Gap in Signal Reception Caused by Refraction in Condensed Exhaust Cloud**

The dropout events occur when the Shuttle is well down-range, which means that signals must traverse a long path through troposphere, stratosphere, and ionosphere, increasing the likelihood of effects such as the above.

### 2.3.3 Multipath Reflection and Diffraction From Shuttle Orbiter and ET Surface Features

The antenna pattern contributes greatly to the received signal strength. Antenna patterns for aircraft radio systems that use supposedly omni-directional antennas often have multiple lobes separated by deep nulls. Such antenna patterns result from multipath reflections or diffraction off of aircraft surfaces. The secondary rays interfere with the direct RF signals, alternatively causing reinforcement and cancellation as aspect angle changes.

In the 417 MHz range ( $\approx 0.7$  m wavelength), the sizes of orbiter and ET features range from less than one wavelength to many wavelengths, so reflection and diffraction modes can both exist. Exhibit 2-10 is a polar plot of a hypothetical stub antenna mounted on a complex (nonplanar) surface, illustrating the effects of multipath signal interference.

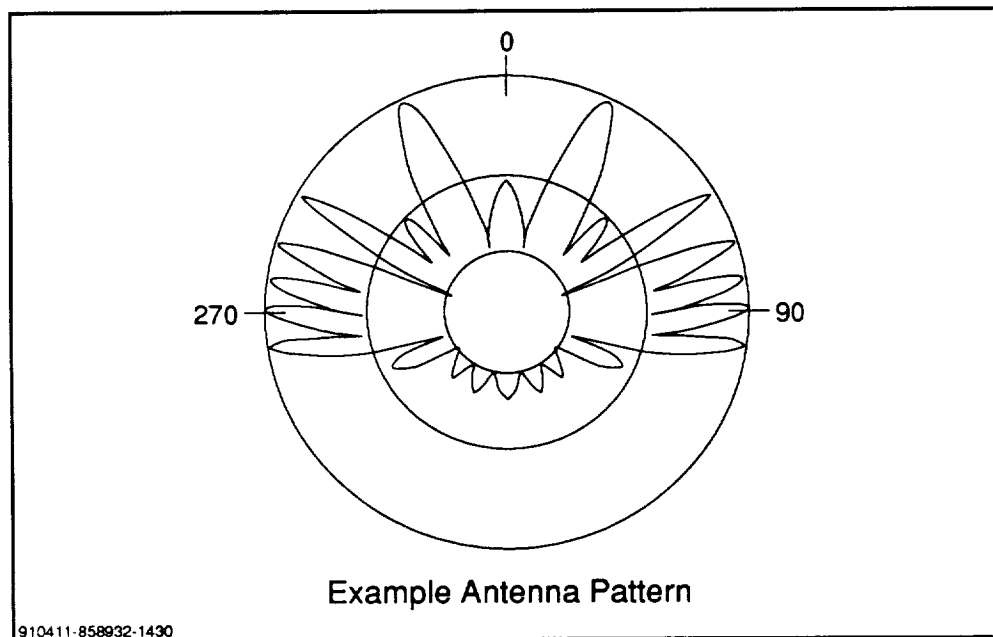


**Exhibit 2-10 Hypothetical Antenna Pattern of a Stub Antenna over a Complex Shape Conductive Surface**

Analysis - To verify the presence of conditions that could cause atmospheric or ionospheric effects on a given Shuttle flyout would require historical meteorologic data and ionospheric sounding data respectively for the date and approximate geographical location of the RF link. We were not able to obtain such data for the Shuttle flights analyzed and, as a result, the possibility of occurrence of atmospheric or ionospheric effects could not be eliminated.

Most of the severe IRD signal fading events found in Shuttle telemetry records were repeatable for similar Shuttle trajectories and command link geometries. The repeatability would tend to indicate causes other than meteorologic or ionospheric phenomena, because these phenomena are transient. Both atmospheric and ionospheric effects have daily, seasonal and random variations probability of occurrence.

The effects of SSME exhaust clouds could not be rejected as possible IRD dropout causes by this analysis, because the exhaust cloud geometry does follow a repeatable pattern for Shuttle flights of similar trajectories.

Sections 4.2 through 4.4 provide more detailed discussions of the study conclusions regarding atmospheric/ionospheric effects.

Analyses and simulations performed by SRS indicate that when the Shuttle is well down-range from the transmitter site, both ET antennas can be shadowed by the orbiter wings, which could shield the antennas or cause periodic nulls from knife-edge diffraction around the wing edge. If diffraction patterns are complex, a variety of multipath and attenuation modes are possible. Exhibit 2-11 illustrates the ray geometry for multipath and diffraction effects of the vehicle.

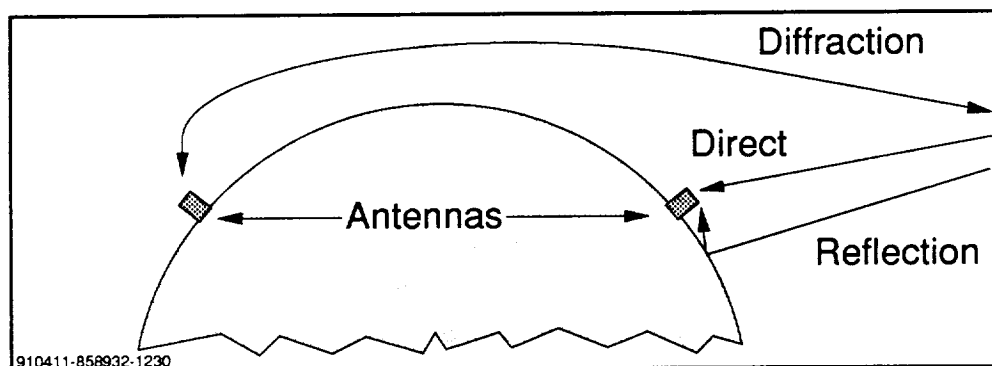


**Exhibit 2-11 Multipath Propagation by Reflection and Diffraction at Vehicle Surfaces**

Also, the two ET antennas both connect coherently to a single receiver input port through a hybrid coupler. This type of arrangement can cause destructive interference if the geometry is such that approximately equal signals reach both antennas with certain phase differences. Diffraction could cause such conditions to occur.

Static IRD antenna pattern measurements made in the orbiter/ET configuration were reviewed to attempt to identify possible fading causes related to the vehicle structures. As discussed in later sections, fidelity of scale model antenna measurements was limited in aspect regions relevant to this analysis effort.

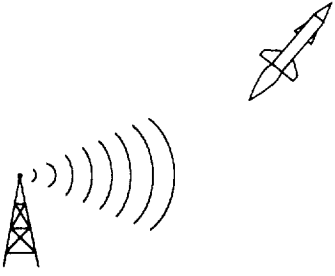
### Theoretical Signal Strength Modeling

The basis for determining the theoretical signal strength of either the CCT or the telemetry signal can be found in the radar beacon range equation in Exhibit 2-12. By solving the equation for signal strength at the target object, a Reference Range may be calculated. The reference range is that range to which the vehicle may fly, and at which point the signal strength reaches the minimum effective value.

$$R^2 = \frac{\lambda^2 P_t G_t G_r}{(4\pi)^2 P_r L}$$

where;

- R = Range
- $P_t$  = Transmitter Power
- $G_t$  = Transmitter Antenna Gain
- $G_r$  = Receiver Antenna Gain
- $P_r$  = Received Power
- L = Insertion Loss Factors
- $\lambda$  = Wavelength



The radar beacon range equation provides the algorithm with which signal strengths may be calculated.

910412-858932-1116

**Exhibit 2-12 Radar Beacon Range Equation**

With the exception of rocket plume attenuation, known path attenuating factors are considered in the calculation. The modified radar beacon range equation is transformed to a logarithmic base 10 form to facilitate manipulating the various signal loss factors involved in the analysis. The reference range (in dB) is used in the SRS computer program, "RFLINK" to provide a measure of the predicted link margin for both telemetry and CCT signal paths.

## 2.5 Outline of the Study Tasks

For each of the possible IRD dropout mechanisms we described above, we first synthesized basic geometric and RF transmission loss models, including calculation of the specific loss functions for that mechanism. We constructed scenarios for the different Space Shuttle flyout profiles represented by missions that have and have not encountered significant IRD signal loss. The models we produced took into account the primary relevant characteristics of ground station equipment, Space Shuttle vehicle equipment, range, altitude, attitude or aspect angle, and atmospheric/ionospheric conditions known or considered likely for the candidate IRD dropout mechanisms.

We used the basic models to compute nominal theoretical received signal levels and additional parameters such as periodicity of fading events for a number of points in each of the flyout scenarios. We then compared the results with measurements made during the respective missions to evaluate compatibility of the observations with the model calculations.

For candidate signal loss causes whose model results are within the bounds of actual data, we carried out empirical assessments, using statistical and physical-effects computational models as needed. These assessments made extensive use of the IRD signal measurements from various Shuttle launches. The results of this effort are signal loss explanations verified by simulation, with supporting data/rationale.

On the basis of results from the detailed empirical assessment, we have defined preliminary requirements for an experiment to demonstrate the signal loss cause or causes established during this study.

The following paragraphs summarize the specific tasks we have performed to complete the IRD Dropout Study.

The sequence of tasks is shown in Exhibit 2-13.

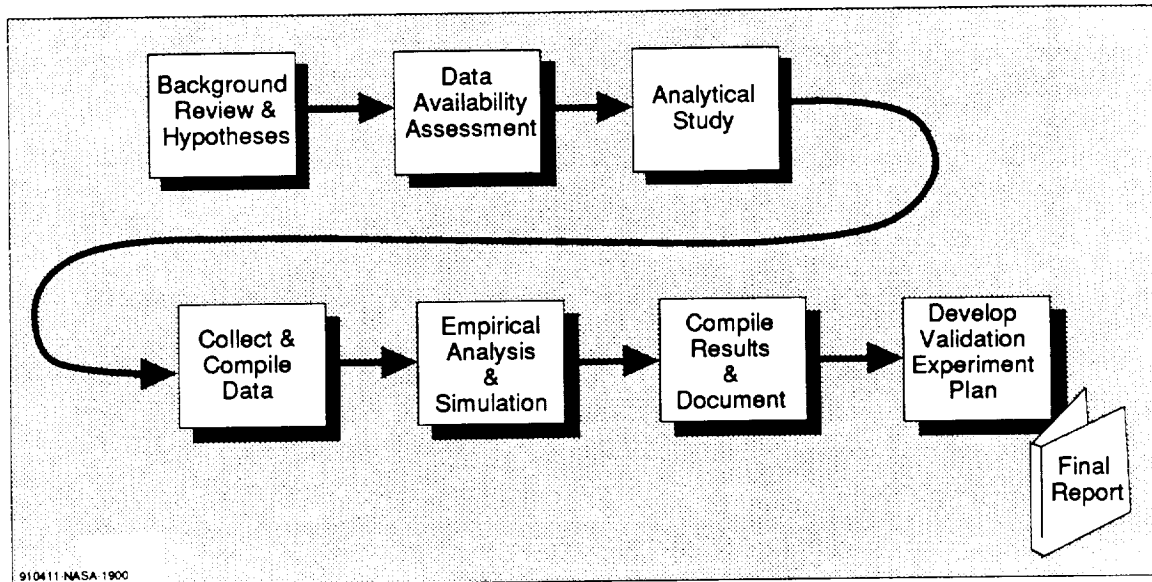


**Exhibit 2-13 IRD Dropout Study Task Steps**

The following paragraphs are an explanation of what was undertaken in these tasks:

**Background Review and Hypotheses Development** - We thoroughly reviewed the background material supplied by NASA to gain a better understanding of the problem. This effort included a review of the report included in the solicitation, A.R.A.P Report No. 494, entitled "Range Safety Signal Attenuation by the Space Shuttle Main Engine Exhaust Plumes" [1]. We discussed data requirements with the NASA engineers who have direct information on the dropout problem. From this background information we developed one or more hypotheses on what may be causing the dropouts. These hypotheses and the candidate methods were discussed with the NASA technical personnel in a project review and at several informal meetings.

**Data Availability Assessment** - We assessed the availability of the data required to perform the hypotheses testing. The level or fidelity of hypothesis testing is directly affected by the quality and quantity of data that can be acquired. The scheduling of subsequent hypothesis testing and analysis is also affected by the availability of data. We then reviewed the Shuttle database referenced in the solicitation work statement to determine what data would be useful for this study. We discussed the data requirements with NASA technical personnel and established methods and schedules for acquiring the desired data.

**Analytical Study** - We performed analytical studies on the hypotheses presented. These

studies applied the theoretical knowledge about related phenomena to the situation or circumstances of the Shuttle launches. These analytical studies were performed to the extent possible with readily available data on the Shuttle launches. The analytical studies showed which phenomena could have a greater influence on the resulting signal dropouts. These analytical studies were used to prioritize and direct the subsequent empirical analyses.

**Collect and Compile Data** - Often data exists in several forms and formats. Considerable time and effort can be saved if unnecessary collection and conversion of data can be avoided. With the guidance of NASA personnel we determined what data, including its form and format, would be the most useful and economical to use. We worked closely with the NASA technical personnel in collecting and compiling the data required to perform the subsequent empirical analyses and simulations. Much of the data came from Shuttle mission databases and from analysis results compiled previously by NASA personnel.

**Empirical Analyses and Simulations** - We performed empirical analyses and simulations to evaluate the presented hypotheses. Empirical data was evaluated to determine if the actual results agree with the analytical models used to describe the dropout causes.

**Compile Results and Document** - The results of the analysis efforts have been collected and are compiled into this report.

**Develop Validation Experiment Plan** - This final report also discusses possible experiments to validate the results and conclusions of the study. The experiment approaches considered may include computer modeling/simulation components, in conjunction with field tests, to take into account factors that are hard to control or extremely costly to incorporate in field test scenarios.

### SECTION 3

## SIMULATION AND ANALYSIS PROCEDURES

To analyze the IRD signal drop effects SRS conducted simulations and performed analytical computations to characterize effects of several phenomena relevant to range safety uplink operation. The focus of this study phase of the analysis was on RF propagation modes, the free space loss computation being the largest magnitude component. To the free space computation we added capability for multipath propagation modes involving land terrain or ocean surfaces. The computations required consideration of antenna patterns for which we depended largely on scale model antenna measurements that had been made previously on a Shuttle model in orbiter-ET configuration. These patterns were made on the antenna range at Marshall Space Flight Center. They are expected to take multipath reflections from vehicle surfaces into account. Some limitations exist in the scale model antenna patterns in terms of the resolution of data and the fidelity at certain aspects angles.

The antenna patterns of the transmitter site omni-directional antennas appear to be quite uniform in azimuth at look angles above horizontal, from inspection of antenna patterns presented in Appendix A of the McDonald 1991 Report [2]. Reflections from the ground or from nearby structures could cause nulls to exist in the pattern. Ground reflection effects are considered in the terrain multipath model used by SRS for propagation analysis (described in Section 3.1). Other antennas and support structures at the site, which appeared in MSFC video recordings reviewed by SRS, could possibly affect the antenna patterns. Determination of the presence of any such effect would require *in site* antenna pattern measurements.

To perform the RF propagation simulation we had to take into account the Shuttle dynamics, consisting of flight path trajectory and spacecraft attitude. Detailed trajectory data was available in the Shuttle databases so we used that empirical data. Flight path data is important in the computation of both the free space path loss and terrain multipath reflections. Attitude data is important to bring into consideration antenna patterns on the Shuttle ET antennas. We also considered the geometric relationship of the Shuttle to the transmitter in terms of range and elevation. We also considered handoff points from one transmitter site to another. The handoff patterns were fairly consistent from flight to flight of given launch trajectories, but they differed for the different trajectories. For example, easterly flights used either Cape Canaveral Air Force Station or Jonathan Dickenson transmitter sites from early in the flight until approximately 400 seconds after launch. Handoff at this time was usually to the Bermuda Transmitter site. Receiver



characteristics were modeled primarily in terms of the received power, which was manifested in the AGC voltage telemetered down from the external tank to the ground. During this study Bill Hopkins of Marshall Space Flight Center measured AGC time constants and did dynamic range measurements using an example receiver.

Because plume effects had been investigated as possible causes of signal drop outs in previous studies, the current study did not concentrate on those. However, we did review the investigations of possible plasma attenuation effects. We also investigated possible refraction or diffraction modes that could occur in either plasma or water vapors states. Refraction or diffraction modes could cause signal enhancement as well as signal loss.

Receiver signal downlink telemetry records were used in simulations for comparison with data obtained from RF propagation calculations. By comparing the telemetry records with results computed from our models on the same time lines and trajectories, we were able to test hypotheses about possible attenuation and loss modes.

The following subsections provide details of the simulation analysis procedures.

### **3.1 RF Propagation (Theoretical)**

The RF propagation model used by SRS for this study included free space and multipath propagation components and antenna pattern effects. The free space model propagation consists of the standard free space attenuation equation which takes into account the inverse-square-law power dispersion and the transmitter and receiver antenna gains. The standard equation that was included in the SRS RF Link model had been developed previously for use in missile range safety assessments. The RF Link model included fly-out trajectories and other bookkeeping functions considered to be of value for the IRD Dropout Study. We added terrain multipath fading code to the RF Link model. The terrain multipath model used is a round-earth reflection model that uses optical ray paths. Provisions were incorporated to permit use of the 4/3 earth radius convention to simulate effects of atmospheric refractivity. Heights of the transmitter and receiver sights above sea level or surface level are taken into account. A simplified model of complex reflection coefficients was used in the terrain multipath simulation. Depth of fades simulated by this model depend on the magnitude of the reflection coefficient. Exact locations of occurrence of the nulls and peaks depend on the detailed geometry and are hard to model effectively. For small reflection angles, i.e., reflection angles close to grazing angles, the phase angle of vertically polarized components reverses, causing a change in the relative shape of the peaks and nulls. For the circular polarized range safety signal, this Brewster's angle effect is expected to cause a wider

variation between multipath peaks and nulls at low angles of reflection. Multipath RF propagation models are described in detail in the references (DeWolf and Salter 1968) and (Griffiths 1980).

The antenna patterns in the RF propagation model were empirical patterns taken from scale model antenna tests at Marshall Space Flight Center. The data was provided to SRS in paper and electronic form. These antenna patterns represent full spherical coverage ( $4\pi$  steradians) in a rectangular matrix of 2-degree x 2-degree cells. The antenna gain values for each RF propagation computation were selected from the antenna pattern matrix considering the Shuttle vehicle position in space and its attitude relative to the transmitter sites. Gains of transmit antennas on the ground did not appear to change significantly through the phases of flight considered for this study. Constant transmit antenna gain values were used in the simulation. The values were taken from published specified transmitter equipment and antenna characteristics descriptions.

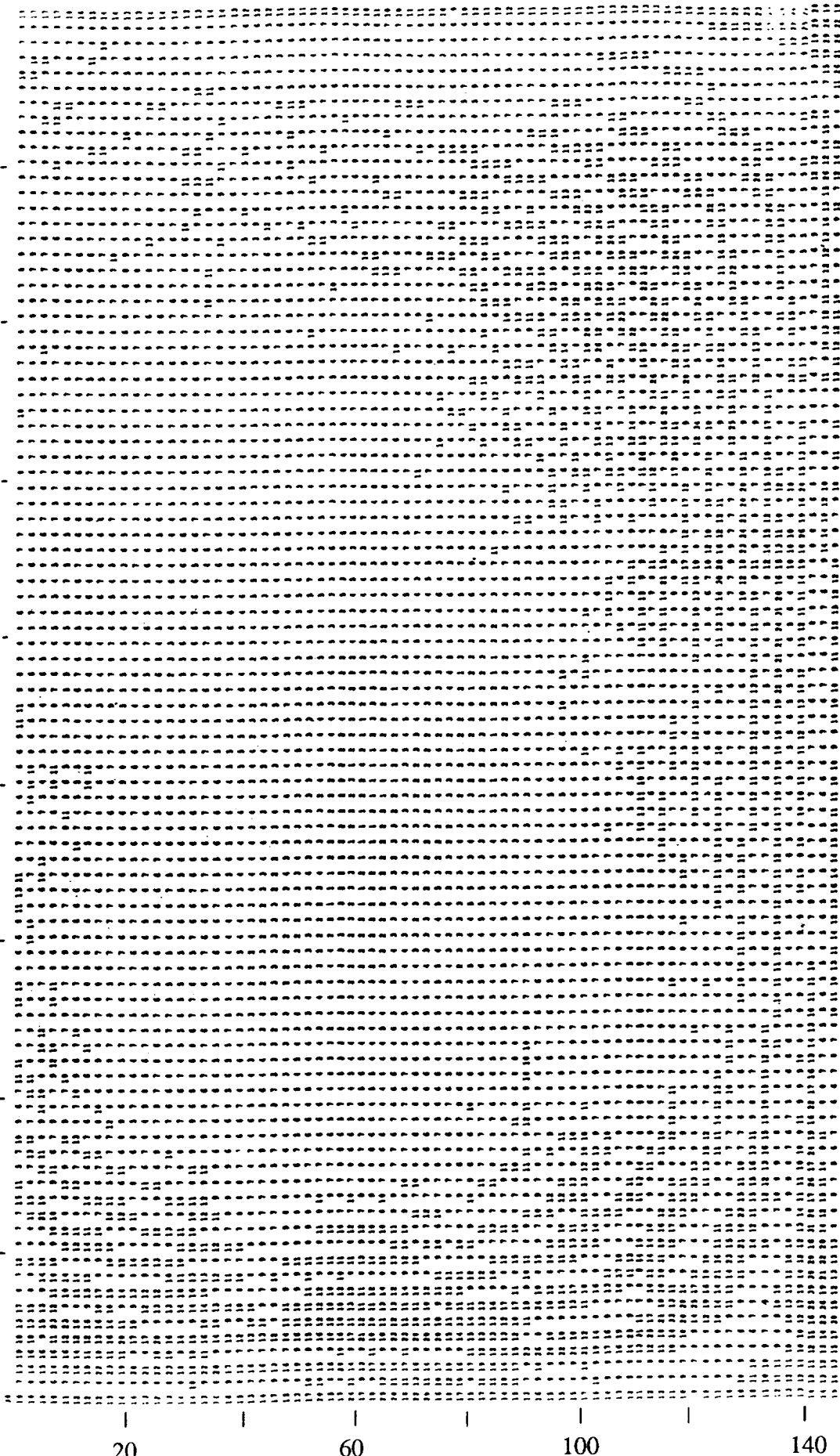
Exhibit 3-1 is a printout of the antenna pattern array showing in each cell the gain value relative to the maximum gain. Shuttle orientation is shown for cardinal points in this sphere.

### 3.2 Shuttle Dynamics

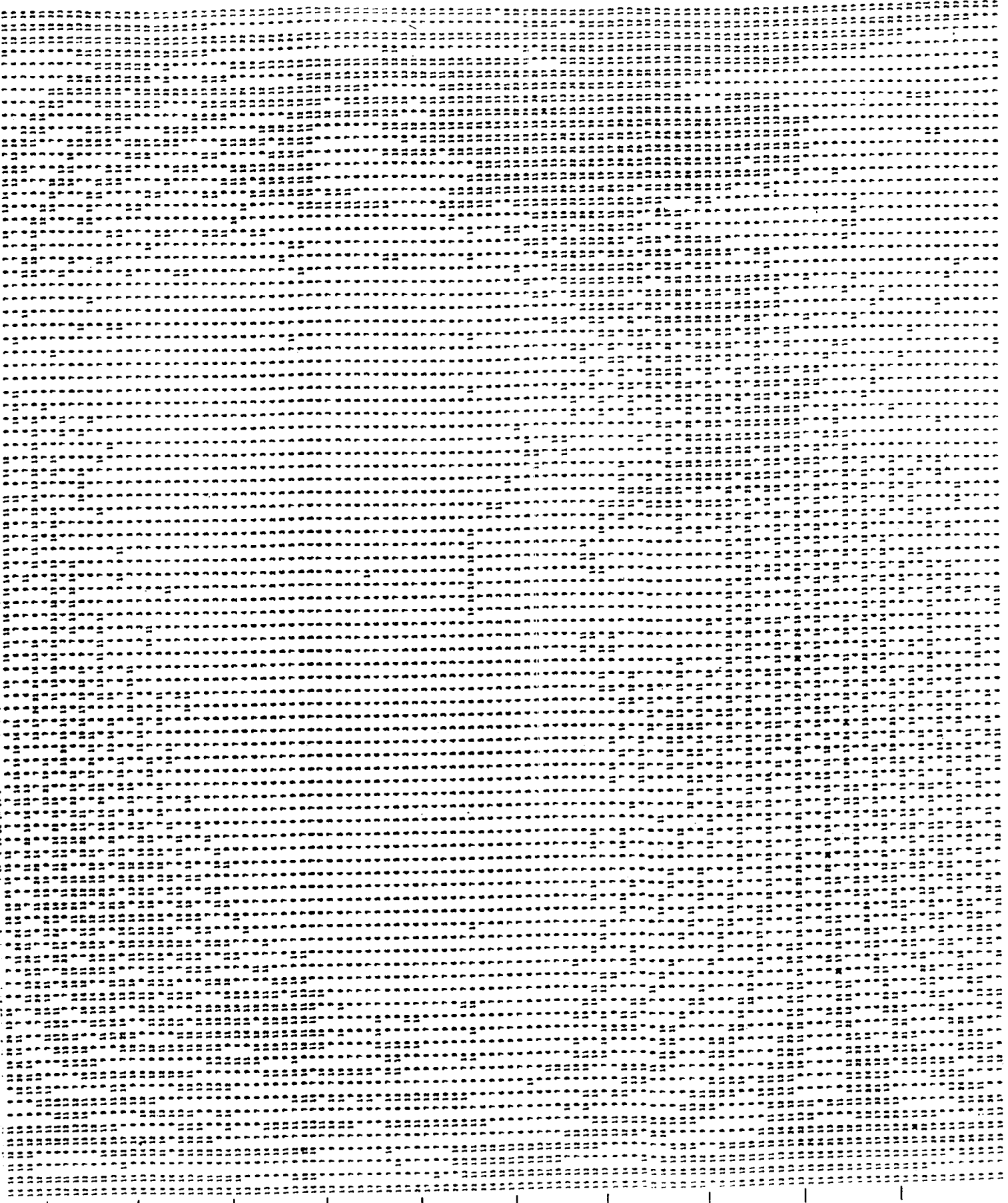
The position and attitude of the Shuttle as a function of time after launch was considered to be an important part of the simulation conditions. A significant part of our effort was oriented toward determining the state of the Shuttle at times when IRD signal fades occurred, to determine correlation of RF effects with differences between the vehicle states. We analyzed downloaded trajectory data from the Shuttle database for times of fades and times when signal fades did not occur for each of the Shuttle flights. It was then stored in computers at SRS for use in the simulation and analyses. The trajectory data (the path of flight and the attitude data consisting of vehicle pitch, yaw, and roll relative to the velocity vector) were combined in the computer model and related to the transmitter sight locations by range and elevation body angles. Results of these trajectory computations were used as described above to determine the locus of antenna pattern cells in Exhibit 3-1 from the time of SRB separation through the time of main engine cutoff (MECO). Other Shuttle flight records were used to identify handoff times from one transmitter site to the next (reference the previous study). Exhibit 2-2(a) shows a typical profile of a Shuttle trajectory after launch. Two common launch trajectories are (1) easterly launch trajectory for low inclination ( $28^\circ$ ) orbits and (2) a northeasterly launch trajectory for high inclination orbits.

Yaw Degrees

20  
40  
60  
80  
100  
120  
140  
160



FOLDOUT FRAME



180  
Roll Degrees

140

100

60

20

of Angles of Arrival on ET Antenna Pattern

FOLDOUT FRAME 2

### 3.3 Receiver Characteristics

The IRD receiver characteristics are as follows: The IRD receives, demodulates, and decodes the Range Safety command signal. The IRD provides a telemetry output that indicates the signal level it receives [11]:

SIGNAL LEVEL	TELEMETRY OUTPUT
No signal input	0.1 to 0.5 Vdc
-97 dBm	0.25 to 0.76 Vdc higher than no signal level
-53 dBm	4.5 Vdc (min) but not saturated
$\leq +13$ dBm	$\leq 5.25$ Vdc

The characteristics of the receiver section are listed in exhibit 3-2.

Exhibit 3-2 Integrated Receiver/Decoder [11]	
Frequency, Fixed tuned	416.5 MHz
Voltage Standing Wave Ratio	
-20 °C to +50 °C	1.5 (max)
-40 °C to -20 °C	2.0 (max)
+50 °C to +80 °C	2.0 (max)
RF Sensitivity	-97 dBm
Capture	$\leq 3$ dB audio output reduction with interfering 416.5 MHz unmodulated carrier 2 dB below desired
Operational Bandwidth	$\pm 45$ kHz (min) from 416.5 MHz
IF Passband Ripple	3 dB (max) within $\pm 45$ kHz of 416.5 MHz
60 dB Bandwidth	$\pm 180$ kHz (max) from 416.5 MHz
Response $> \pm 10$ MHz from 416.5 MHz	80 dB image rejection required
Specification Assembly Drawing	10SPC-0132 10406-0143

The plots of voltage vs. signal strength from two different IRDs are presented in Exhibit 3-3.

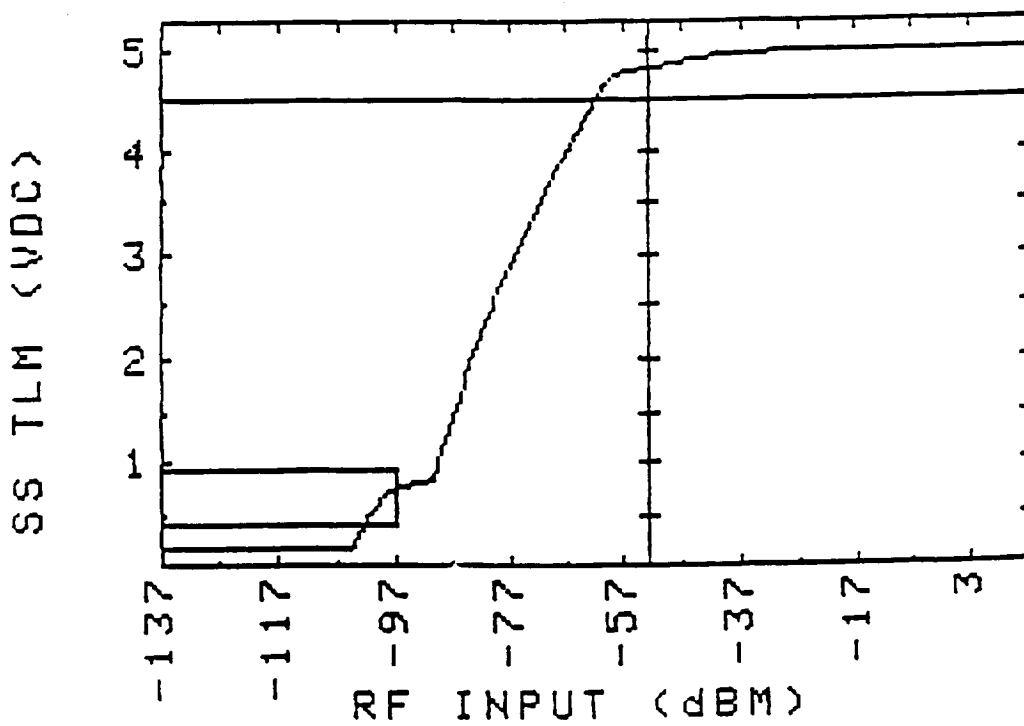
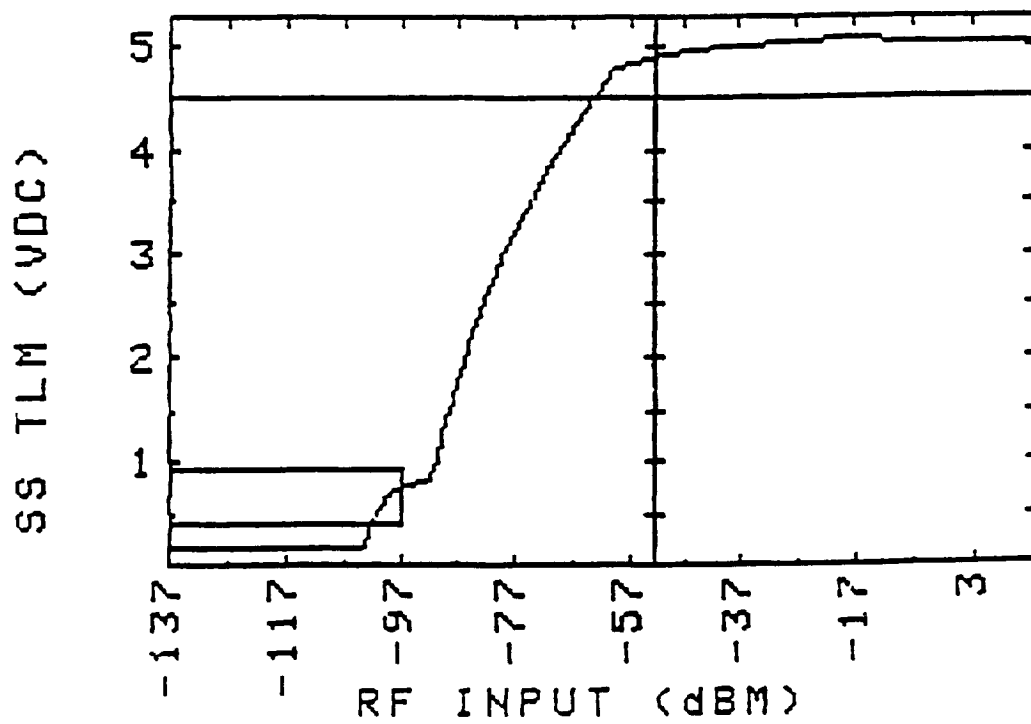


Exhibit 3-3 Voltage vs. Signal Strength Plots From Two IRDs [11]

## SECTION 4 SIMULATION/ANALYSIS RESULTS

The computer model used in the performance of this contract was a computer code called RFSignal. RFSignal is written in FORTRAN and executes on a Macintosh personal computer. RFSignal was generated from an SRS existing code called RFLINK which was used primarily for range safety analysis of Flight Termination System radio link margins. The RFLINK code used a worst case measure of antenna nulls for antenna loss and did not provide the capability to compute antenna loss from antenna pattern data. Several redundant features were added to RFLINK to generate the the RFSignal code. RFSignal has the capability to accept an input antenna loss pattern as an input array. The code also computes a directional site vector to the vehicle which is used to index into the antenna pattern array to determine directional antenna loss. The capability to model terrain multipath effects was also added to the code to model the multipath signal fades due to the changing phase of the two received signals. The output from the RFSignal program was then used as input to a commercial plotting program available on the Macintosh to produce the graphs contained in this report. The results of the analysis using these computer tools are described in the following paragraphs.

### 4.1 Terrain Multipath

In studying the signal loss measurements from a number of the Shuttle flights there appeared to be some recurring cyclical nulls very similar to the effects of terrain multipath fades. Using the RFSignal computer model, we studied the effects of terrain multipath on several Shuttle flight trajectories. The results showed that, due to the velocity of the Shuttle, the cyclical rate of the terrain multipath fades are at a much higher rate than the fades observed in the initial study effort. The results of the terrain multipath study indicates that terrain multipath fades are occurring but are not causing the large signal dropouts that are the issue in this study.

We considered the possibility that a combination of receiver AGC response time and the instrumentation sample rate may be causing a cyclical null pattern at a lower rate than the terrain multipath cyclical rate. However, after discussions with the NASA technical personnel on the instrumentation sampling rate and some AGC sampling rate tests performed in the lab, it was determined that the AGC response rate and the instrumentation sampling rate prevent this from occurring. The AGC measurements indicated that the AGC response is "fast-attack, fast-decay", with time constants less than 50 milliseconds. With such response characteristics, the AGC will tract terrain multipath power envelopes accurately to within the 0.045 telemetry sampling interval at

which AGC response waveforms were recorded.

## 4.2 Antenna Patterns

We traced the Shuttle flight directional site vector through the antenna pattern to determine if the nulls are the result of the antenna pattern. From this analysis we can only draw a marginal conclusion that the antenna patterns cause the dropouts. On some occasions there appear to be some correlation between antenna cells and the recorded instrumentation data. However, because of the granularity of the cell measurements it is difficult to determine if the cell measurement accurately reflects the signal result. On different flights the traces may pass through the same cell with differing results. The two most noticeable differences are that the path across the cell can be different and that the time period spent in the cell can be significantly different. It appears that significant nulls may exist within the actual antenna pattern but the two-degree-granularity scale model antenna pattern does not have sufficient resolution to capture the null.

Conversely, ET IRD signal level fading patterns exhibited consistencies from flight to flight that suggest the influence of stable structural or geometric phenomena. Exhibit 4-1 is a superposition of signal strength records for ET IRD reception of transmissions from Bermuda during several of the early Shuttle flights that used an easterly launch trajectory. The spacing of peaks and nulls appears to be quite similar for all of these flights, although absolute times and magnitudes vary. Earth-surface multipath and antenna patterns (including Shuttle surface multipath effects) are both stable phenomena.

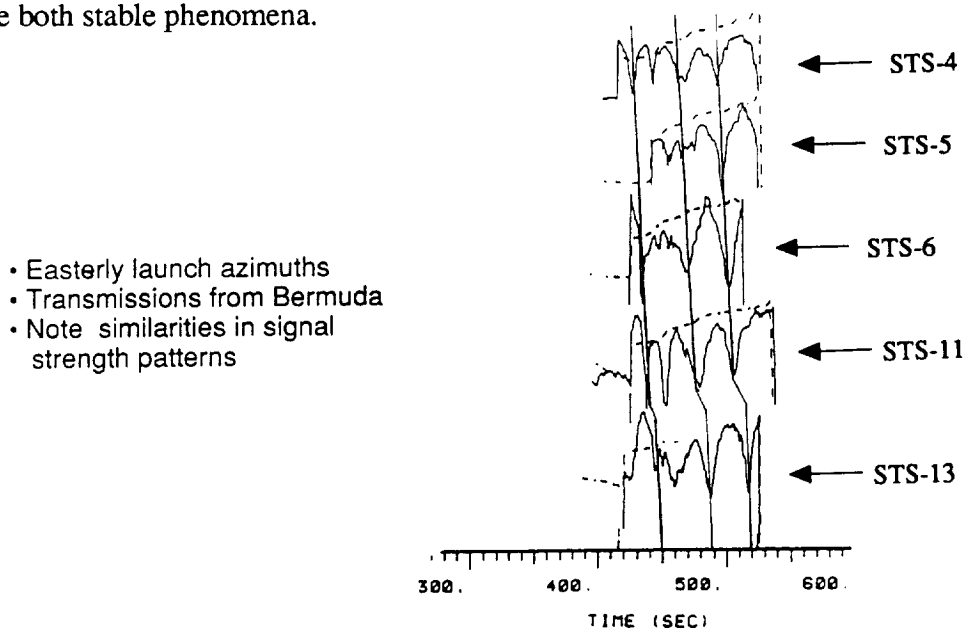


**Exhibit 4-1 Comparison of ET RSS Signal Strength Patterns**



Our simulation of earth-surface multipath indicated a faster variation with time than observed in these cases. We believe that these effects could be caused by fine-grained features in the ET antenna patterns that were not evident in the discrete-cell scale-model antenna pattern data. Scattering theory and radar cross-section (RCS) measurements from complex objects demonstrate frequent and violent signal level fluctuations with aspect angle.

### 4.3 Trajectories/Attitudes

Shuttle flights STS-26, STS-27, STS-29, STS-30, STS-33, and STS-36 appeared to have encountered the most severe IRD signal fades. We analyzed flight trajectories of these flights to search for geometric indications of the underlying cause(s) for the dropouts. The flight trajectories, including vehicle attitude, and the location of the FTS transmitting sites, were considered in the analysis.

Exhibit 4-2 shows the angular measurement off the centerline, looking from aft, the time in flight, and the time when the deep nulls occurred. The STS-27 and STS-36 flights have similar characteristics that are noticeably different from the other flights, due to the northeasterly launch azimuth for these flights. STS-30 looks quite different because of a turn performed in its flight. This turn can be seen in the trajectory data plotted in the attached appendices for these flights.

STS #	Yaw Look Angle	10°	9°	8°	7°	6°	5°	4°	3°	2°	1°	0°	-1°	-2°
26c	(E)	192	203	211	231	248	270	307	334*	*391				
29c	(E)	191	201	213	237	258	284	326*	*351					
30c	(E)	230	237	246	255	265	276	289	303	319	340*	*364	391	429
33c	(E)	196	199	202	235	252	273*	*303	348*	*420				
27c	(N)	286	306	329	358	393	434*	*451						
36c	(N)	274	299	326	356	390*	*400							

\* Deep nulls occur at times between the asterisks (note: STS-33 has two nulls)

(E) Easterly launch azimuth

(N) North-Easterly launch azimuth

### Exhibit 4-2 Yaw Look Angles vs. Shuttle Flight Time

In our analysis, the vehicle-to-site vector was computed in a yaw and roll angle so the angles could be used to index into the antenna pattern data array. Exhibit 4-3 shows the combination of yaw and roll angles at the point of the deepest signal fades. The roll angle is measured from the vertical stabilizer with the Shuttle in the inverted (180° roll flight regime). Positive is to the right, rotating in the counterclockwise direction, a negative number indicates the

site vector crossed over the centerline to the left, rotating in the clockwise direction. Note again that flight STS-33 has two nulls.

Flight	Time (sec)	Yaw Angle	Roll Angle
26c (E)	385	2.4°	-2.4°
29c (E)	330	4°	4°
30c (E)	364	0°	14°
33c (E)	290	4.4°	7°
	400	2.2°	-6.5°
27c (N)	440	4.8°	76°
36c (N)	390	6°	75°

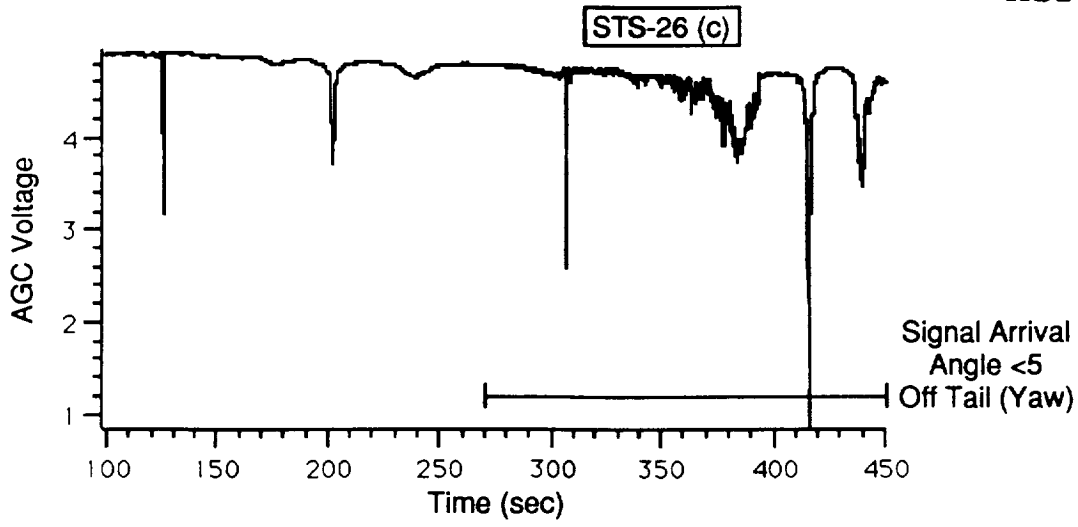
E) Easterly launch azimuth

(N) North-Easterly launch azimuth

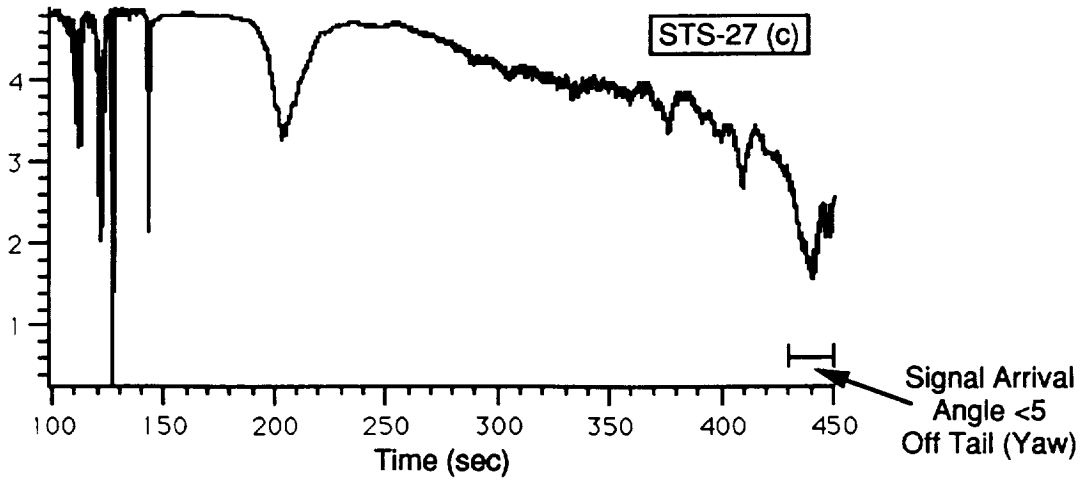
#### Exhibit 4-3 Attitude Angles at Times of Deep Signal Fades

Exhibit 4-4 contains AGC voltage records from the ET IRD as functions of time after launch for flights STS-26, STS-27, STS-29, STS-30, STS-33 and STS-36; with transmissions from Cape Canaveral. The time intervals during which signal arrival angles were within 5° of directly aft (in yaw) are indicated for all of these flights except STS-36. For STS-36, handover of transmission to Bermuda occurred just at the time the signal arrival angle decreased to 5° from directly aft. In all the other cases shown, deep signal fades occurred only during the interval of aft signal arrival. In the STS-36 case, the decreasing signal level trend near 400 seconds after launch suggests that if Cape Canaveral transmission had continued as the arrival angle decreased further, a deep fade might have occurred within a short time.

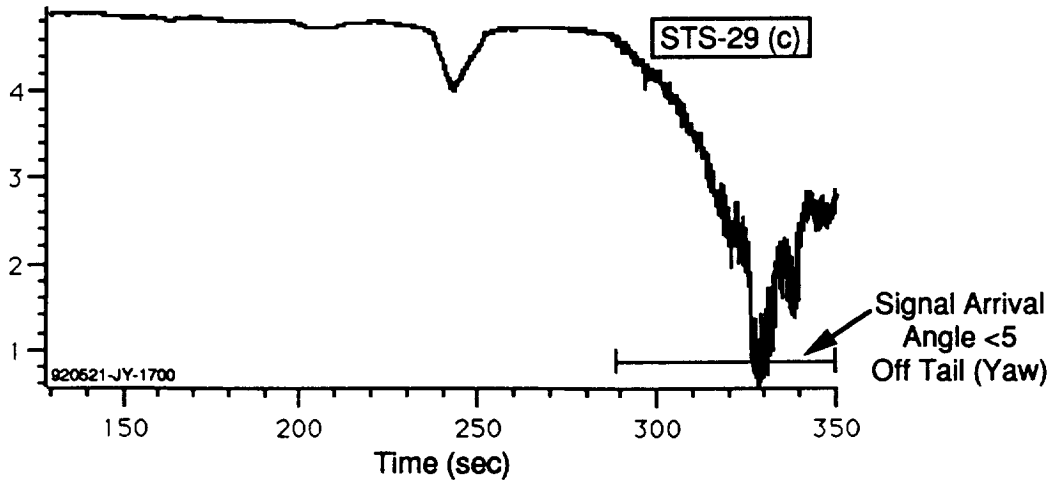
These results indicate the dropouts may be related to aspect angles nearly directly aft, with some contribution from the roll (pitch) angle also being a contributing factor. However, it is not clearly indicated with this data. For example, flights STS-26 and STS-33 have similar trajectories, and they both have signal fades at approximately 300 seconds and 390 seconds. However, the signal fades on flight STS-33 are much longer and deeper than the fades on STS-26. This seems to indicate that indeed there may be very sharp antenna nulls that the Shuttle antenna patterns do not reflect and/or there may be other contributing factors involved.



a. STS-26

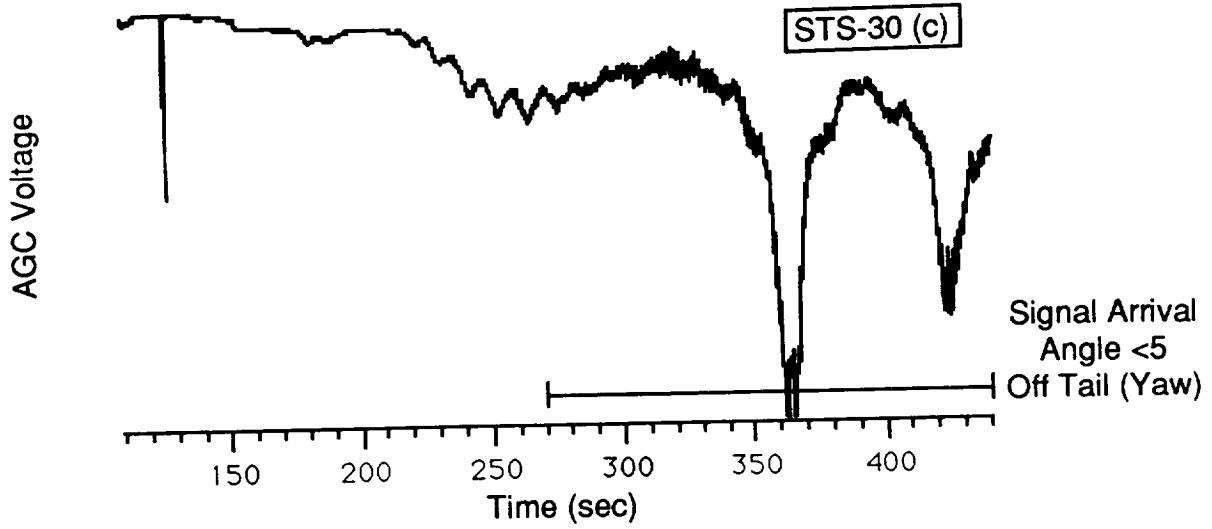


b. STS-27

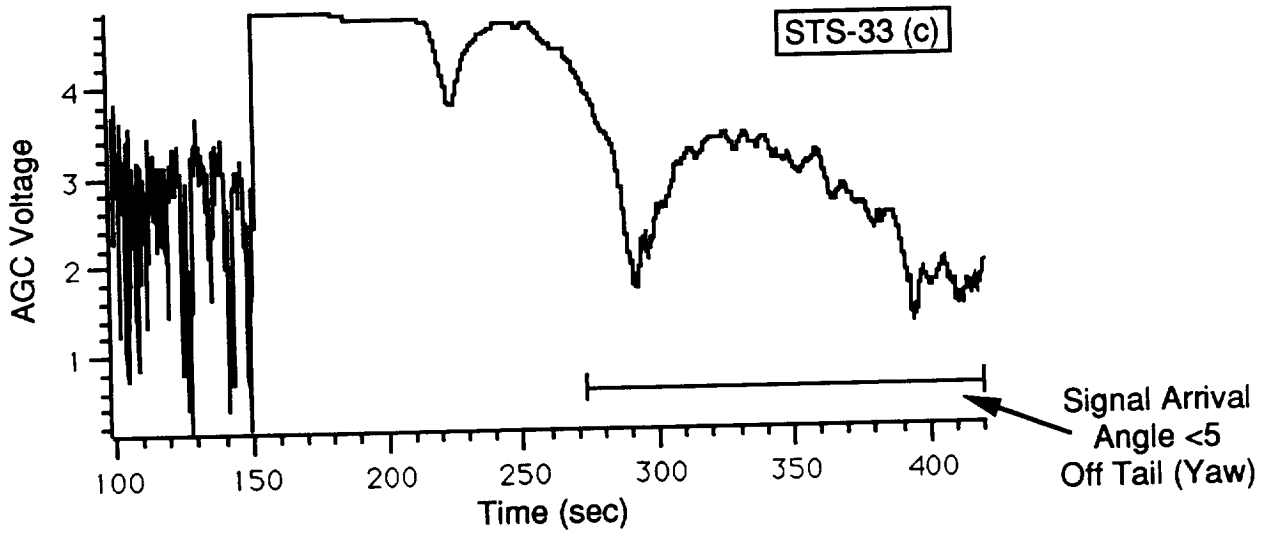


c. STS-29

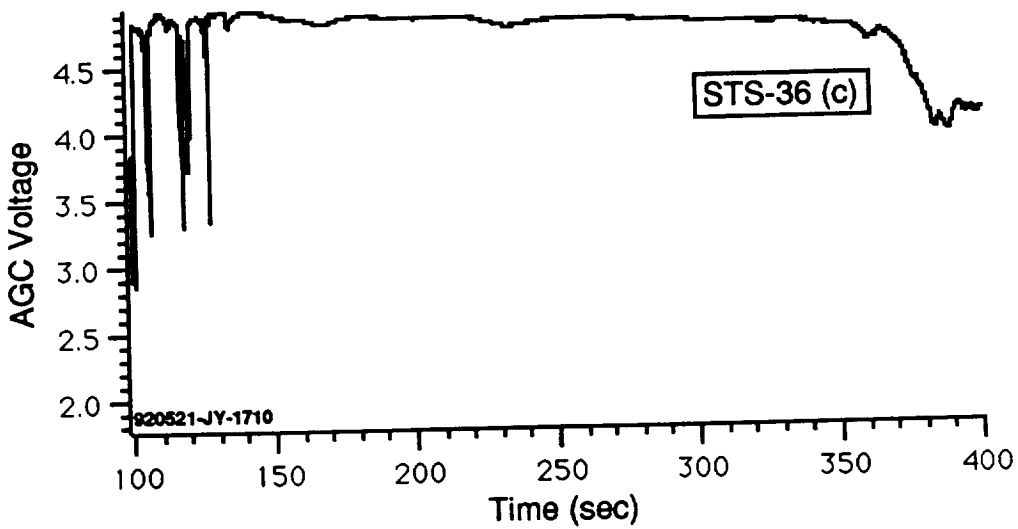
**Exhibit 4-4 Record of ET Receiver AGC Voltages vs. Time After Launch (Transmission from Cape Canaveral)**



a. STS-30



b. STS-33



c. STS-36

An important question in light of these results is: What is the mechanism that causes the signal nulls to occur at arrival angles nearly directly aft? Possibilities include the following:

- Both ET antennas are blocked by Shuttle surfaces.
- Nulls occur in the basic ET antenna patterns at arrival angles nearly parallel to the ET skin.
- One ET antenna is blocked while the other is subject to destructive multipath interference from Shuttle surfaces.
- Signals arrive at the two ET antennas in such a phase relationship that, with the effects of RF cable lengths, cancellation occurs at the output of the RF coupler device that combines the RF signals for input to the IRD.
- Signal diffraction and/or refraction involving Shuttle surfaces or the SSME exhaust plume/cloud.

The source data needed to isolate these possible causes of aft nulls was not available to SRS in sufficiently high resolution or fidelity during the current study.

Given the knowledge of specific signal arrival angles that cause extended signal nulls (i.e., directly aft) NASA may be able to develop operational methods of avoidance. However, isolation of the mechanism(s) responsible for dropouts may permit a solution to be produced that does not require operational constraints. Such a solution could be incorporated in future ET design upgrades or added independently if deemed necessary. Examples of possible solutions (depending on the cause) are replacement of the ET RF combiner, addition of a second IRD using the presently terminated difference port of the existing RF combiner, change in placement of one or both ET antennas for more favorable rearward pattern, or selection of an ET antenna type with higher gain at angles nearly parallel to the ET skin.

The high-fidelity data needed to isolate these mechanisms and to identify the specific cause(s) can be obtained through additional scale-model antenna pattern measurements, detailed electromagnetic computer modeling/simulation, or (probably most efficiently) with a combination of these experimental and analytical approaches. These approaches are discussed in the following conclusions and recommendations sections.

#### **4.4 Atmospheric Effects**

Atmospheric effects were not studied because the fades appear to be consistent from flight to flight as a function of the trajectory. Severe weather conditions, which are usually the cause of

signal fades and interference, would not be a factor since the Shuttle does not launch in such weather. Less critical weather conditions such as inversion layer and ducting problems would be much less predictable. Since the fade patterns appear to be a function of flight and transmitter geometry, the problems and expense of collecting weather data did not seem warranted.

#### 4.5 Plume Attenuation

Various STS trajectories were examined to determine if rocket plume attenuation may have been a cause, in part, of the observed IRD dropout. The relatively clean burning LO<sub>x</sub>/liquid hydrogen SSMEs, however, are expected to contribute no more than three to six dB signal attenuation at the very worst aspect angle, i.e., zero degrees, looking into the plume.

In the analysis of plume attenuation for various U.S. Army Strategic Defense Command rocket tests (all analyzed employed solid propellant motors, and include HOE, Queen Match, ERIS, and BP Target Vehicle), SRS modeled multiple trajectory geometry's and conditions that led to both early-in-flight and late-in-flight onset of the plume attenuation phenomenon. Attenuation onset, in all cases, was shown to be a function of the aspect angle in conjunction with the plume exit angle. Although SRS saw cases where the onset was quite sudden, the rate of onset never approached the nearly "step function" dropout that appeared in the external tank signal strength traces. Also, the attenuation, once encountered, did not cease until booster burn-out, or a change in vehicle attitude occurred which increased the vehicle aspect angle to a value outside of the envelope defined by the plume exit angle and aspect angle combination.

SRS also examined expected signal levels for the portion of a shadow zone of a plume formed super conductive disk where a diffracted command destruct (416.5 MHz) signal might be expected to impinge. Using the Poehler method [5], values for signal strength in the diffraction illuminated zone were calculated to be on the order of 20 dB lower than direct illumination intensities. These values are far in excess of the expected attenuation for the SSMEs, therefore, this exercise seems to be of no value in the analysis. Details concerning the calculation of these values are presented in Exhibit 4-5.

Since most of the IRD dropouts occur with near step-function rapidity, and occasionally cease with equal rapidity (and without discernible change in vehicle attitude), and since the expected value of plume attenuation from the SSMEs is of a relatively minor magnitude, SRS can not associate the dropout with a plume attenuation phenomenon.

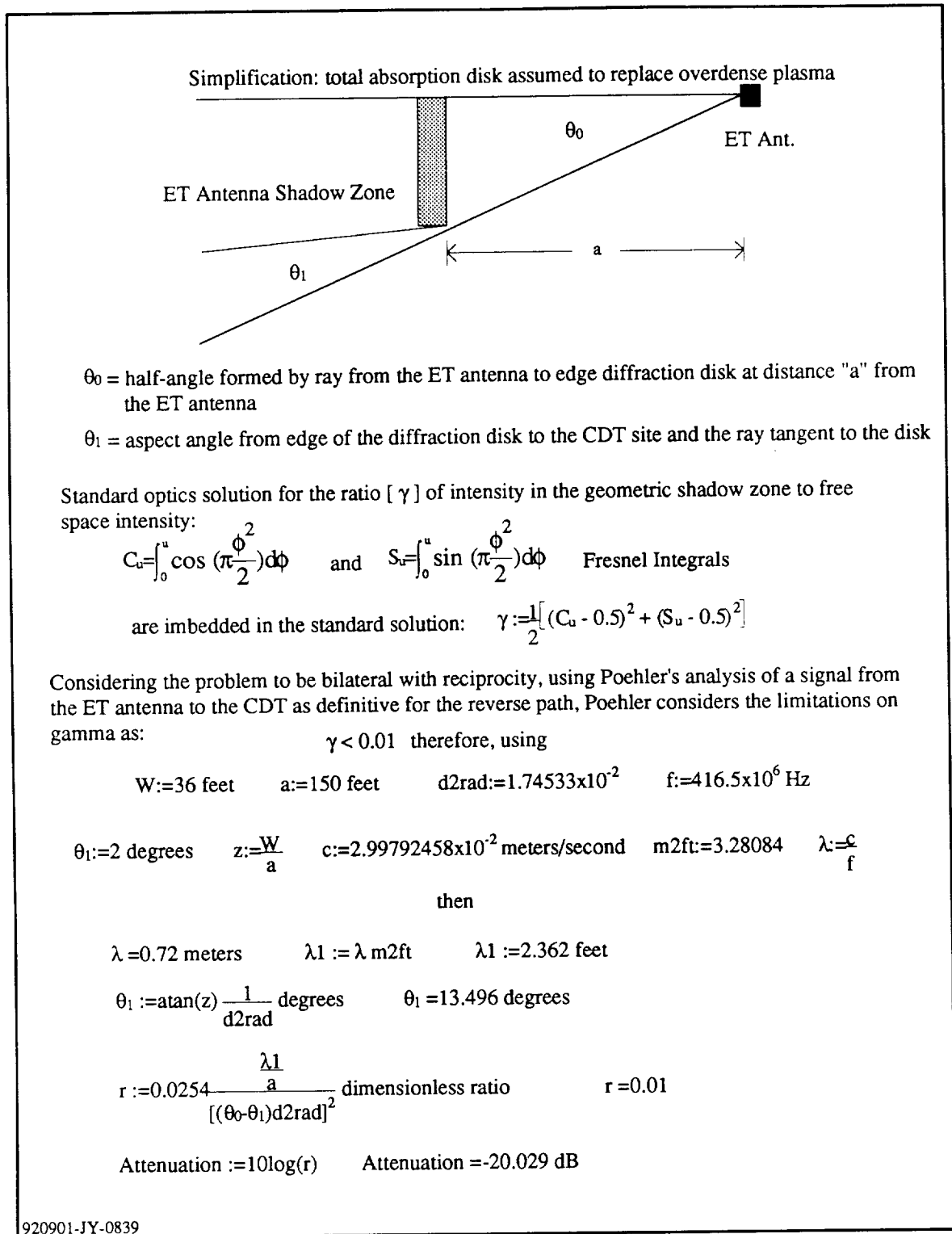


**Exhibit 4-5 Calculation of Signal Strength Attenuation in the Diffraction Illuminated Zone**

#### 4.6 Line-of-Sight Comparisons

SRS developed the plots in Exhibit 4-6 to aid in visualizing the line-of-sight range between the Shuttle and the visual horizon at selected points during the fly-out of the vehicle. The trajectory of STS-43 was chosen as adequately illustrative for this exercise, and vehicle sub-points at 60, 121, 300, and 450 seconds time-of-flight (TOF) were used to develop essentially orthographic projections which were then limited in extent to the line-of-sight range from the vehicle to the horizon, based on vehicle altitudes at the respective times. The last chart was developed using the 121 second TOF sub-point, but arbitrarily forcing the vehicle altitude to 150 NM to show the line-of-sight capability from an orbital altitude. Corrections for refraction were not included as the charts are intended only as an aid in visualizing the vehicles capability to “see” selected ground stations at the various altitudes.

The sub-point of the present position of the vehicle at the annotated TOF is represented by a small square at the center of each chart. In addition, the locations of the Command Control Transmitters (CCT) are annotated as follows:

CCAFS	Cape Canaveral Air Force Station
JDMTA	Jonathan Dickinson Missile Tracking Annex
WFF	Wallops Flight Facility (Wallops Island Flight Center)
BDA	Bermuda

Of particular note is the not-intuitive realization that the CCT at Wallops Flight Facility comes into visual range of the Shuttle prior to the CCT located at Bermuda. The charts may also be used to observe the relative aspect angles between the CCT sites and position of the Shuttle at the various points portrayed.



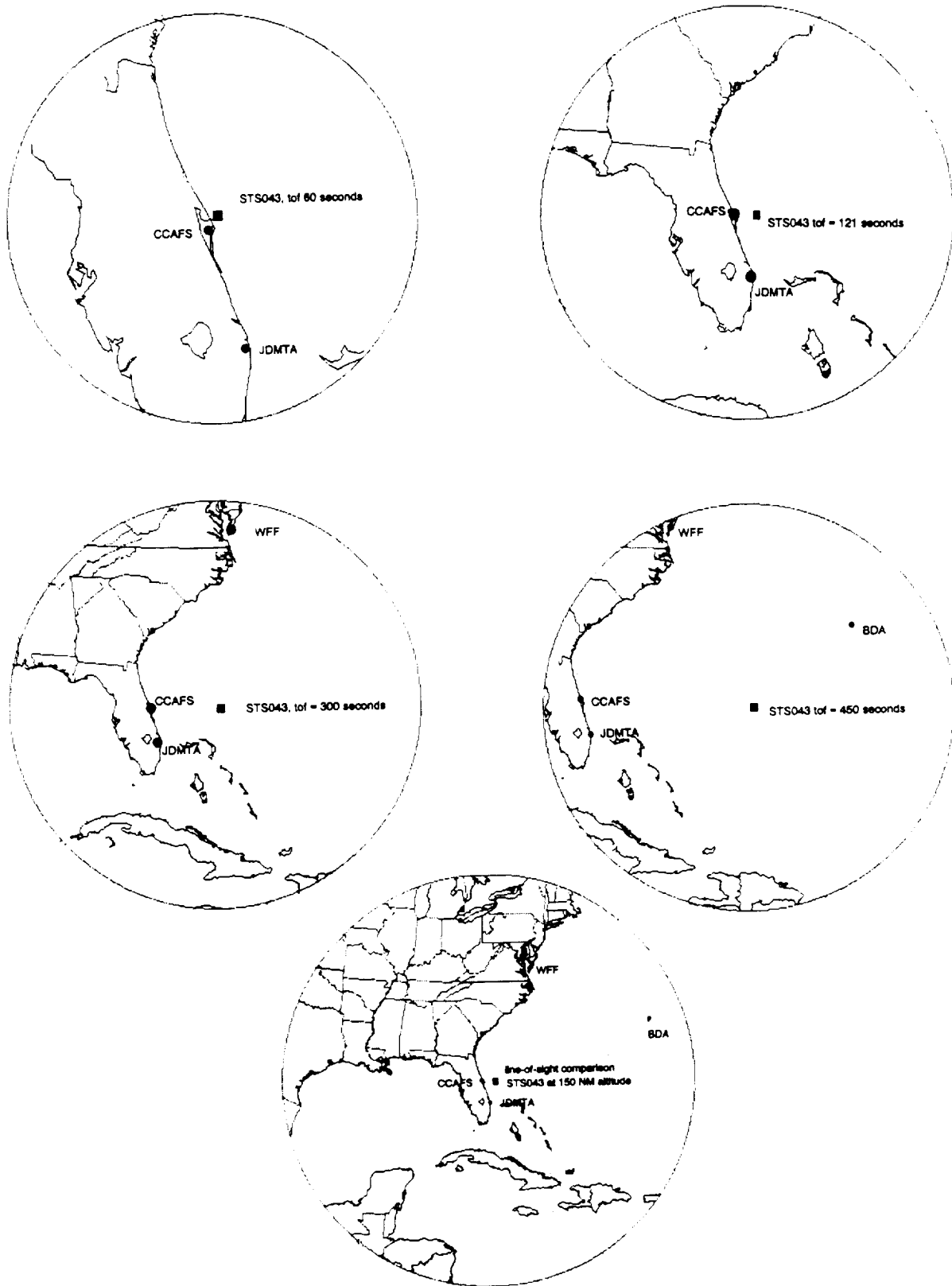


**Exhibit 4-6 Line-of-Sight Range Between the Shuttle and the Visual Horizon at Selected Points During Fly-Out**

## SECTION 5 CONCLUSIONS

Following are findings of the IRD Dropout study:

- Deep IRD signal fades of extended duration occur when the signal arrives at the Shuttle from almost directly astern of the Shuttle (within approx 5 degrees).
- Direct line of sight paths do not always exist to either ET antenna in the UHF range when the signal arrives from astern. In this case blockage is caused by the orbiter body, orbiter wings, and ET body.
- Because the Shuttle surfaces are predominantly parallel to the longitudinal axis, the paths of signals arriving have small incidence angles to the surfaces, below the Brewster angle, so that direct and reflected signals can be in phase or out of phase in both polarizations at the antenna.
- When geometric line-of-sight does not exist, signals must arrive at the ET antenna(s) by reflection as above, by surface waves ducted along the ET skin, or by diffraction around Shuttle surfaces (a possible alternative is diffraction through the exhaust plume).
- The measured scale model antenna patterns do not contain the nulls at aft angles of arrival that appear in flight test data and in our predictions from analysis. Two possible reasons are:
  - A phenomena not related to the antenna/Shuttle configuration affects the signal.
  - The measured antenna patterns are not accurate for aft angles of arrival, and/or the 2-degree-resolution is not fine enough to model the situation.
- From discussions with NASA personnel who observed the original scale-model antenna pattern measurements, we learned that the purpose of measuring the antenna patterns was to measure and verify that the antennas had adequate gain over 95 percent of the sphere. This was an Air Force 127-1 requirement that had to be verified. The test model and procedures were set up to specifically verify 95 percent coverage, not to measure where

and how deep interference nulls were in the nose and tail area. NASA and the Air Force have approved these test procedures and test results. It may be advisable, in the future, to extend antenna tests to better characterize pattern nulls but this would require different procedures, higher fidelity test models, and extended test equipment capabilities.

- The two ET range safety antennas are connected to the IRD RF front end through RF cables and an RF combiner. That method can possibly permit destructive interference in cases where RF energy can reach both antennas from a given direction. (RF interferometers use this principle to measure direction of arrival in electronic warfare and radio-astronomy applications.) Combining RF inputs from multiple antennas is often accomplished through the use of diversity combiners, which switch antennas, use phase-locked loops to merge signals at IF, or select data at baseband. The dual IRD scheme used for SRB range safety reception accomplishes diversity combining at baseband.
- Certain other signal fading phenomena we modeled appear to occur at times in the flight data (for instance, sea-surface multipath at low look angles), but the effects are not of large magnitude or long duration, and they do not appear to cause the deep, extended signal fades that are the primary objects under investigation.

## SECTION 6.0

### APPLICATION OF METHODOLOGY TO FUTURE FLIGHTS

The methodology used for this study can be applied to evaluation of IRD dropout phenomena on future Shuttle flights. Analytic portions of the recommended evaluation can be accomplished directly from review of the Shuttle trajectory/attitude data and IRD AGC data. Simulation portions will require use of the simulation/analysis software SRS used in the study.

Given the conclusions presented in the previous section, an objective of evaluating future flight data may be to determine whether observed fades are associated with signal arrival angles directly aft of the Shuttle. Shuttle yaw attitude and position can be extracted and plotted manually, with time tags, as vectors on a map. From these plots, the approximate signal arrival angles from transmitter locations on the map can be determined by ray-tracing. The Shuttle position/attitude time tags can then be compared with signal fade times to identify associations between fades and particular Shuttle states.

The RF signal software can be used with pre-mission trajectory data to evaluate the RF entry angles for a planned flight. Although we are unable to accurately predict when the fades may occur, since they appear to be function of a near aft yaw angle and a less predictable roll angle (combination roll and pitch), the approximate time in the flight that these aspect angles occur can be predicted. This time information could be helpful in pre-mission planning for determining when best to switch to an alternate site. However, there are some limitations to when the switch over can occur. From our analysis we observed that, due to the distances between the transmitting sites (Cape, JDMTA, Bermuda, Wallops) and the curvature of the earth, there is little overlap in coverage area. The use of the JDMTA site seems to overcome the near aft aspect angle problem, but the signal overlap area between JDMTA and Bermuda is small. A study is recommended using the RFSignal program and a trajectory generation program to develop an understanding of the aspect angles, site track elevation angles, and coverage areas.

## SECTION 7 RECOMMENDATIONS

Following are recommendations for future experiment and additional analysis:

- To acquire more detailed antenna pattern data for the orbiter/ET configuration, we recommend performance of antenna range tests on a scale model (possibly the model currently stored at the MSFC antenna range). The Shuttle model configuration should represent as accurately as possible the structure viewed (put the support boom on the nose) from astern. Also, the data should be continuous cuts (conical or great-circle) in the neighborhood of the tail, with close spacing (e.g., less than 1/2 degree) between cuts. SRS will support these measurements, facilitate logging/storage of data, perform data reduction, and analyze the results with regard to the dropout phenomenon.
- To better characterize the potential role of the ET RF combiner in received signal dropouts, we recommend laboratory testing of ET range safety RF and IRD hardware in a configuration representing that of flight hardware. The tests will include static and dynamic RF phase and amplitude input variations from dual signal sources simulating various angles of arrival at ET antennas. SRS will perform the recommended tests in our Huntsville laboratory if MSFC desires. Alternatively, we can support testing at MSFC, in which case we will facilitate logging/storage of data, perform data reduction, and analyze the results.
- To provide analytical support for the experiments identified above, we recommend construction of a computer model of relevant features of the orbiter/ET configuration (e.g., plane and knife-edge representation of the wing and vertical stabilizer; cylinder representation of the ET). We will use multiple-ray or wave-theory RF propagation analysis algorithms with the computer model to determine theoretical relative signal levels and phases at the range safety antenna output ports in the presence of reflections and diffraction from the Shuttle surfaces.

## REFERENCES

1. Blaine E. Pearce, "Range Safety Signal Attenuation by the Space Shuttle Main Engine Exhaust Plumes", ARAP Report No. 494, 19 April 1983
2. Malcolm W. McDonald, "An Investigation of Pre-Launch and In-Flight STS Range Safety Radio Signal Degradation and Dropout", The University of Alabama at Huntsville, Contract No. NGT-01-008-021, 15 February 1991.
3. Jacob P. Digulla, "Eastern Space and Missile Center Instrumentation Handbook for the Eastern Test Range", Report No. ESMC-TR-83-03, 15 February 1984.
4. G. Sandhu, E. Kells, and John E. Dickson, Jr., "Rocket Plume Effects Report," SRS Technologies Report No. TR87-016, 1 December 1986.
5. H.A. Poehler, "Rocket Exhaust Attenuation and Degradation Final Report," Pan American World Airways, Aerospace Services Division, 1969.
6. John Griffiths, Radio Wave Propagation and Antennas, Prentice-Hall International, London, 1987.
7. David F. deWolfe and Robert E. Salter, "Propagation Characteristics and System Parameters for Design of Microwave Links for Airborne and Surface Terminals", Electronic Communications, Inc. Report No. 1-SER-68-7346, 15 October 1968.
8. Arvids Vigants, "Space Diversity Engineering," Bell System Technical Journal, Vol 54, No. 1, January 1975.
9. Kenneth Davies, Ionospheric Radio Propagation, National Bureau of Standards Monograph 80, U.S. Government Printing Office, 1 April 1965.
10. R.K. Crane, "Spectra of Ionospheric Scintillation", Journal of Geophysical Research, Vol. 81, No. 13, 1 May 1976.
11. Contract NAS8-39077, Attachment J-2, George C. Marshall Space Flight Center, NASA
12. Eastern Space and Missile Center Instrumentation Handbook for the Eastern Test Range, ESMC-TR-88-02, 8 May 1989.
13. 45th Space Wing Geometric Coordinates Manual, January 1992, United States Air Force Eastern Range, Patrick Air Force Base, Florida

**APPENDICES**

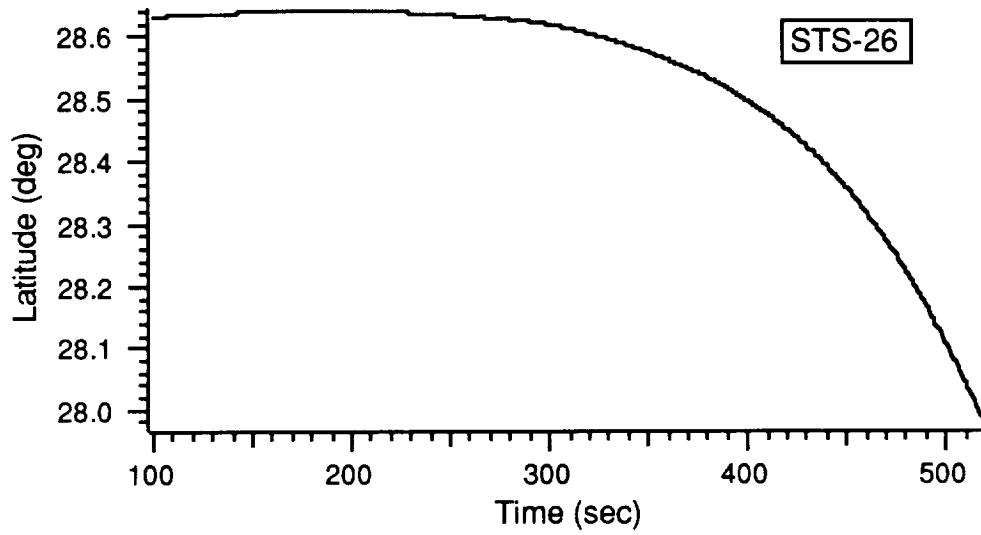
## PREFACE TO THE APPENDICES

The following pages are a series of plots describing the trajectory and signal data for the flight. The trajectory data was downloaded from the NASA database and was used in this analysis. The signal strength data was also downloaded from the NASA database and was plotted on the same timebase as other analysis plots to provide an easier time comparison. Other plots are the products of the computer model used for analysis. The antenna pattern data was provided by NASA personnel on magnetic disk. The antenna pattern tracks are hand drawn to show the antenna cells used and reflect the data shown on other plots.

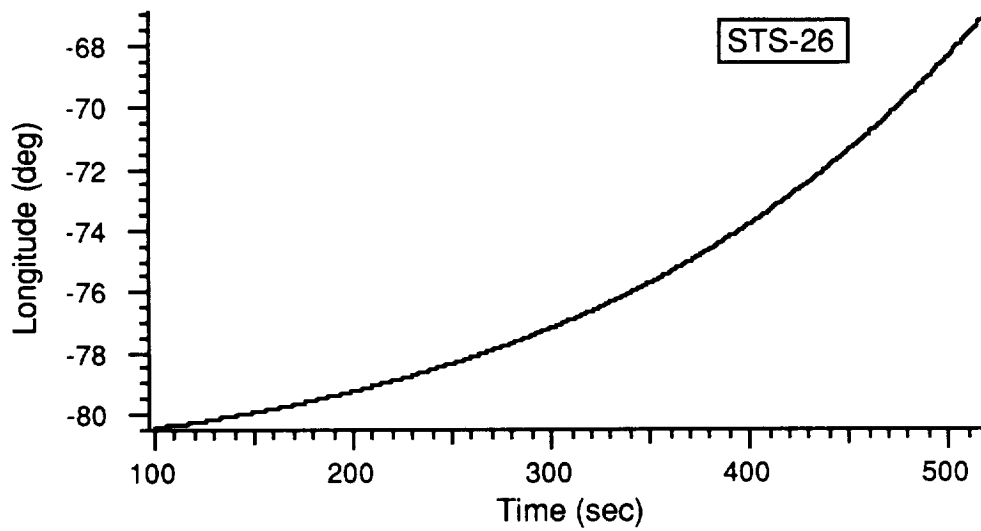


STS-26  
Appendix

STS-26 was a flight launched in an easterly direction. Moderate fading during the time interval from 370 to 390 seconds after launch, and a short, deep fade at 417 to 418 seconds after launch were noted. These fades occurred when the signal arrival angle was less than  $5^\circ$  from directly aft.

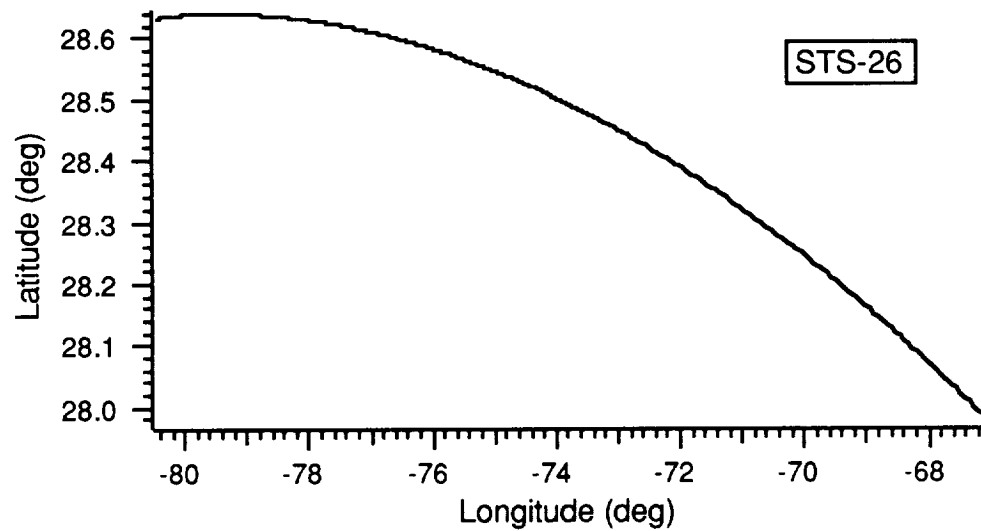


a. Latitude vs. Time

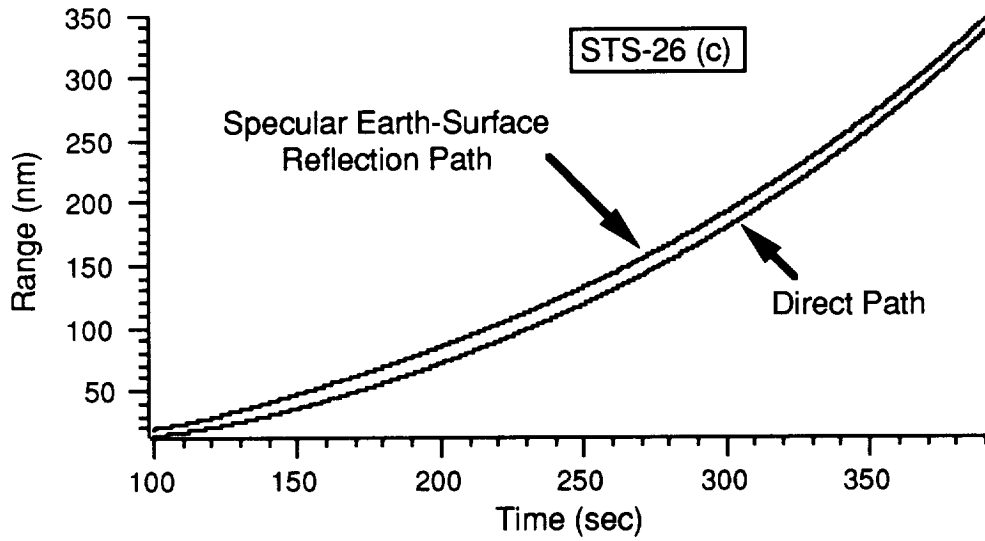


b. Longitude vs. Time

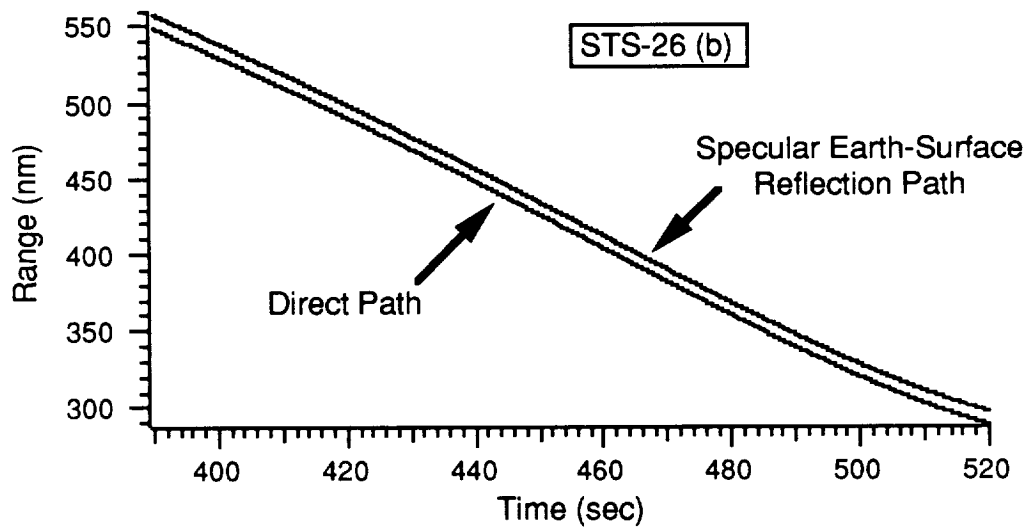
**Plots of Latitude (a.) and Longitude (b.)vs. Time After Launch**



**Ground Trace of Shuttle Trajectory**

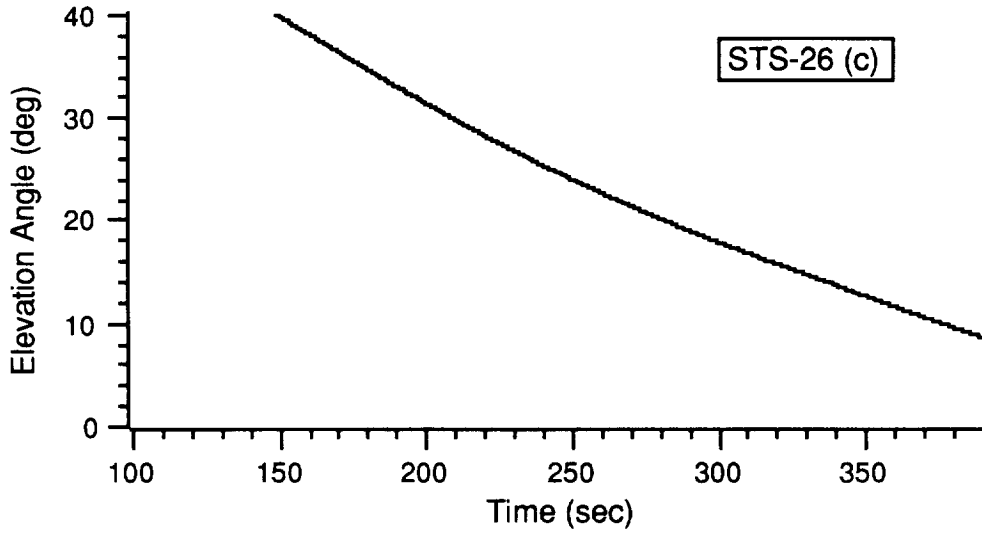


a. Transmission From Cape Canaveral

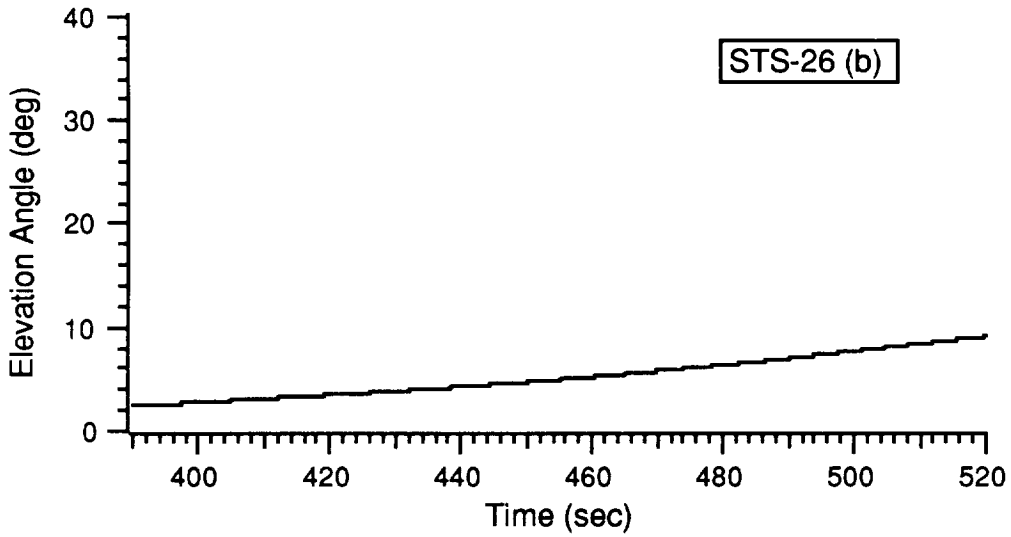


b. Transmission From Bermuda

**Range From Transmitter Site to Shuttle vs. Time After Launch**

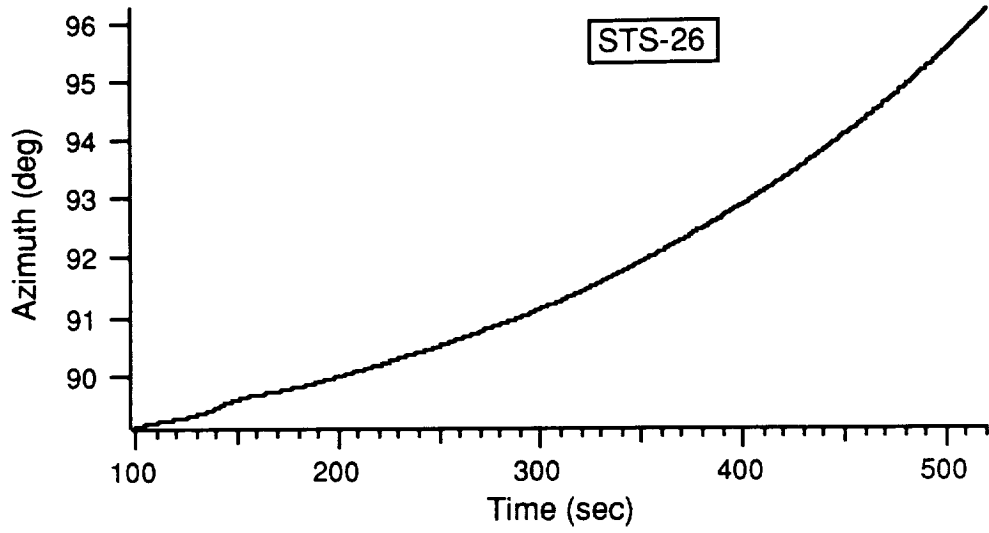


a. Transmission From Cape Canaveral

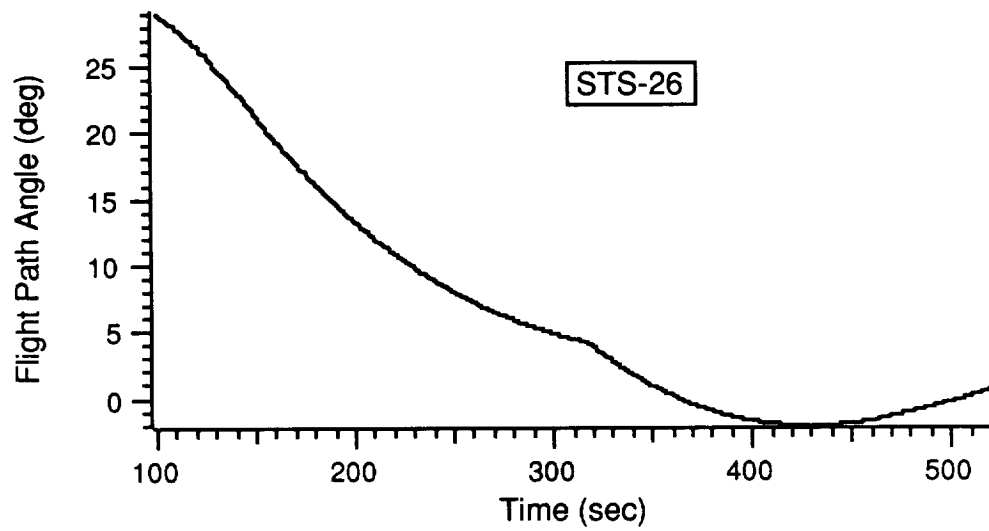


b. Transmission From Bermuda

**Elevation Angle (Transmitting Site to Shuttle) vs. Time After Launch**

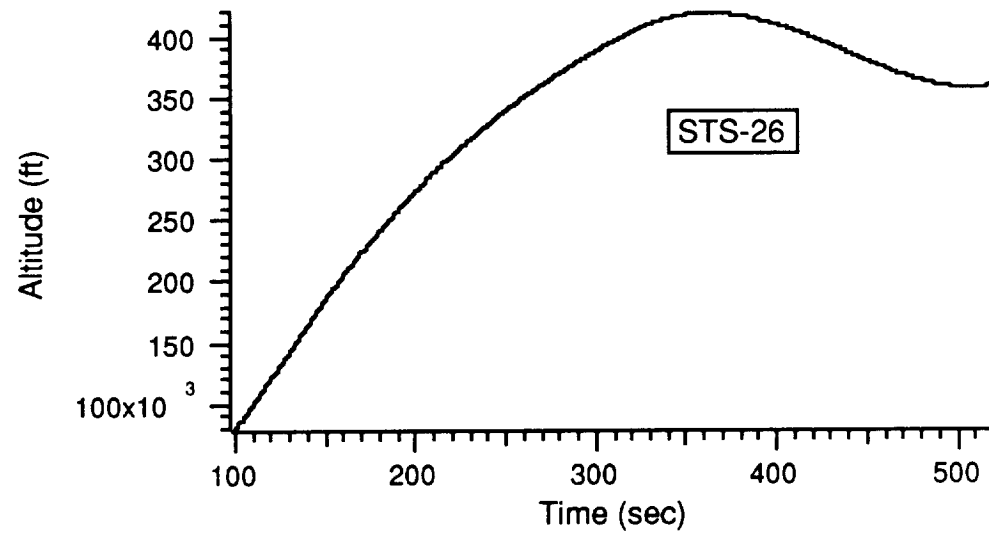


a. Horizontal

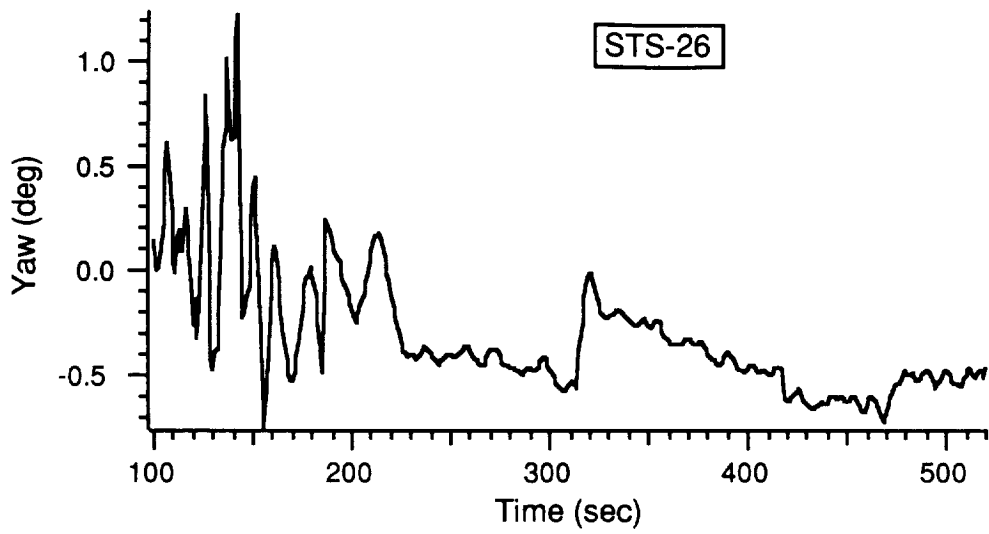


b. Vertical

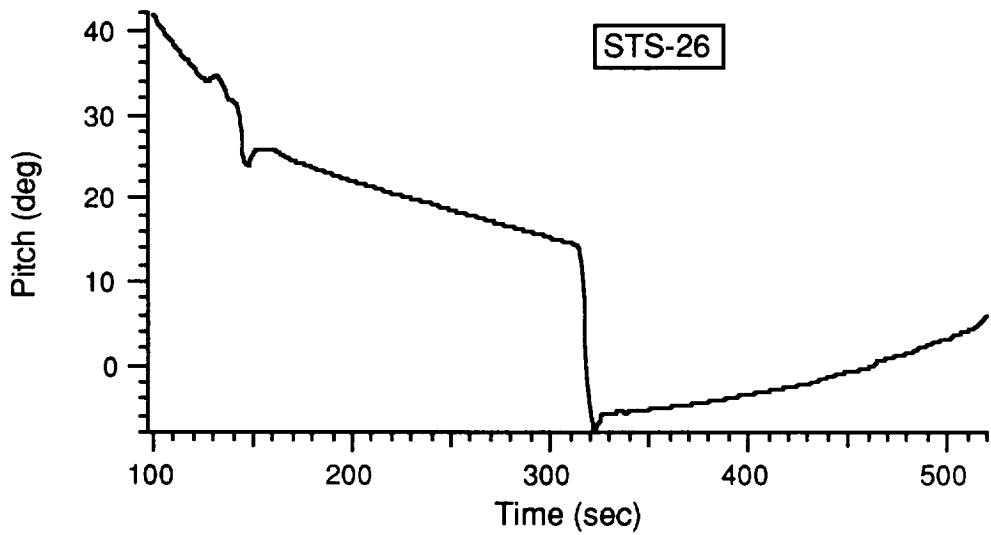
**Shuttle Flight Path Angles vs. Time After Launch**



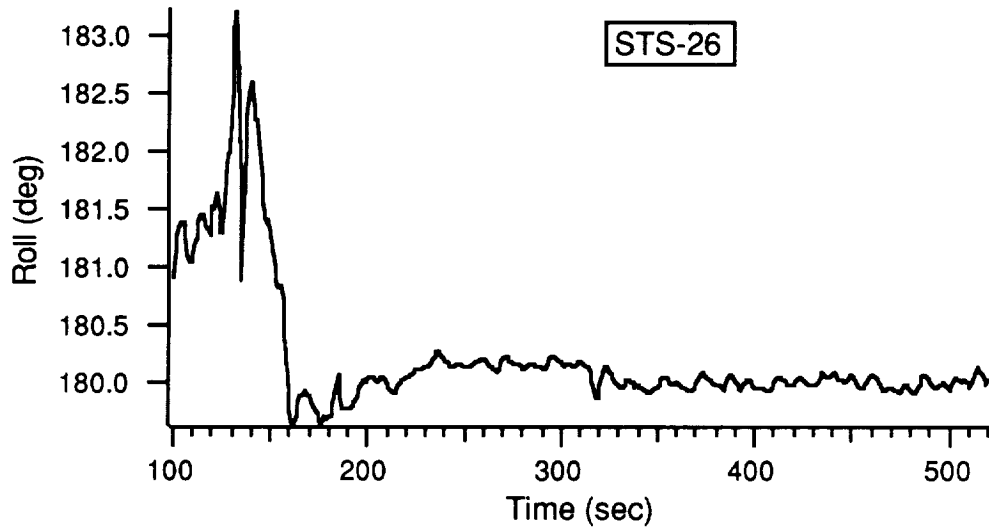
**Shuttle Altitude vs. Time After Launch**



a. Yaw Attitude

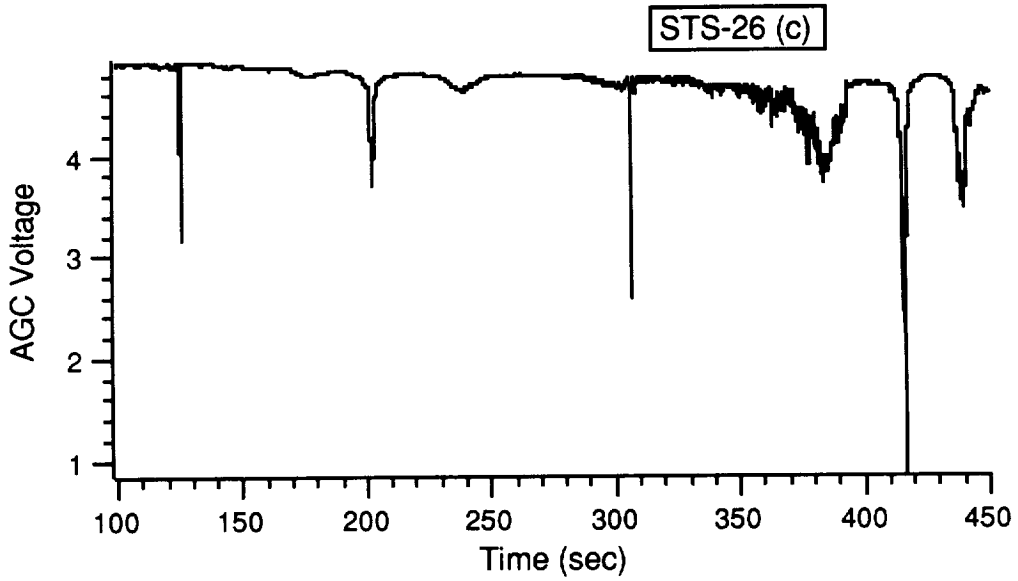


b. Pitch Attitude

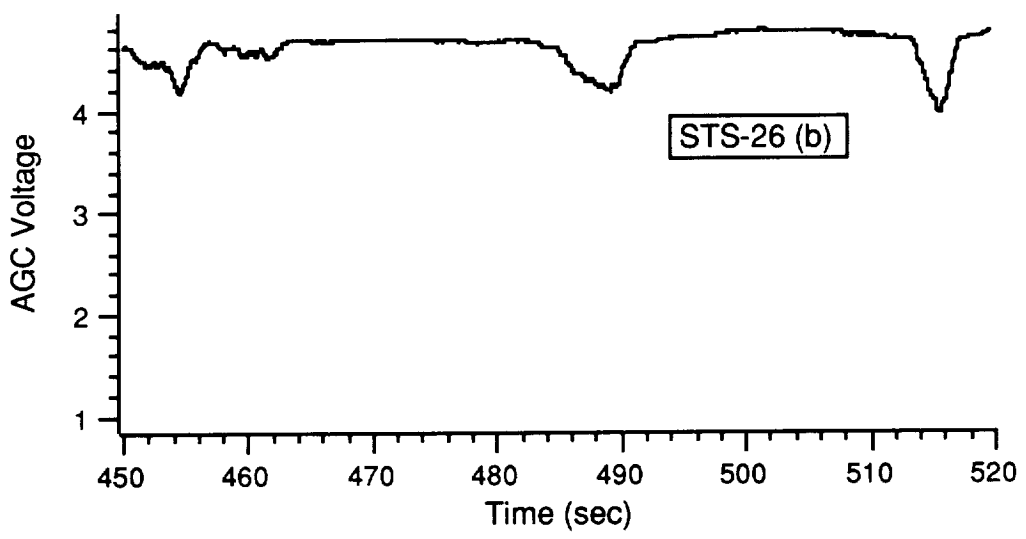


c. Roll Attitude

**Shuttle Attitude Angles (With Respect to Velocity Vector) vs. Time After Launch**

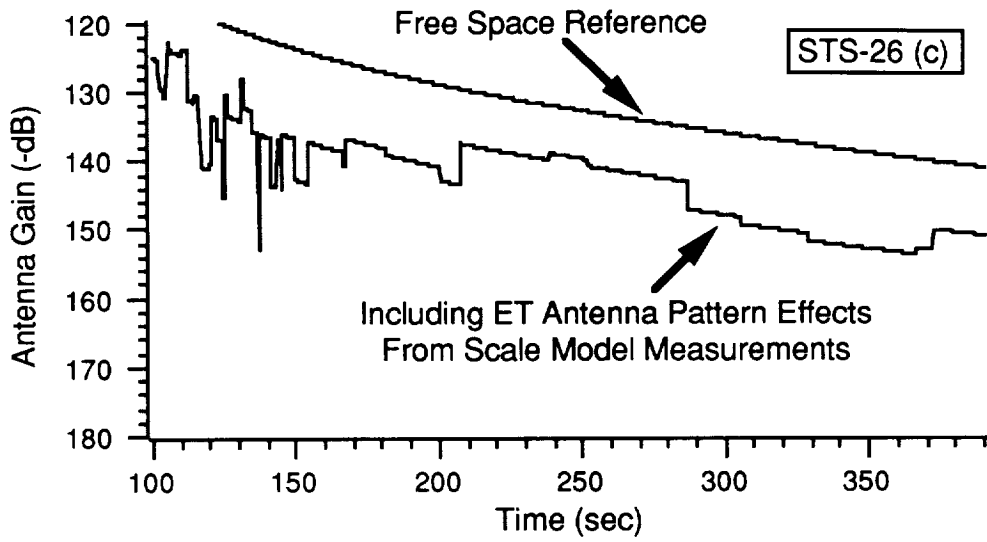


a. Transmission From Cape Canaveral

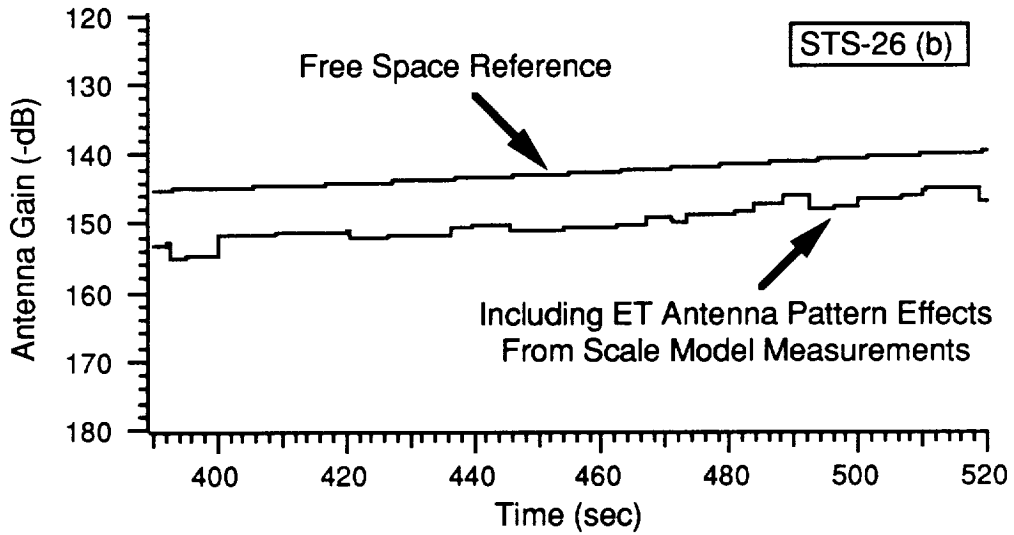


b. Transmission From Bermuda

**Record of ET Receiver AGC Voltage vs. Time After Launch**



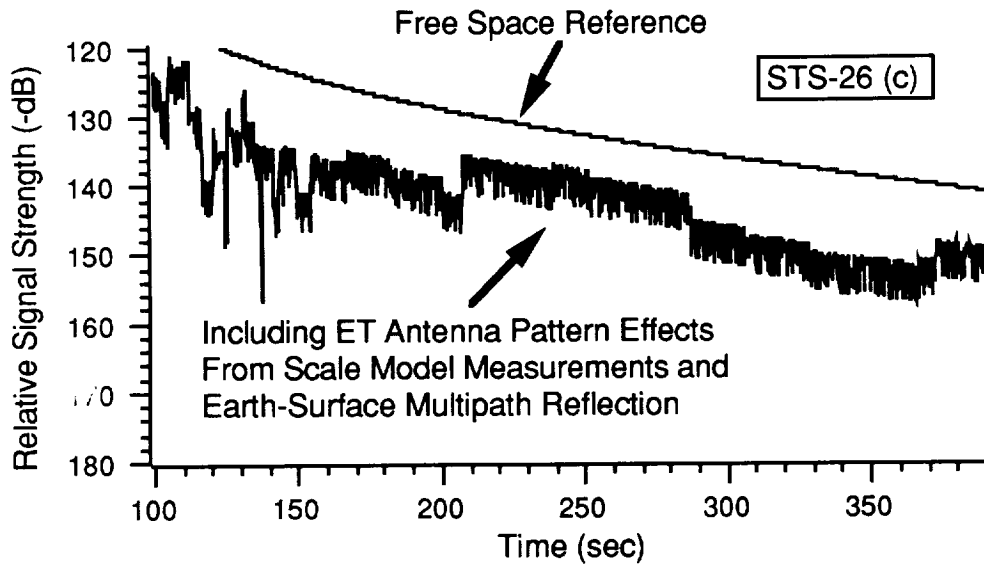
a. Transmission From Cape Canaveral



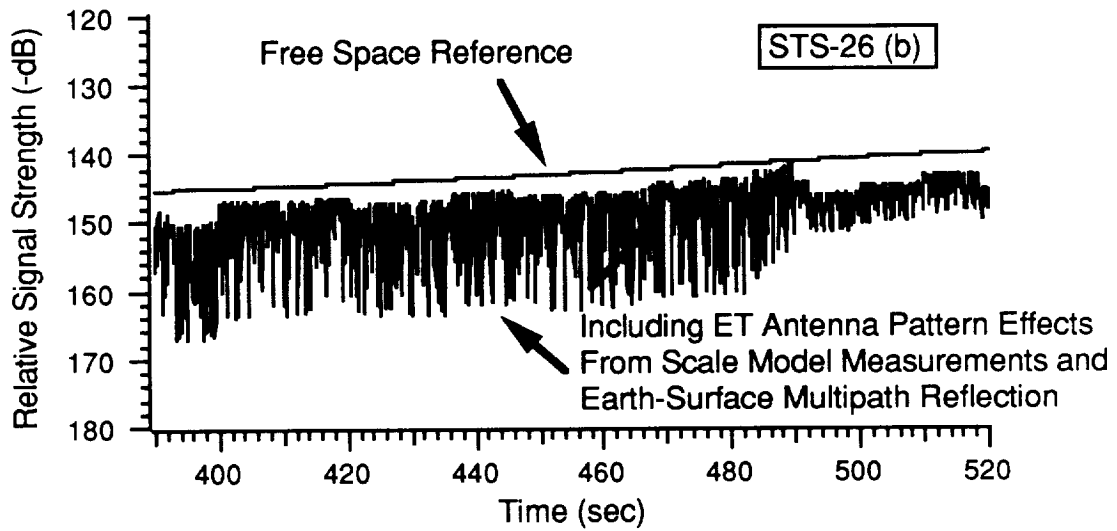
b. Transmission From Bermuda

**Computer Simulation of Relative Signal Strength at ET Receiver vs. Time After Launch (Without Earth-Surface Multipath Reflection)**





a. Transmission From Cape Canaveral



b. Transmission From Bermuda

**Computer Simulation of Relative Signal Strength at ET Receiver vs. Time After Launch (Including Earth-Surface Multipath Reflection)**

Yaw Degrees

20

40

60

80

100

120

140

160

20

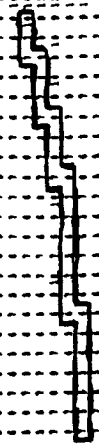
60

100

140

FOLDOUT FRAME

Locus of A



180  
140  
100  
60  
20  
Roll Degrees

STS-26 (Bermuda)

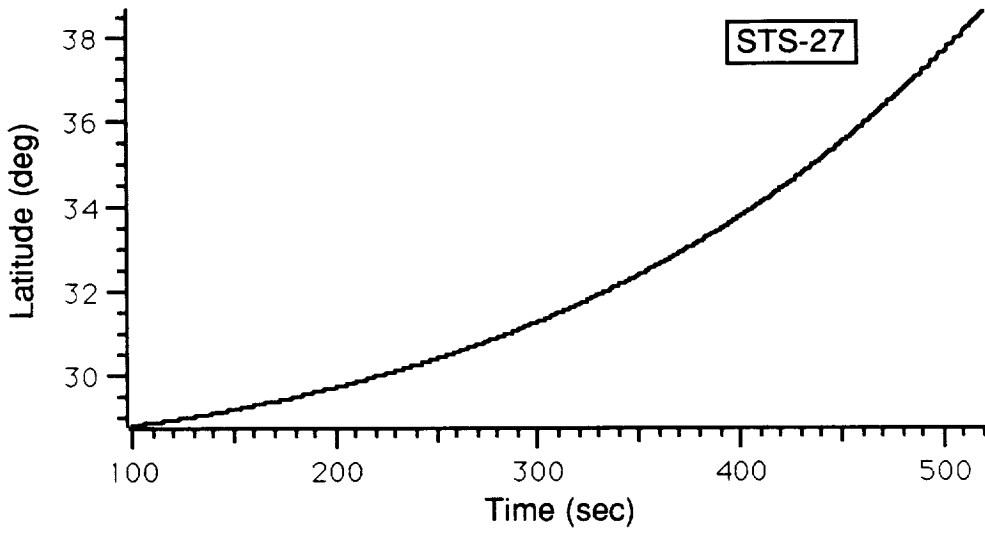
Angles of Arrival on ET Antenna Pattern

FOLDCUT FRAME

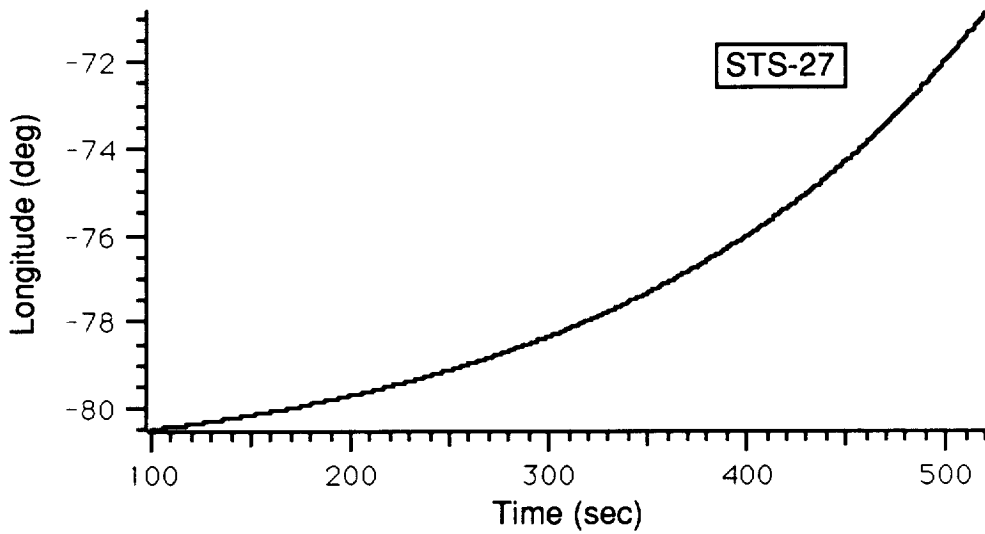
2

STS-27  
Appendix

STS-27 was launched on a more northeasterly launch azimuth (approximately  $57^\circ$ ). The signal strength shows a gradual deterioration of the signal from approximately  $10^\circ$  away from directly aft to  $5^\circ$  when the switch was made to the Bermuda transmitter. The signal strength appears to deteriorate more rapidly between  $5^\circ$  and  $6^\circ$  away from directly aft. The aspect angle on this flight did not drop below  $4^\circ$ .

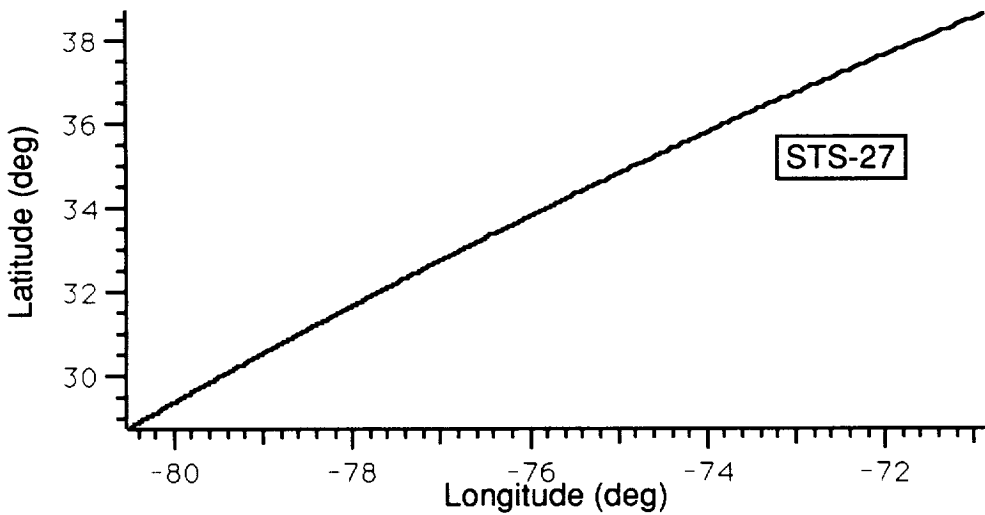


a. Latitude vs. Time

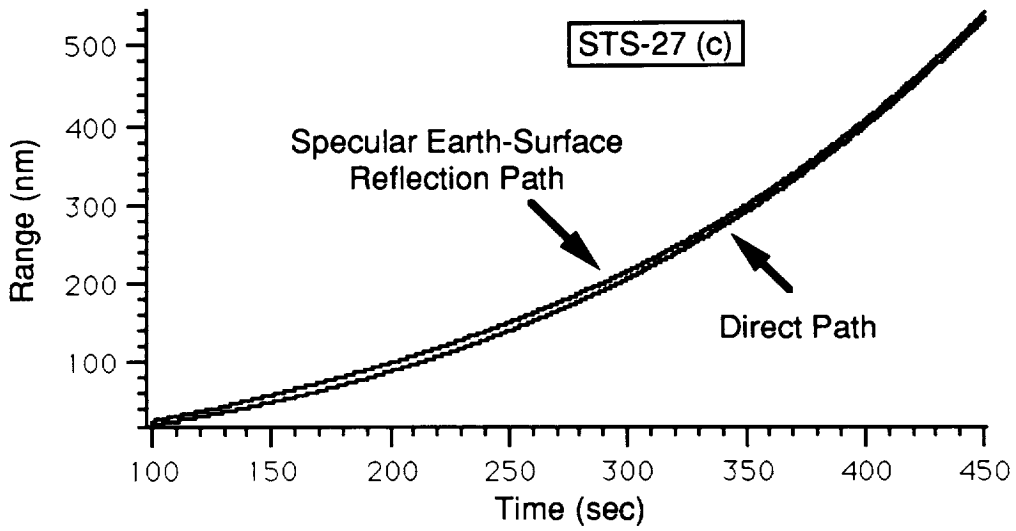


b. Longitude vs. Time

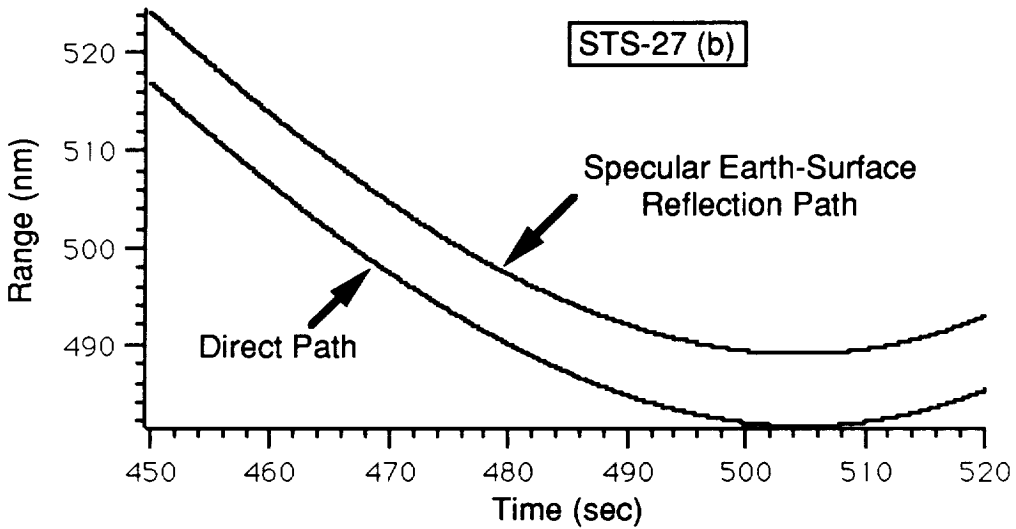
**Plots of Latitude (a.) and Longitude (b.) vs. Time After Launch**



**Ground Trace of Shuttle Trajectory**

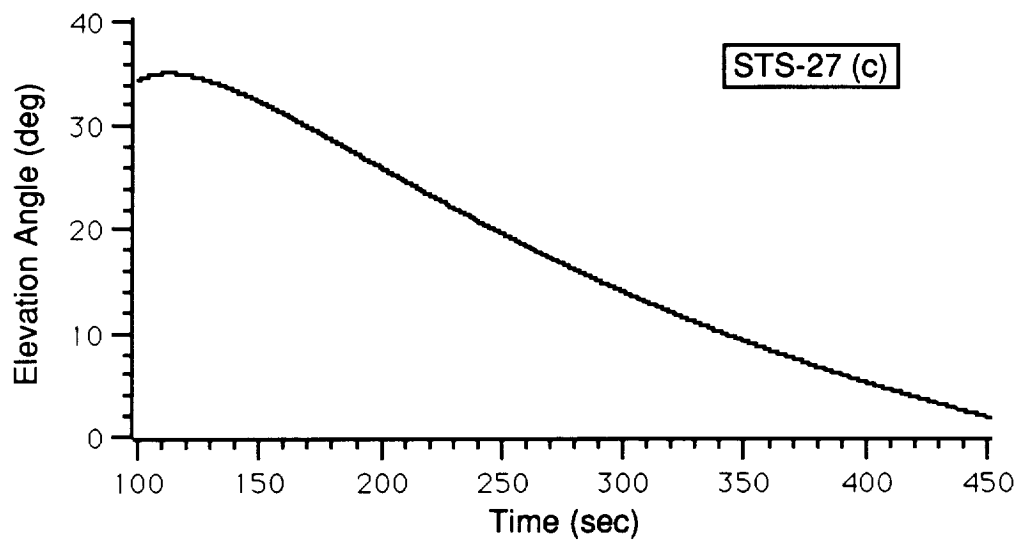


a. Transmission From Cape Canaveral

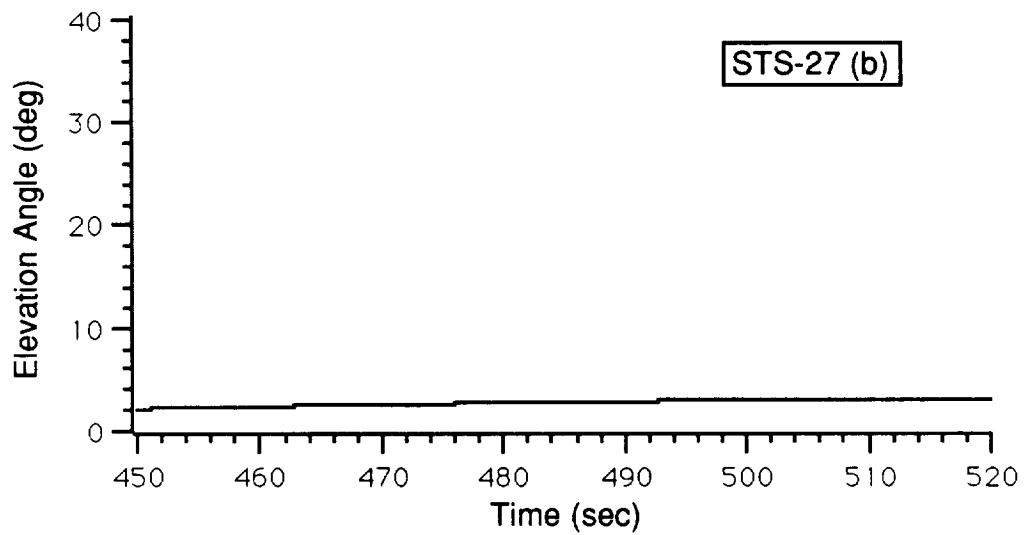


b. Transmission From Bermuda

**Range From Transmitter Site to Shuttle vs. Time After Launch**

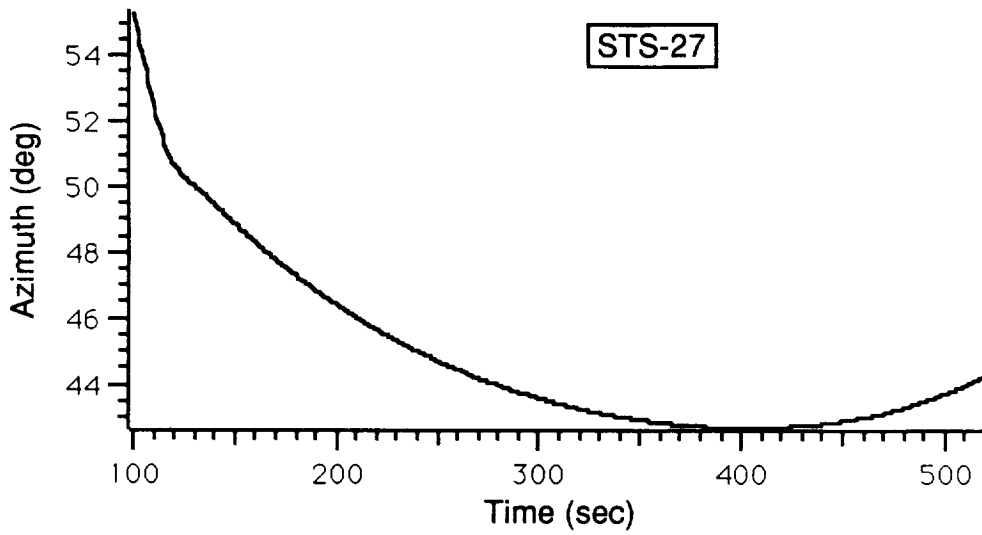


a. Transmission From Cape Canaveral

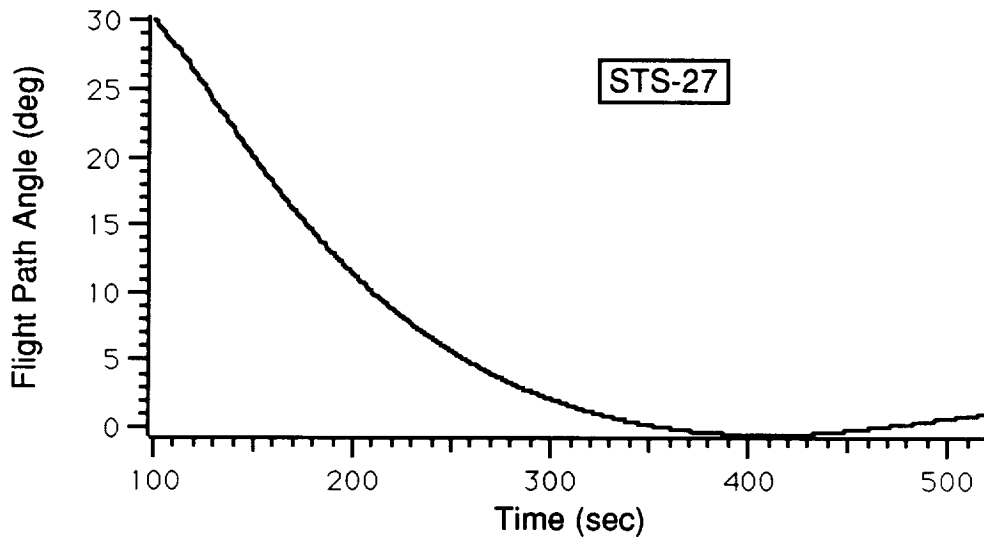


b. Transmission From Bermuda

**Elevation Angle (Transmitting Site to Shuttle) vs. Time After Launch**

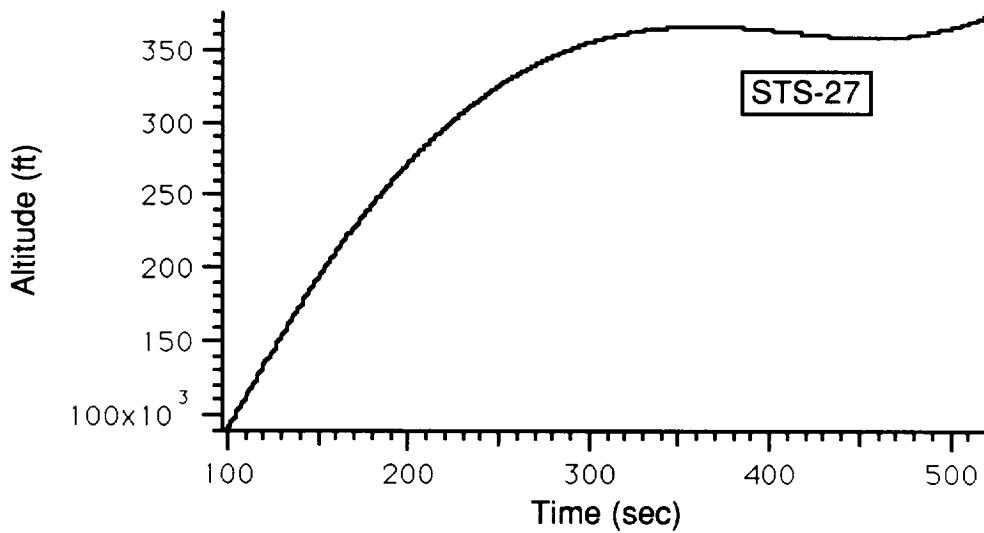


a. Horizontal



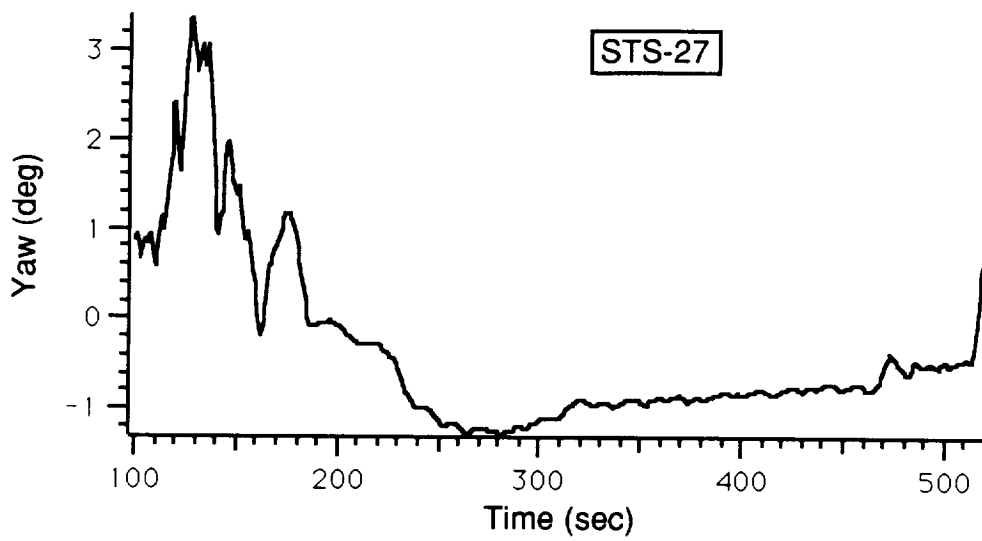
b. Vertical

**Shuttle Flight Path Angles vs. Time After Launch**

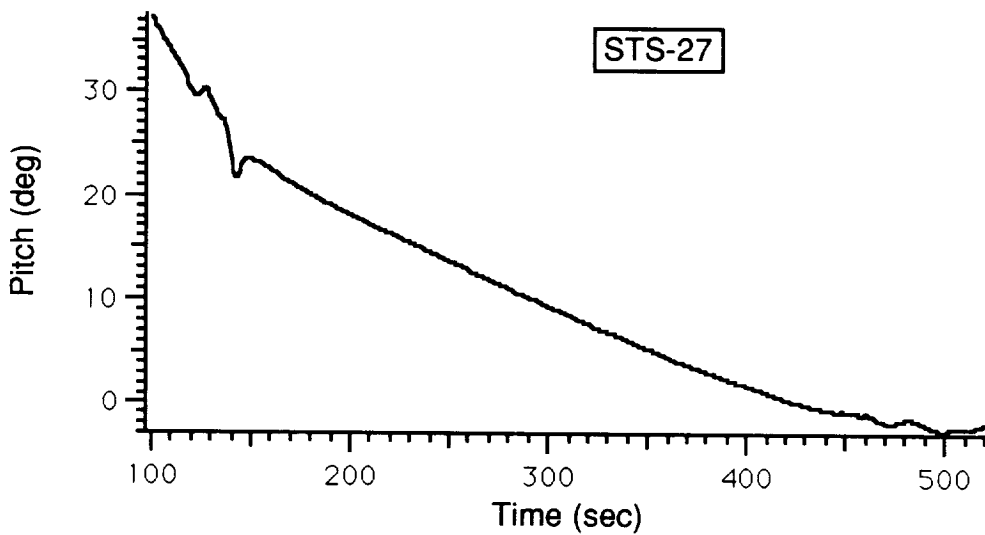


**Shuttle Altitude vs. Time After Launch**

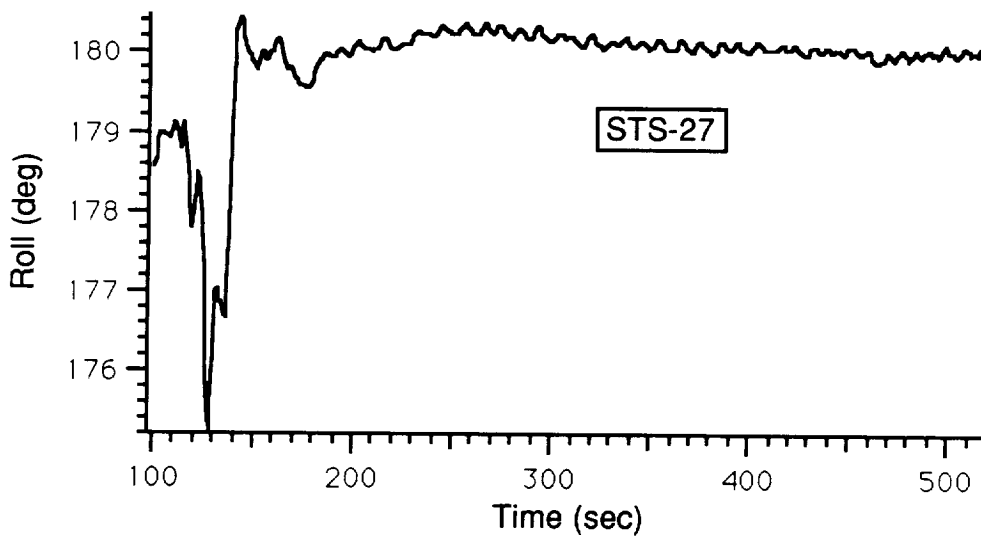




a. Yaw Attitude

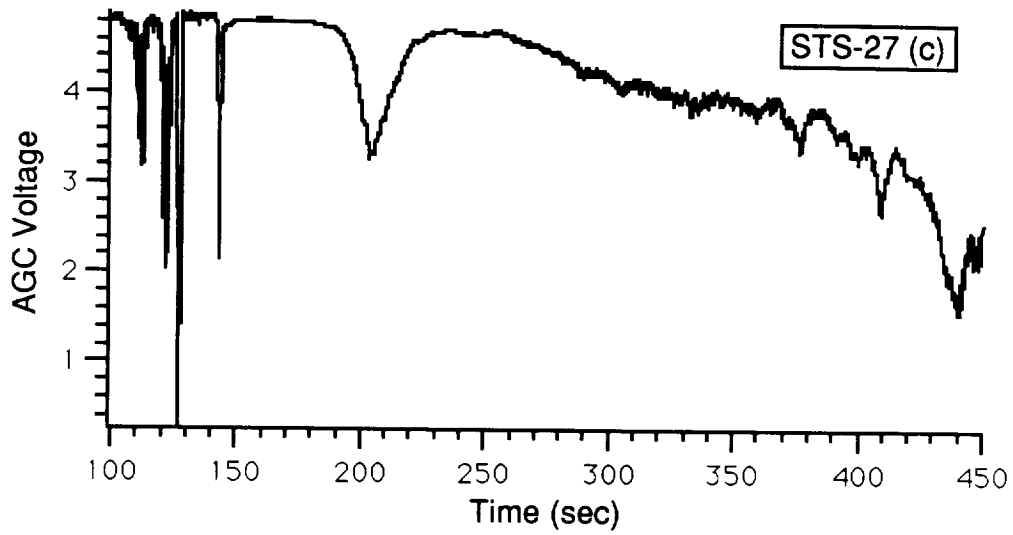


b. Pitch Attitude

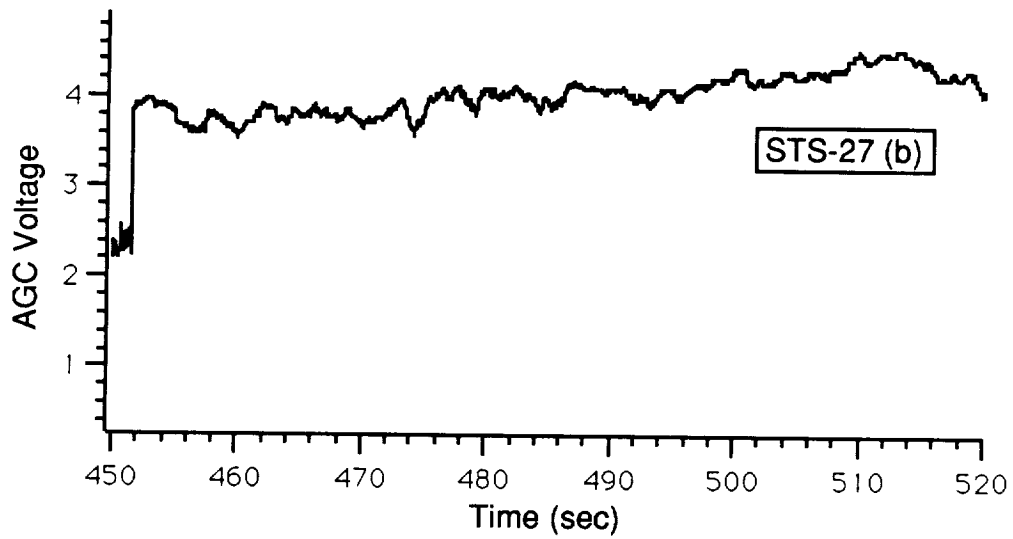


c. Roll Attitude

**Shuttle Attitude Angles (With Respect to Velocity Vector) vs. Time After Launch**

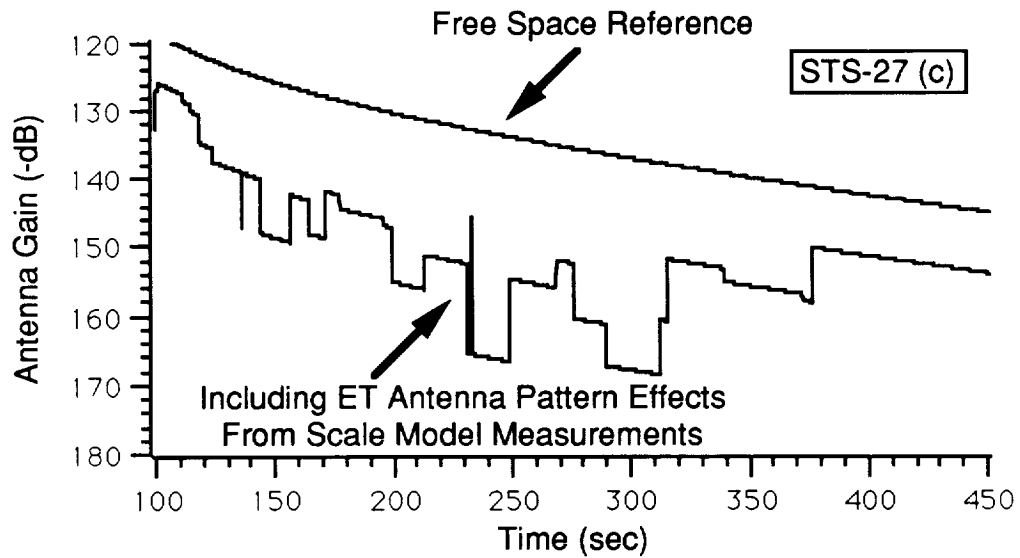


a. Transmission From Cape Canaveral

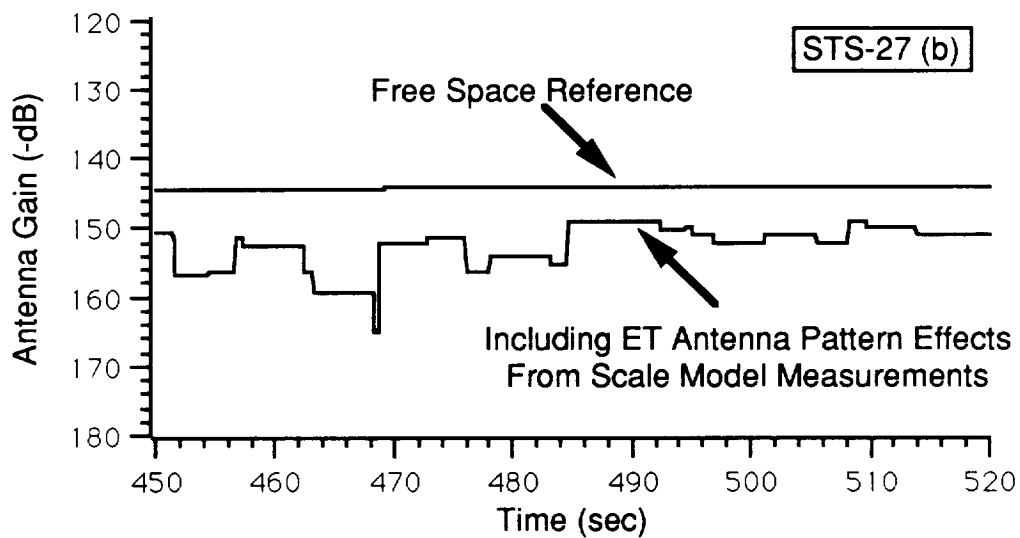


b. Transmission From Bermuda

**Record of ET Receiver AGC Voltage vs. Time After Launch**

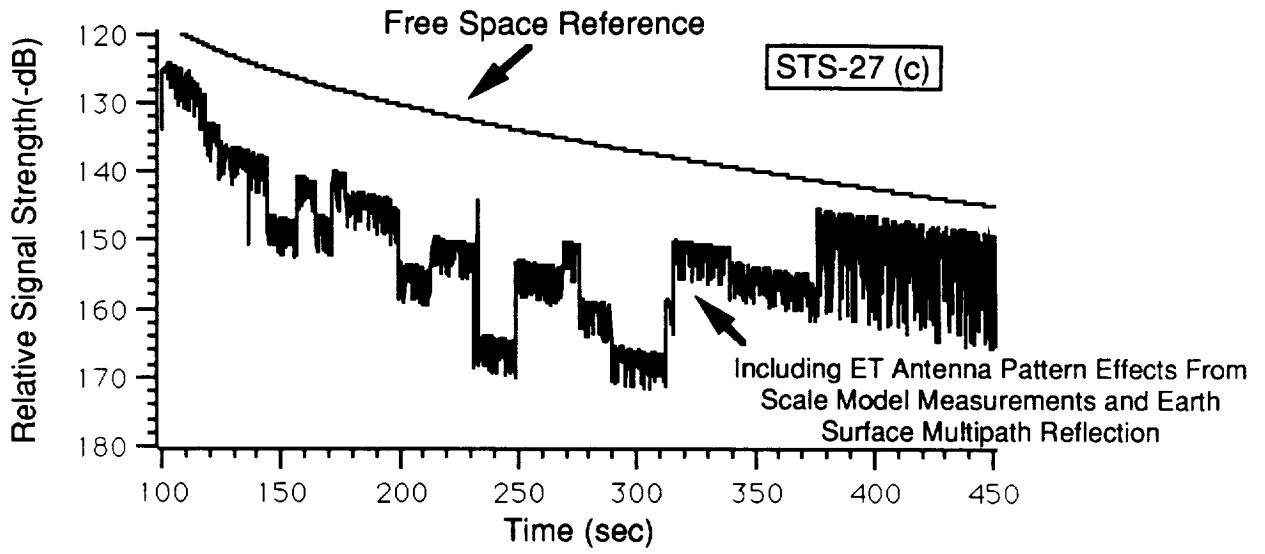


a. Transmission From Cape Canaveral

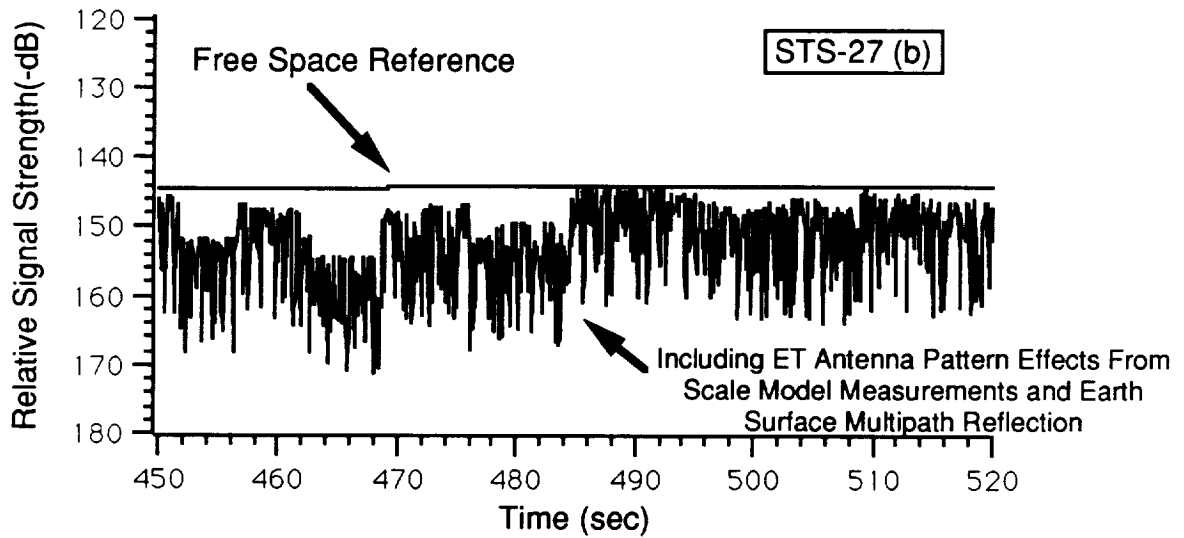


b. Transmission From Bermuda

**Computer Simulation of Relative Signal Strength at ET Receiver vs. Time After Launch  
(Without Earth-Surface Multipath Reflection)**

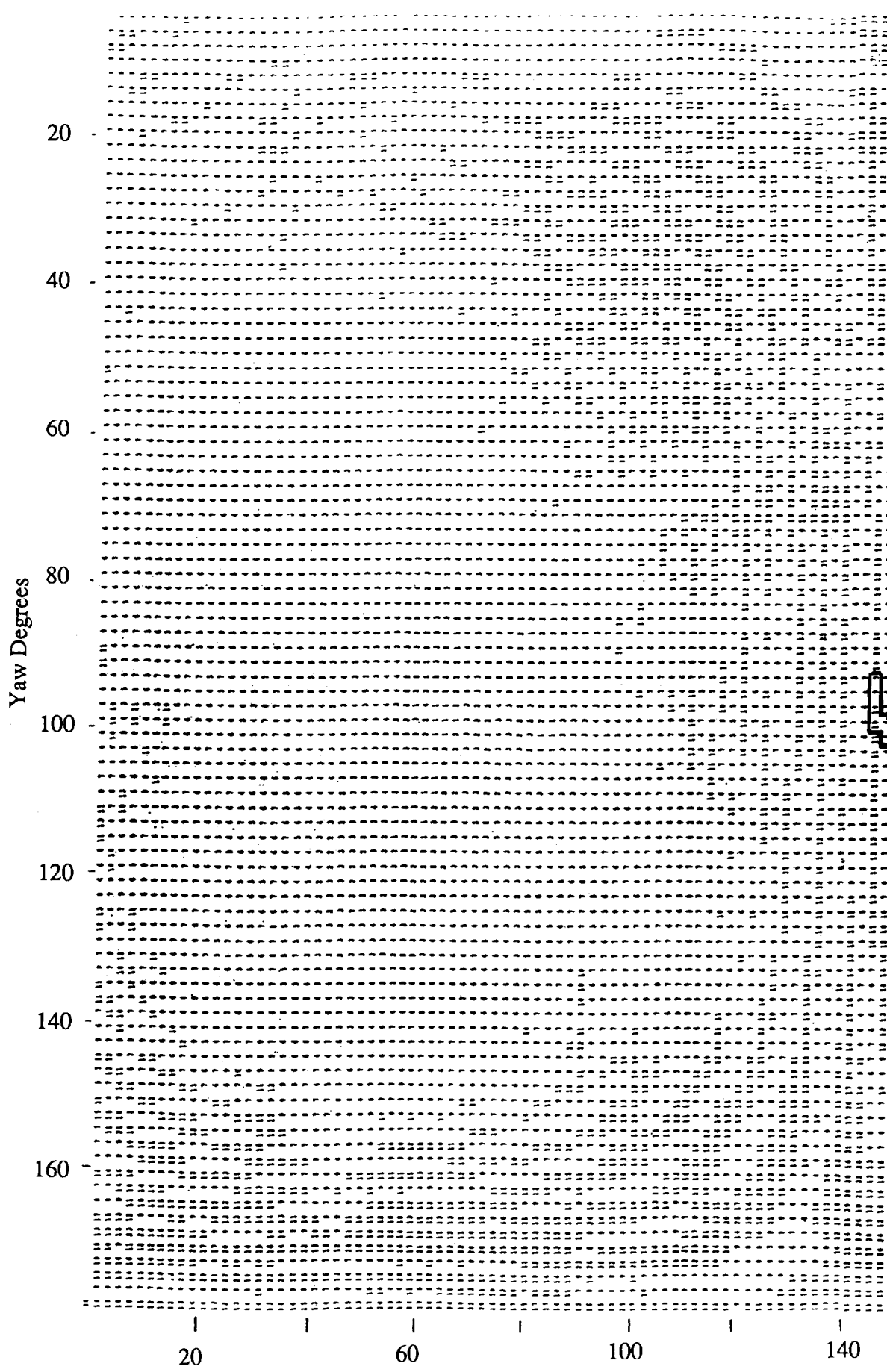


a. Transmission From Cape Canaveral



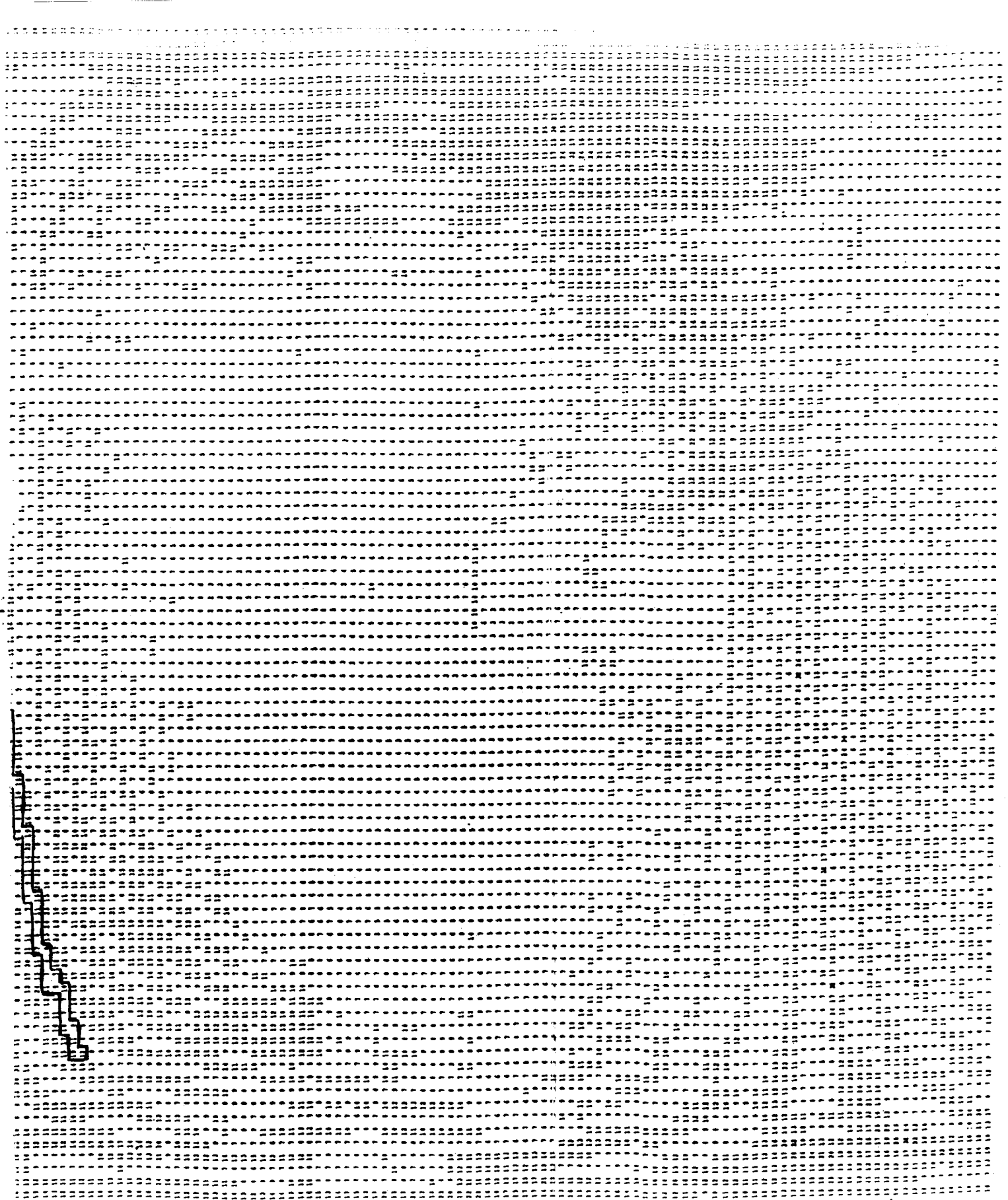
b. Transmission From Bermuda

**Computer Simulation of Relative Signal Strength at ET Receiver vs. Time After Launch  
(Including Earth-Surface Multipath Reflection)**



FOLDOUT FRAME /

Locus of Ang



180  
Roll Degrees

140

100

60

20

STS-27 (Cape Canaveral)

es of Arrival on ET Antenna Pattern

FOLDOUT FRAME 2

Yaw Degrees

20  
40  
60  
80  
100  
120  
140  
160

20

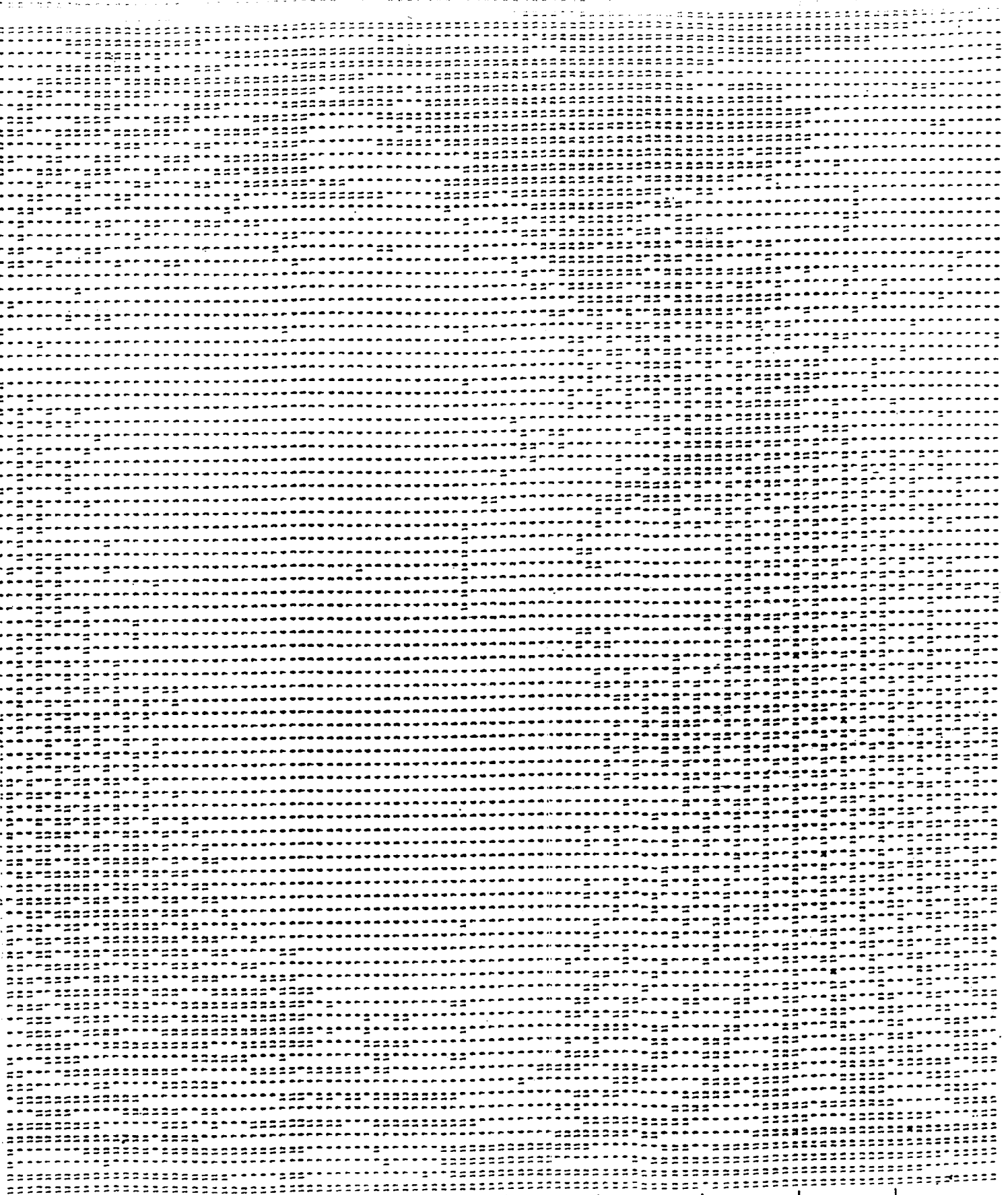
60

100

140

FOLDOUT FRAME

Locus of Ang



Roll Degrees

STS-27 (Bermuda)

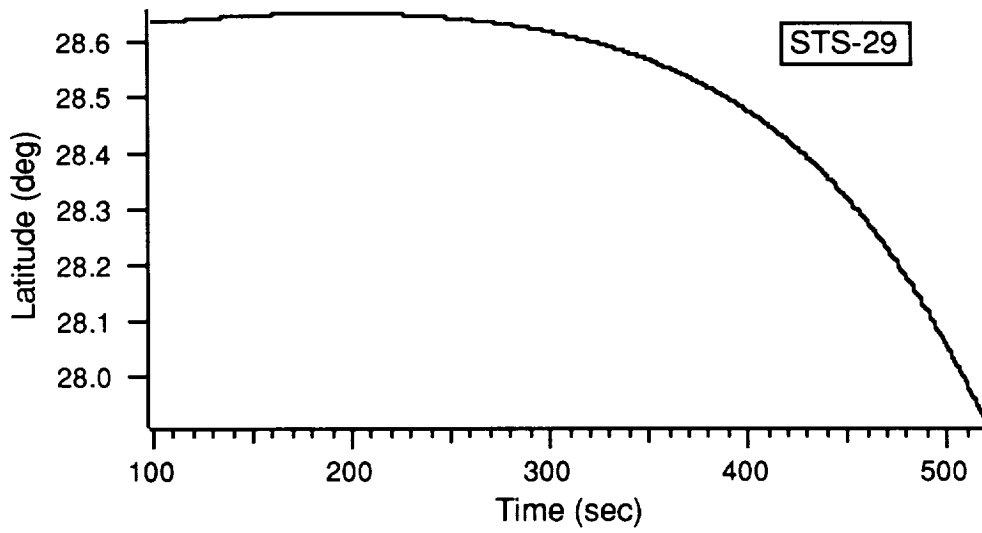
FOLDOUT PAGE 2

es of Arrival on ET Antenna Pattern

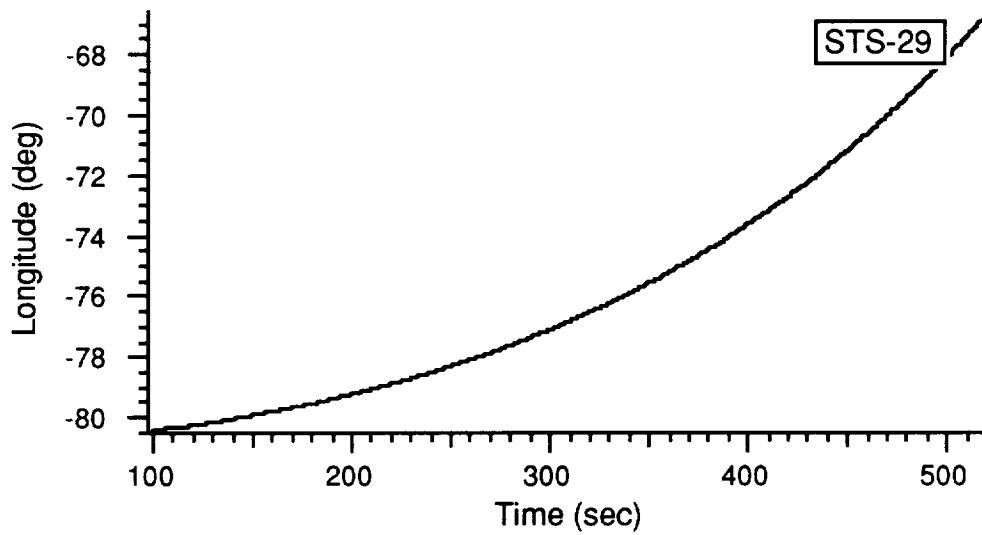


STS-29  
Appendix

The STS-29 flight experienced a deep fade between 300 and 350 seconds in flight, this corresponds to a  $3.5^{\circ}$  to  $4.5^{\circ}$  aspect angle.

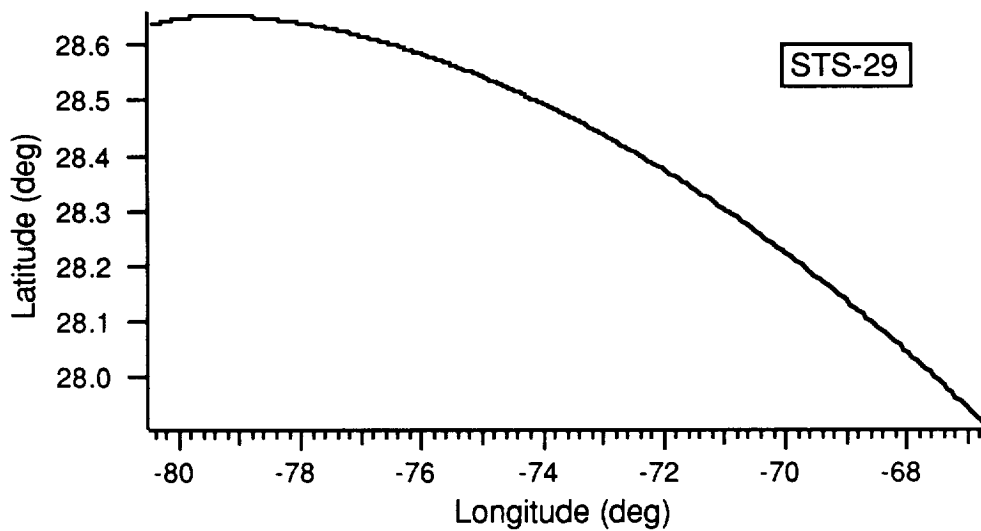


a. Latitude vs. Time

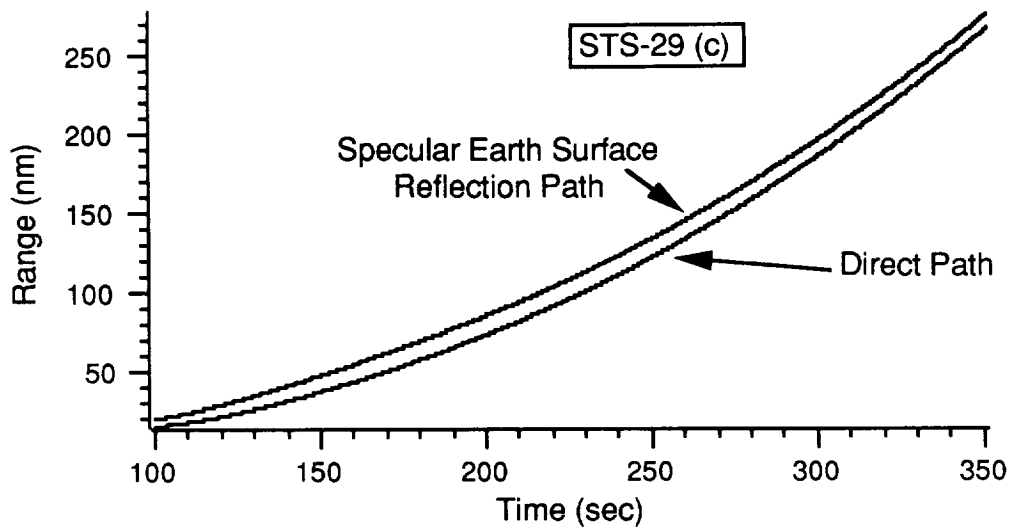


b. Longitude vs. Time

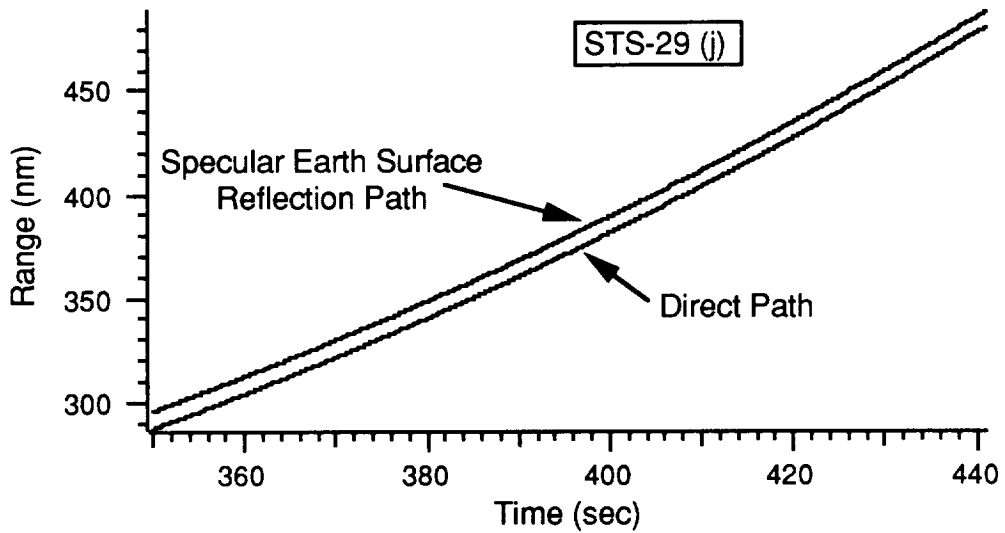
**Plots of Latitude (a.) and Longitude (b.) vs. Time After Launch**



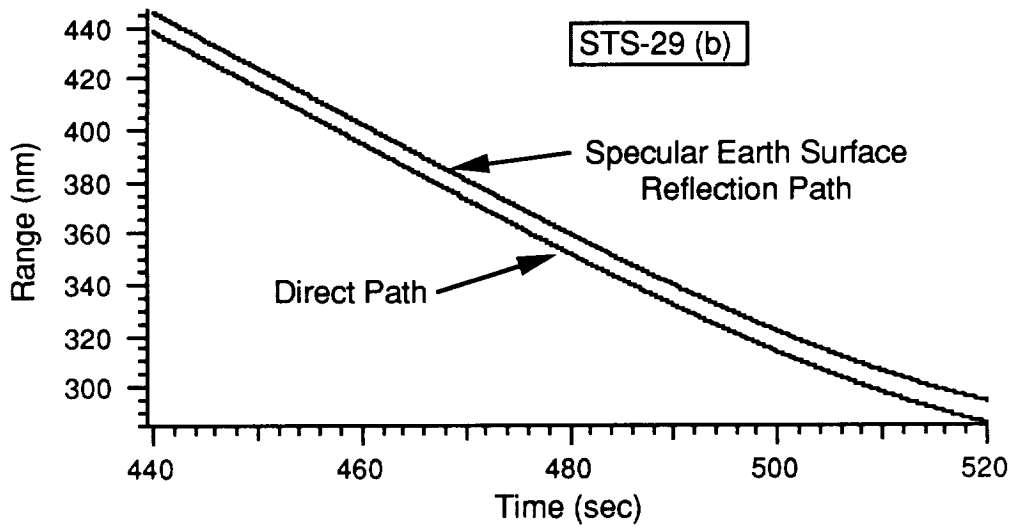
**Ground Trace of Shuttle Trajectory**



a. Transmission from Cape Canaveral

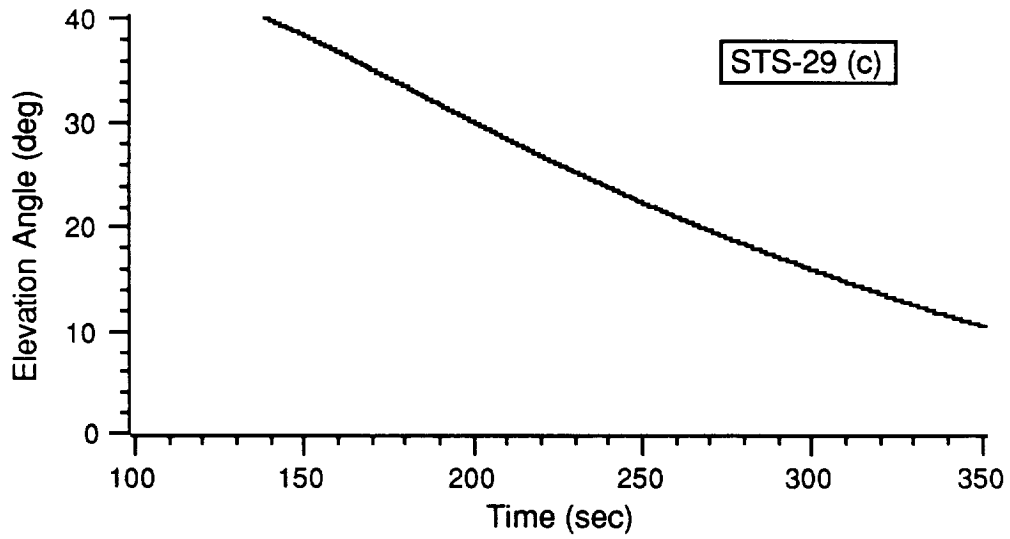


b. Transmission from Jonathan Dickinson

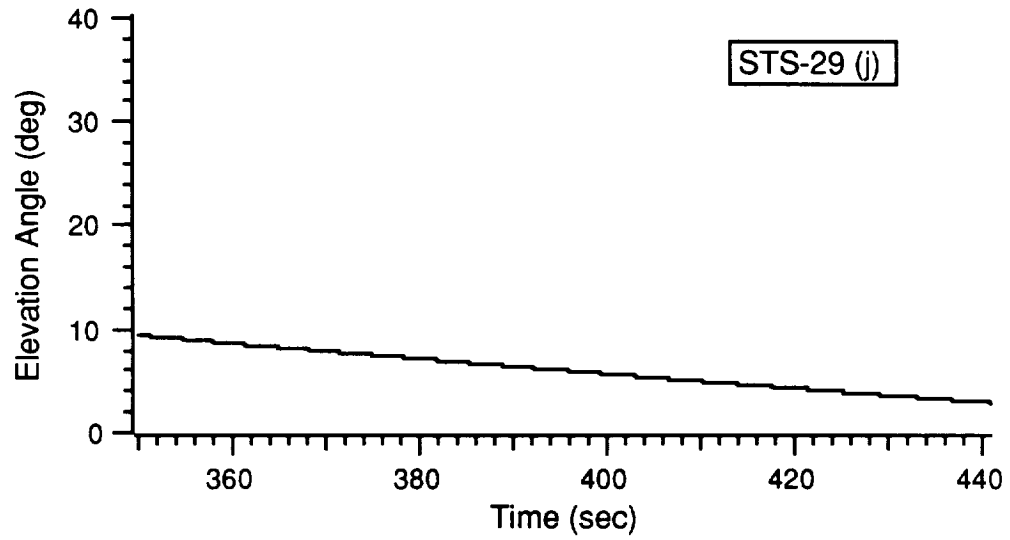


c. Transmission from Bermuda

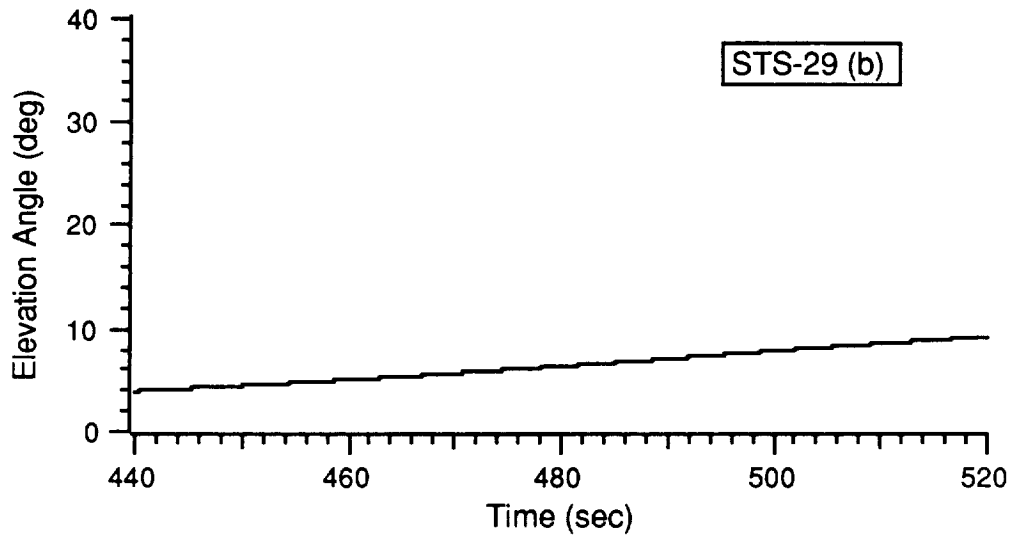
**Range from Transmitter Site to Shuttle vs. Time After Launch**



a. Transmission from Cape Canaveral

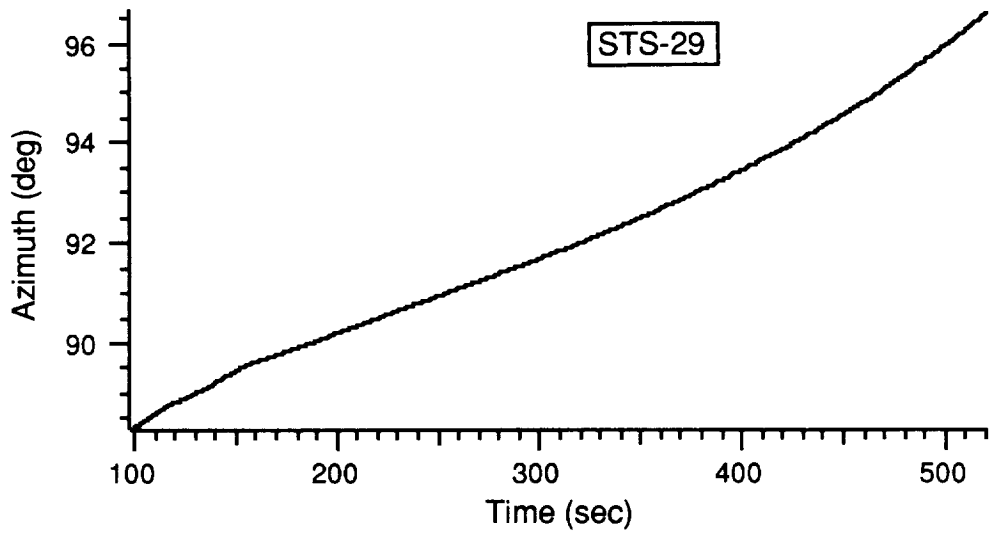


b. Transmission from Jonathan Dickinson

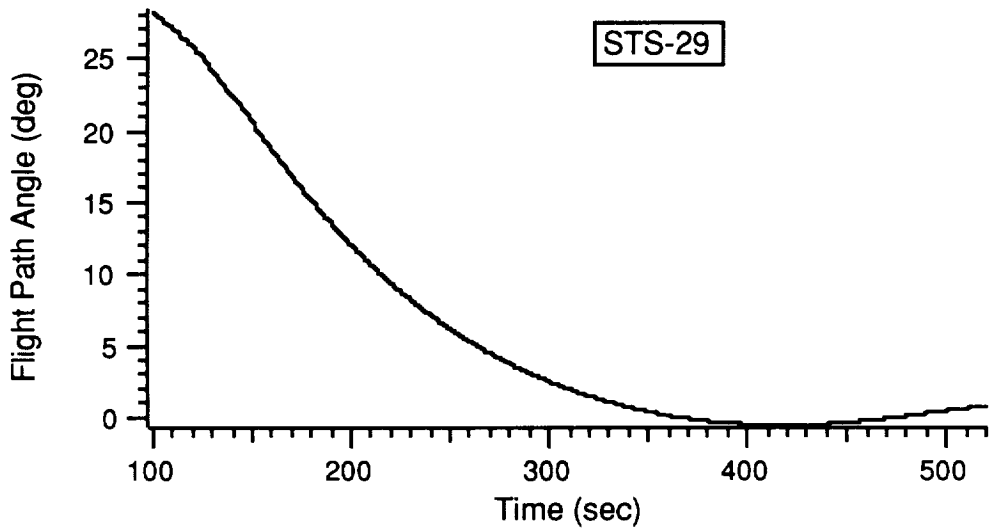


c. Transmission from Bermuda

**Elevation Angle (Transmitting Site to Shuttle) vs. Time After Launch**

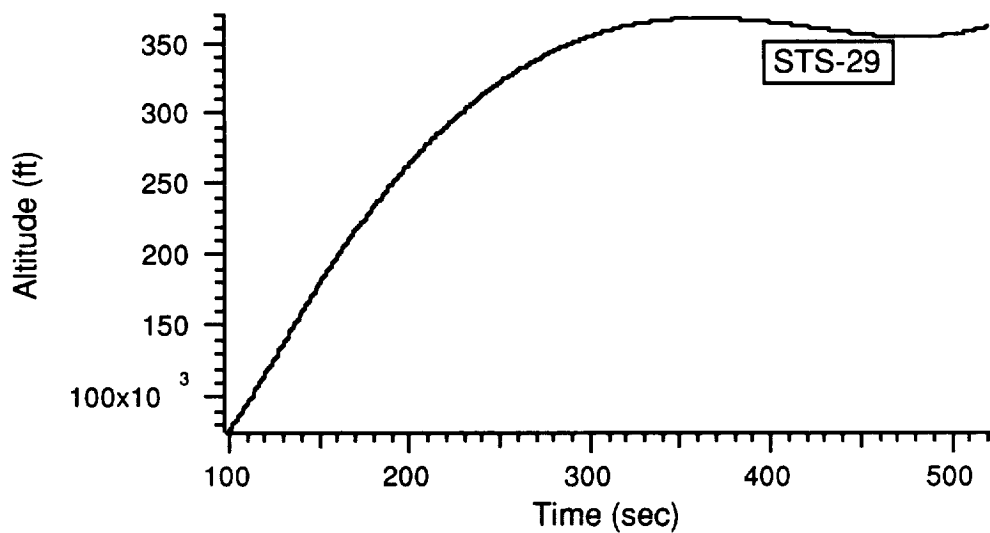


a. Horizontal

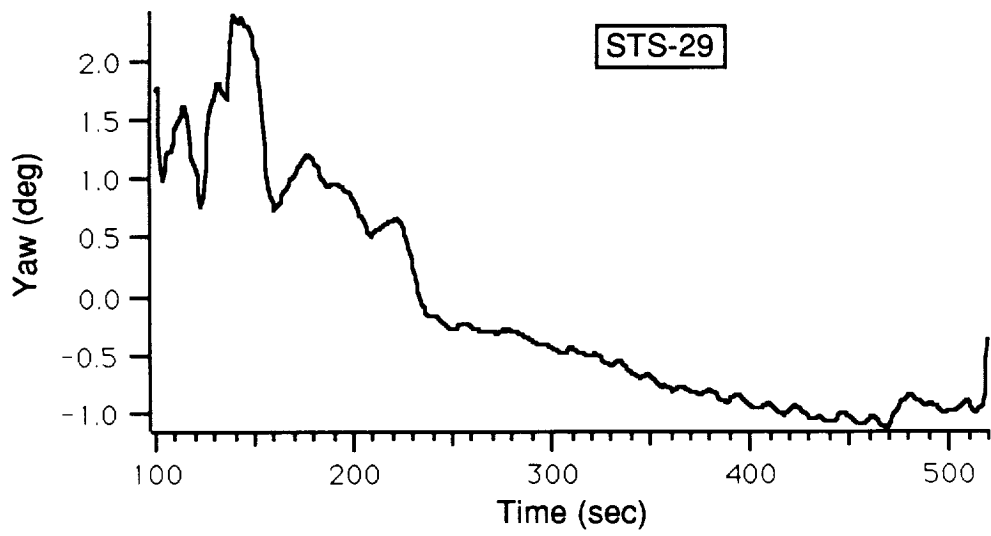


b. Vertical

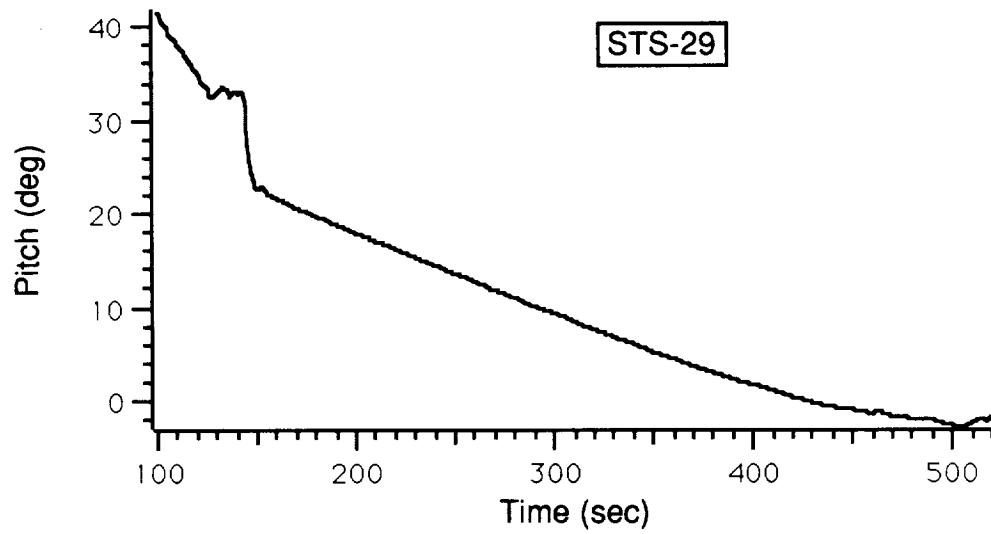
**Shuttle Flight Path Angles vs. Time After Launch**



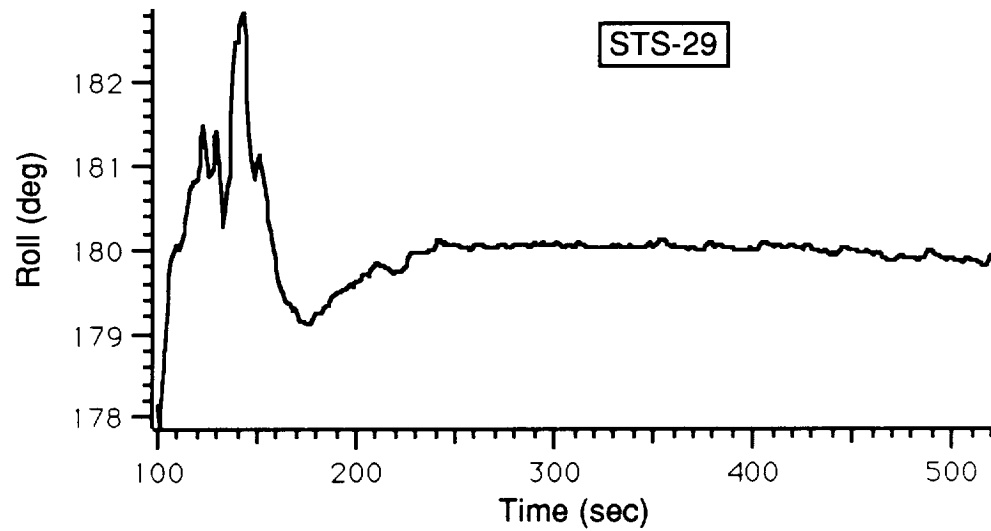
**Shuttle Altitude vs. Time After Launch**



a. Yaw Attitude

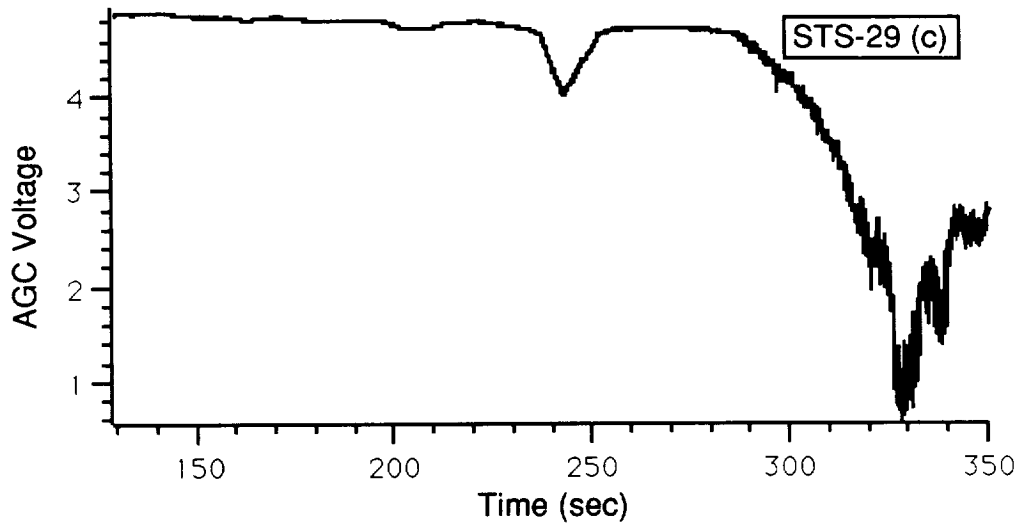


b. Pitch Attitude

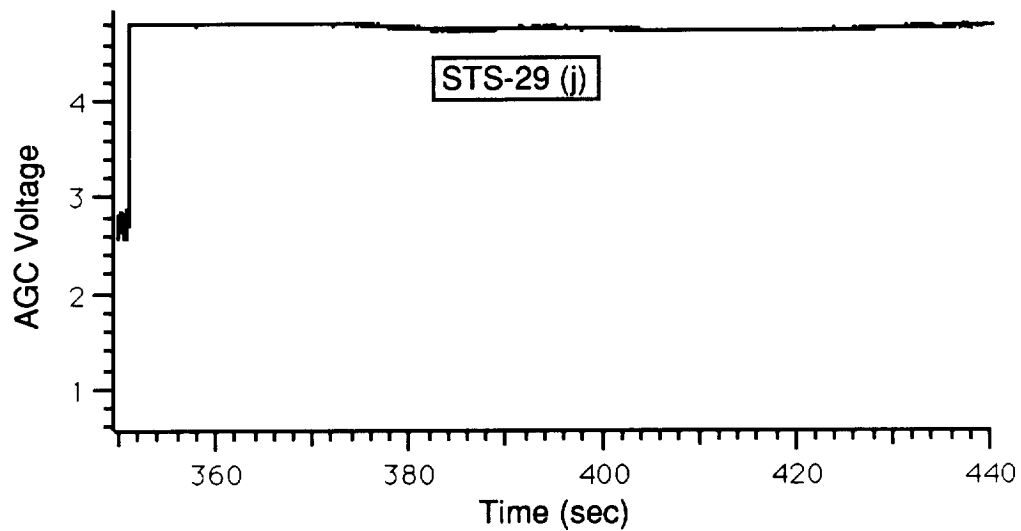


c. Roll Attitude

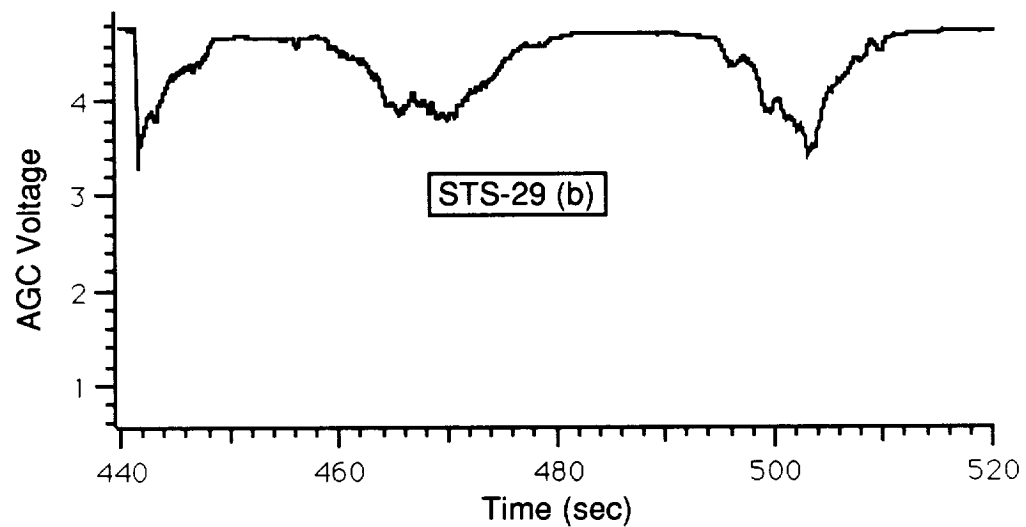
**Shuttle Attitude Angles (With Respect to Velocity Vector) vs. Time After Launch**



a. Transmission From Cape Canaveral

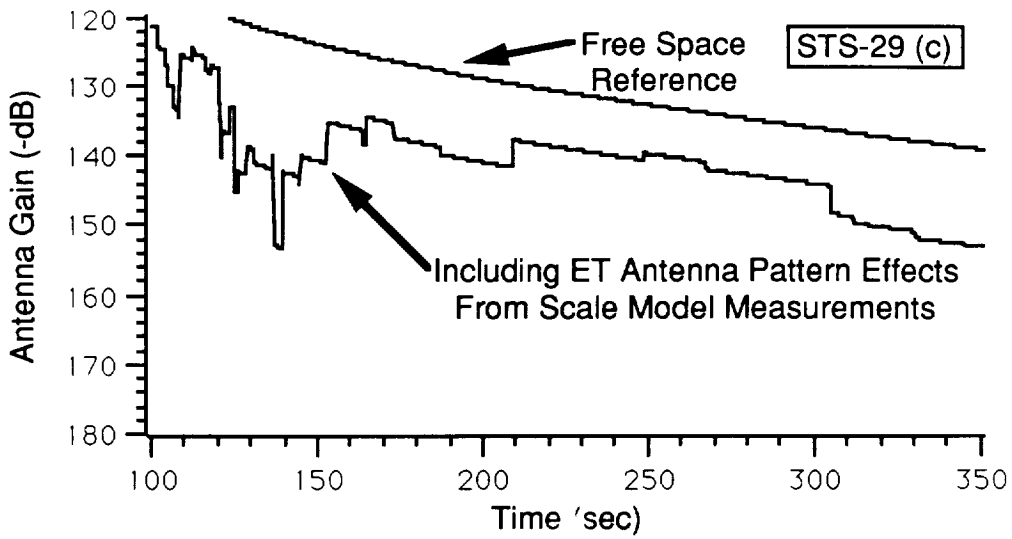


b. Transmission From Jonathan Dickinson

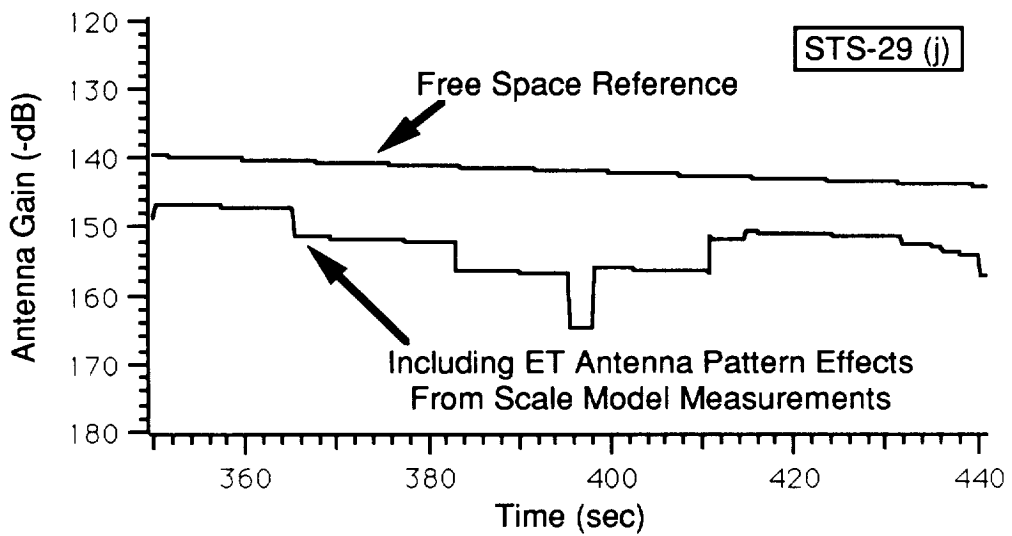


c. Transmission From Bermuda

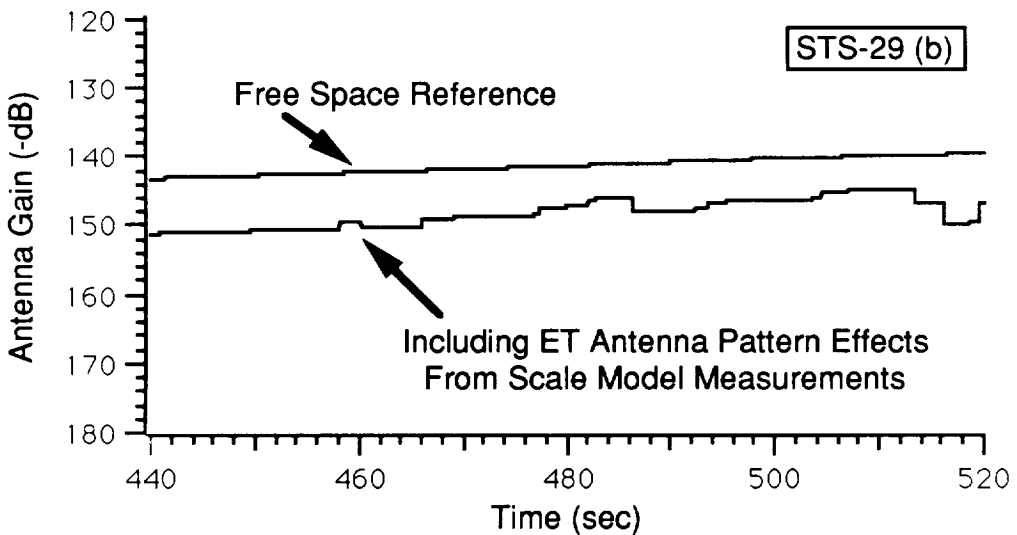
**Record of ET Receiver AGC Voltage vs. Time After Launch**



a. Transmission From Cape Canaveral



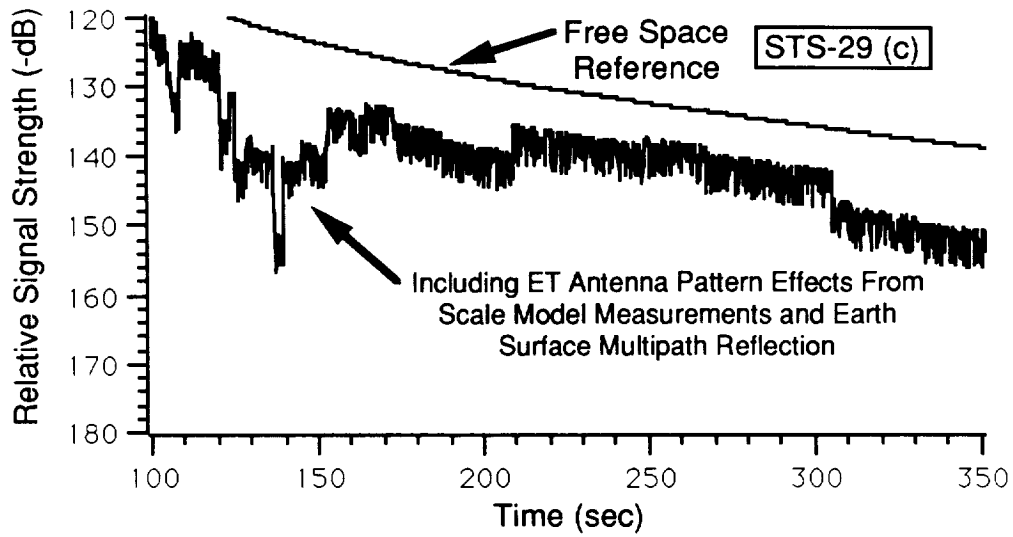
b. Transmission From Jonathan Dickinson



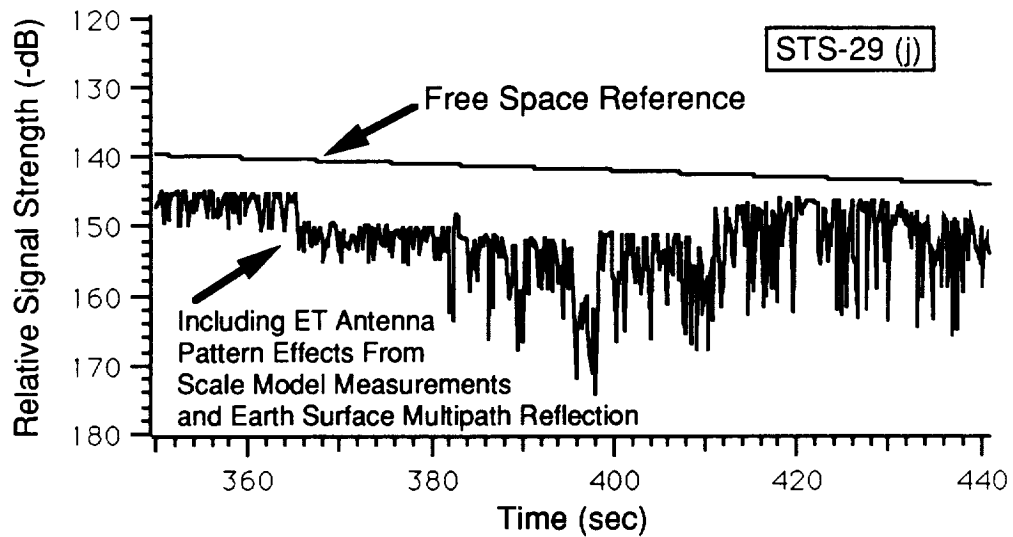
c. Transmission From Bermuda

**Computer Simulation of Relative Signal Strength at ET Receiver vs. Time After Launch  
(Without Earth-Surface Multipath Reflection)**

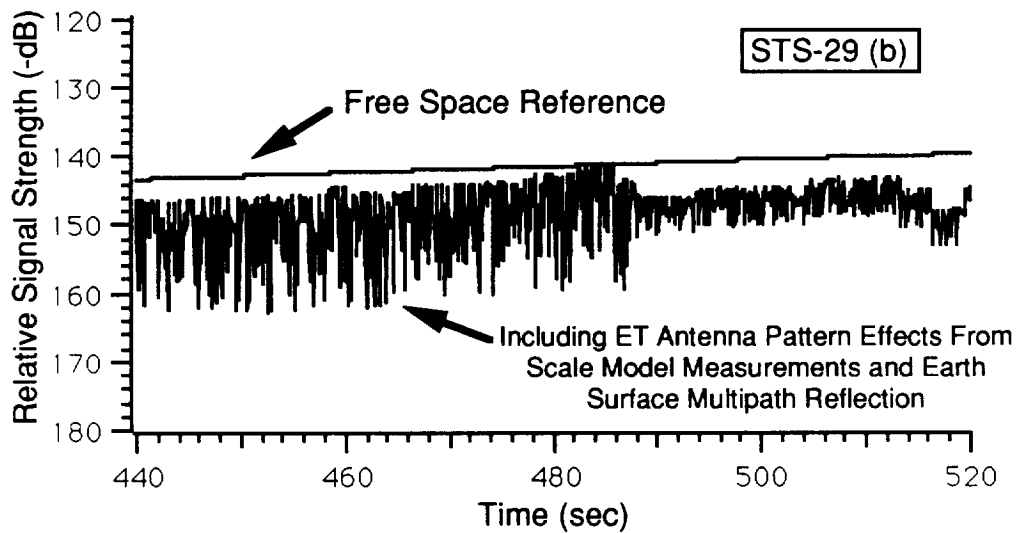




a. Transmission From Cape Canaveral



b. Transmission From Jonathan Dickinson



c. Transmission From Bermuda

**Computer Simulation of Relative Signal Strength at ET Receiver vs. Time After Launch  
(Including Earth-Surface Multipath Reflection)**

Yaw Degrees

20

40

60

80

100

120

140

160

20

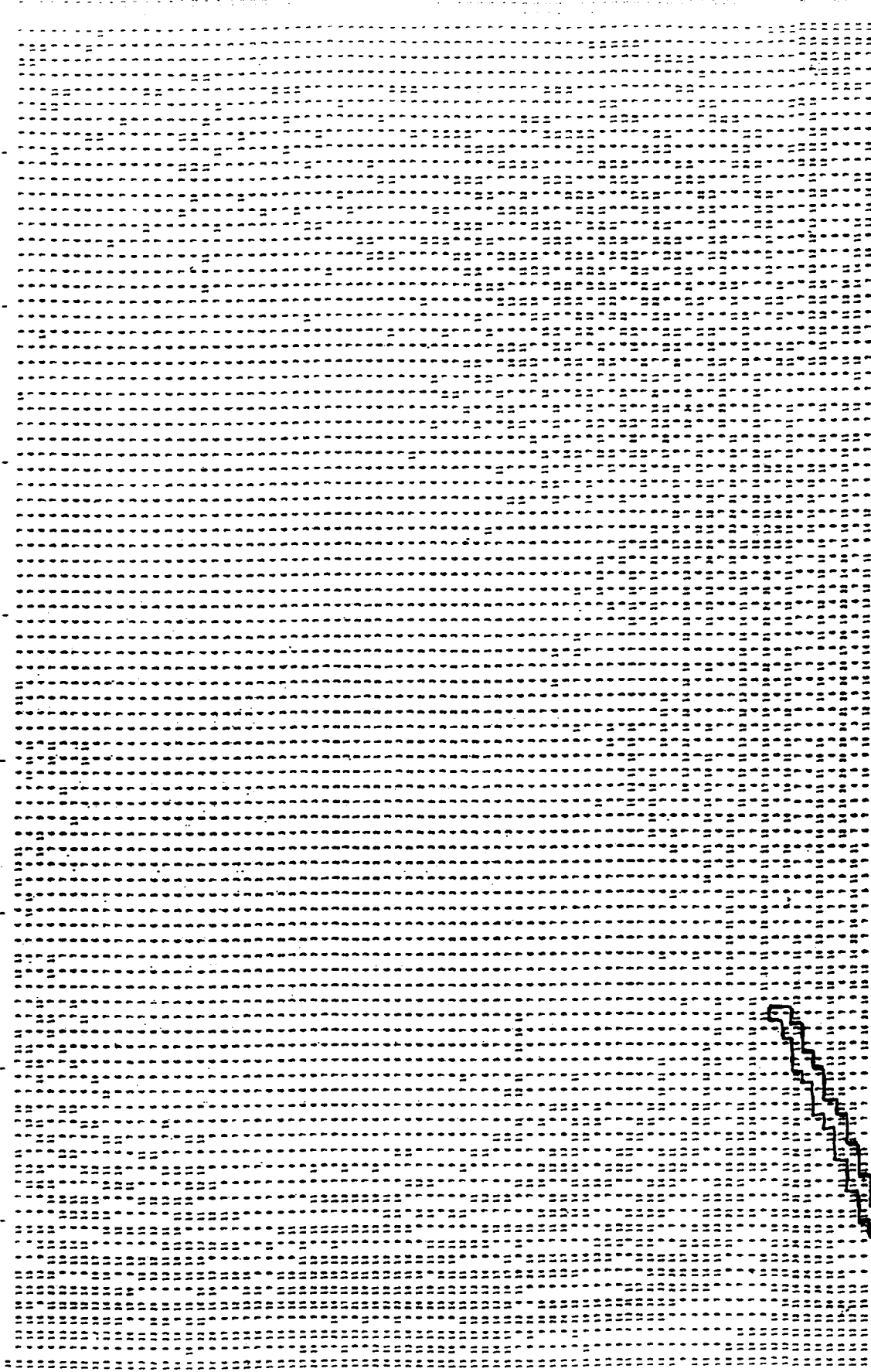
60

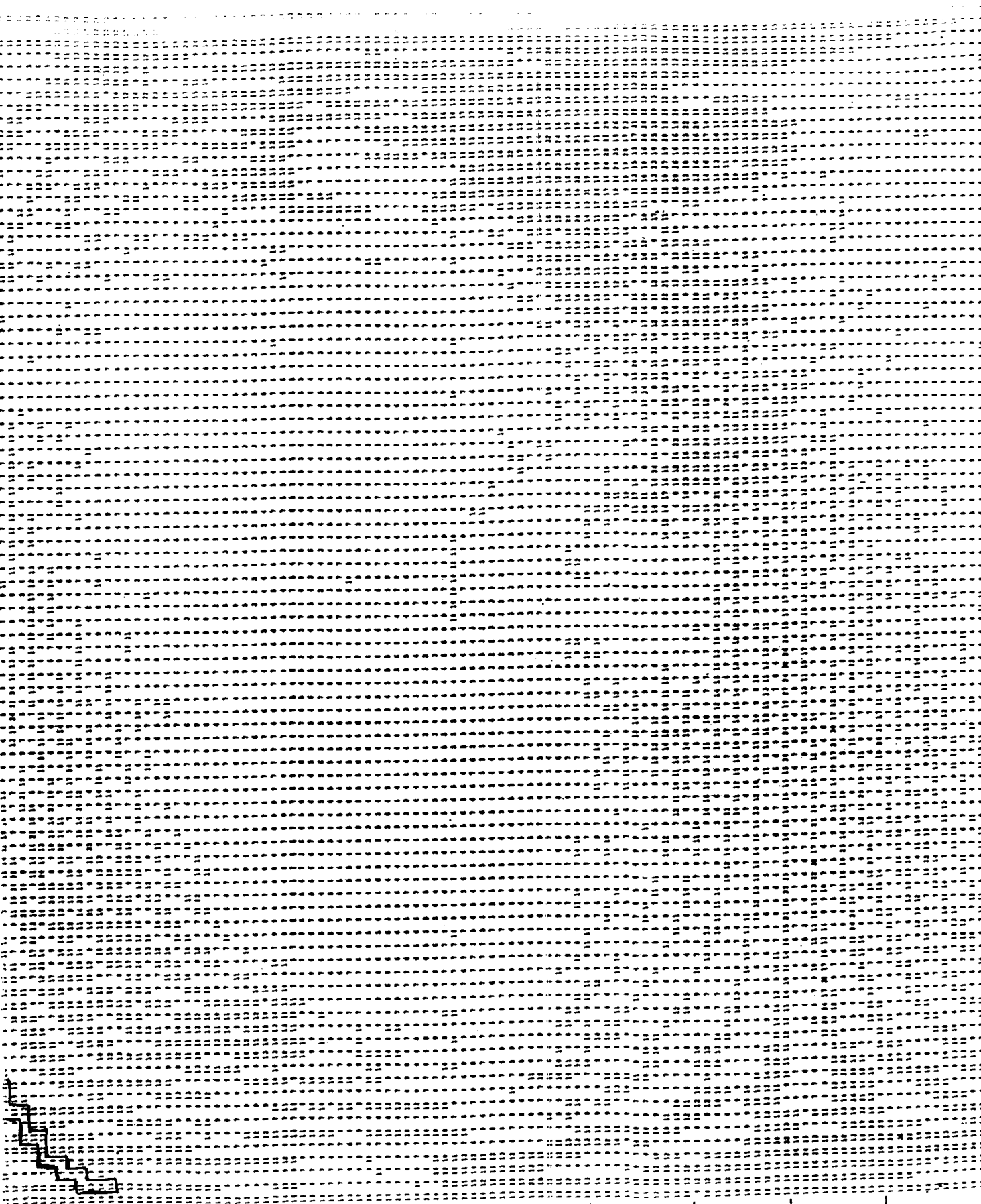
100

140

FOLDOUT FRAME

Locus of Ang

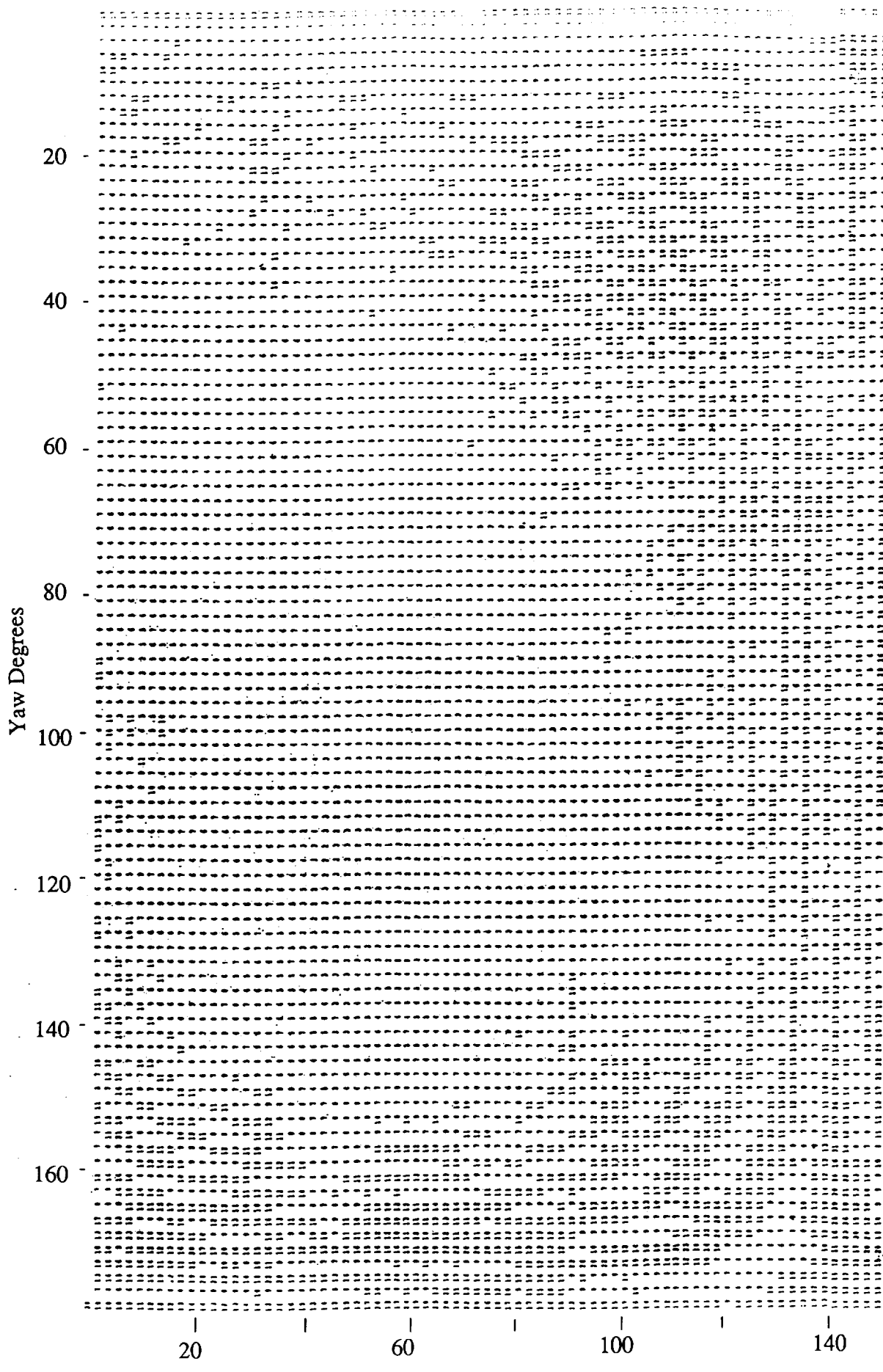




180  
140  
100  
60  
20  
Roll Degrees

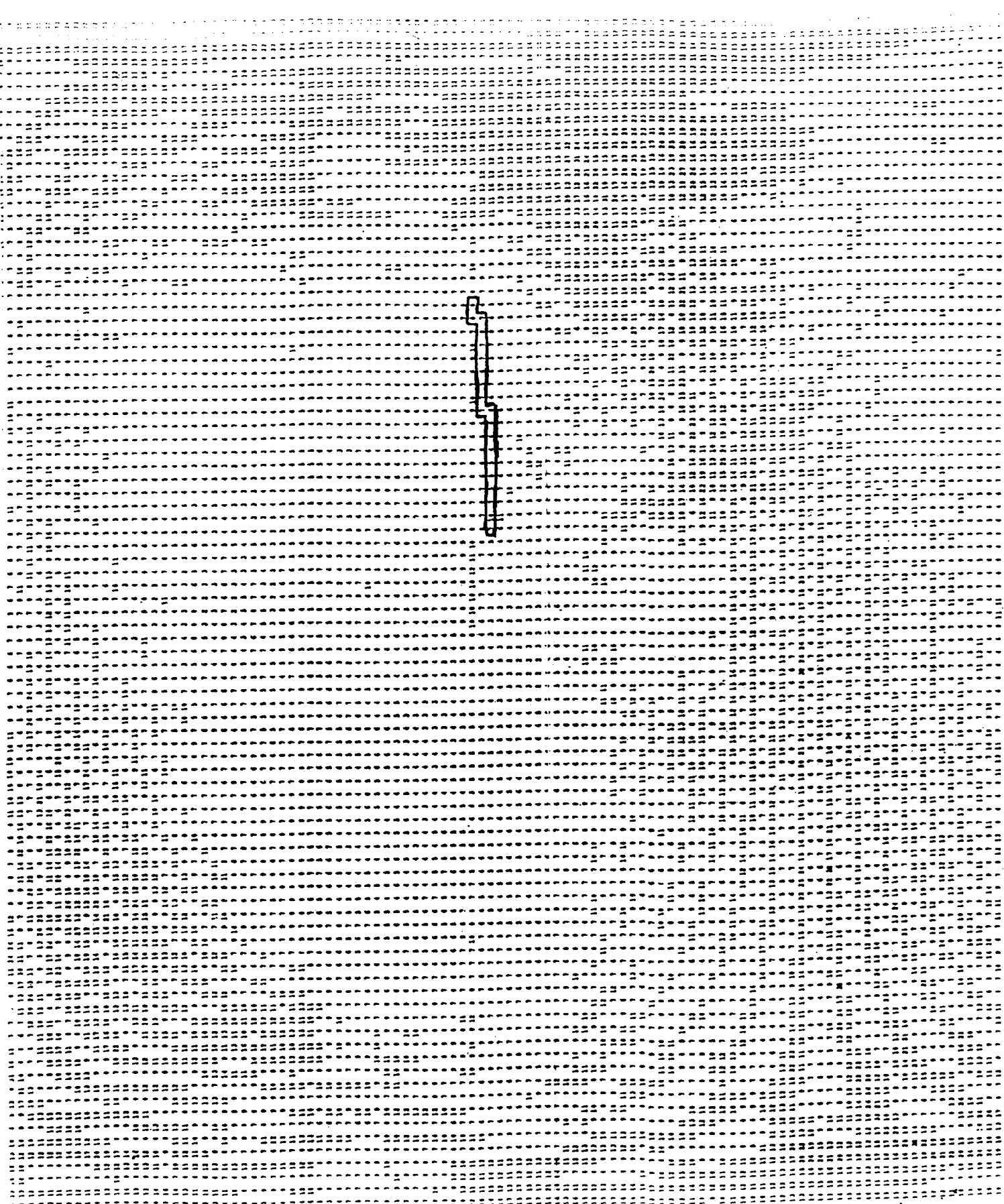
BTS-29 (Cape Canaveral)  
s of Arrival on ET Antenna Pattern

FOLDOUT FRAME 2



FOLDOUT PLANE /

Locus of Ar



180  
140  
100  
60  
20  
Roll Degrees

STS-29 (Bermuda)

FOLDOUT

2

les of Arrival on ET Antenna Pattern

Yaw Degrees

20

40

60

80

100

120

140

160

20

60

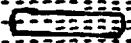
100

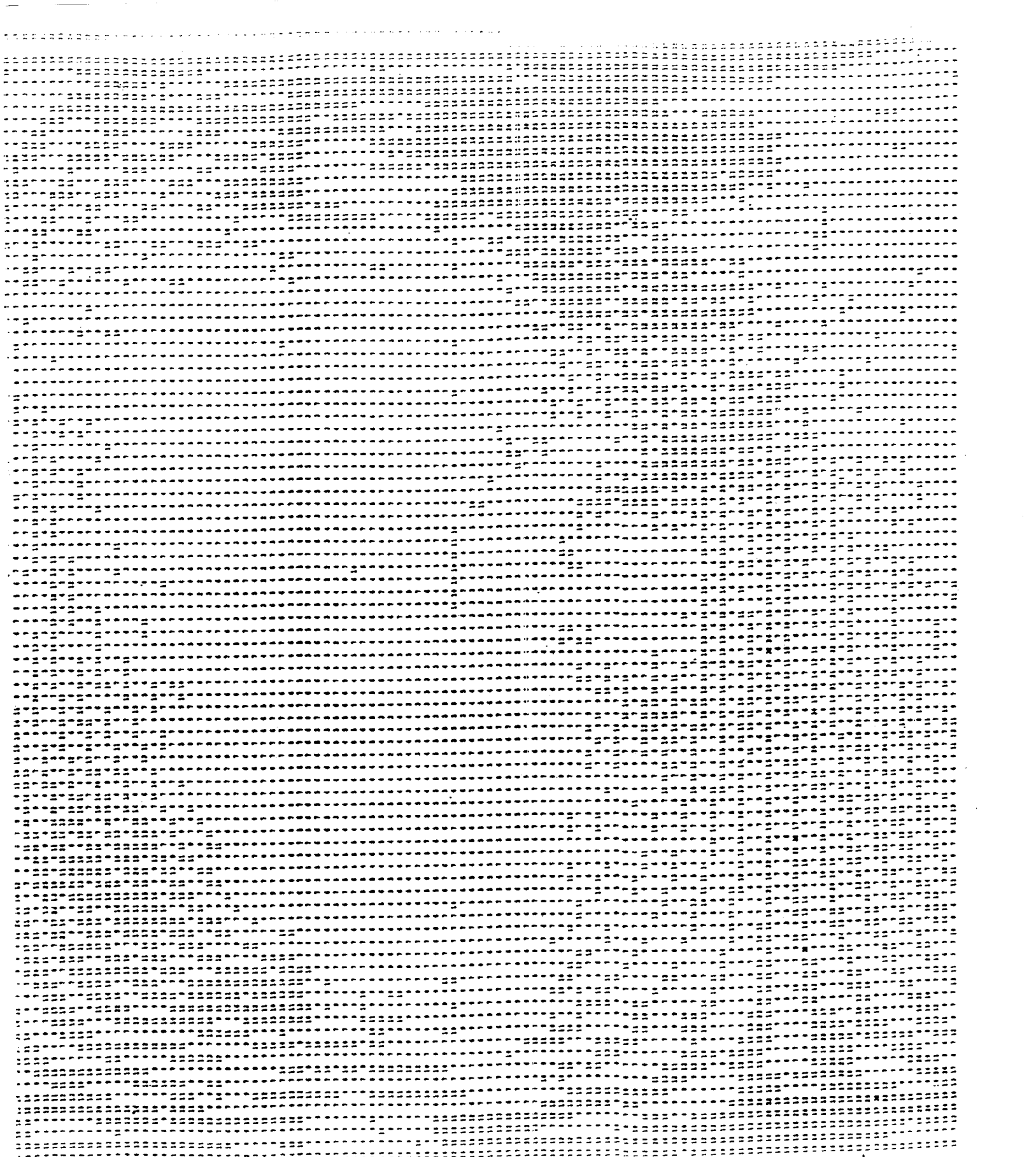
140

FOLDOUT FRAME

Locus of An

S





180  
140  
100  
60  
20  
Roll Degrees

S-29 (Jonathan Dickinson)

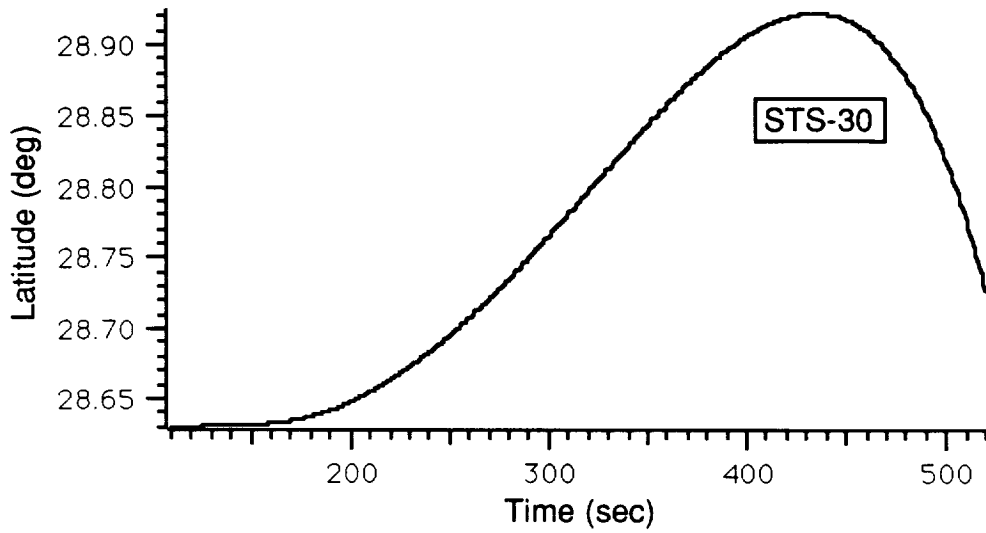
es of Arrival on ET Antenna Pattern

EXHIBIT FRAME 

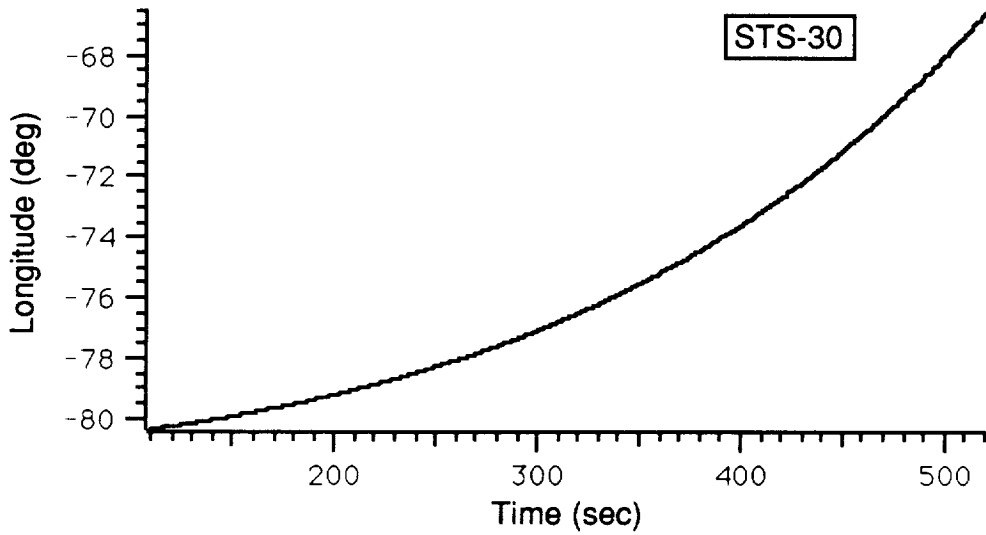
STS-30  
Appendix

STS-30 was launched almost directly east. It experienced two deep nulls. One null appears to be at a directly aft aspect angle and the other within  $2^\circ$  of directly aft.



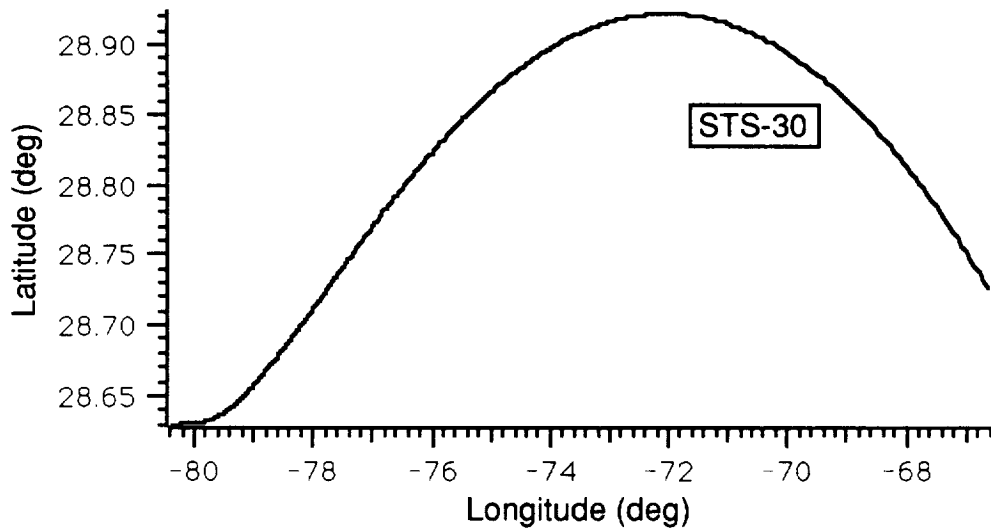


a. Latitude vs. Time

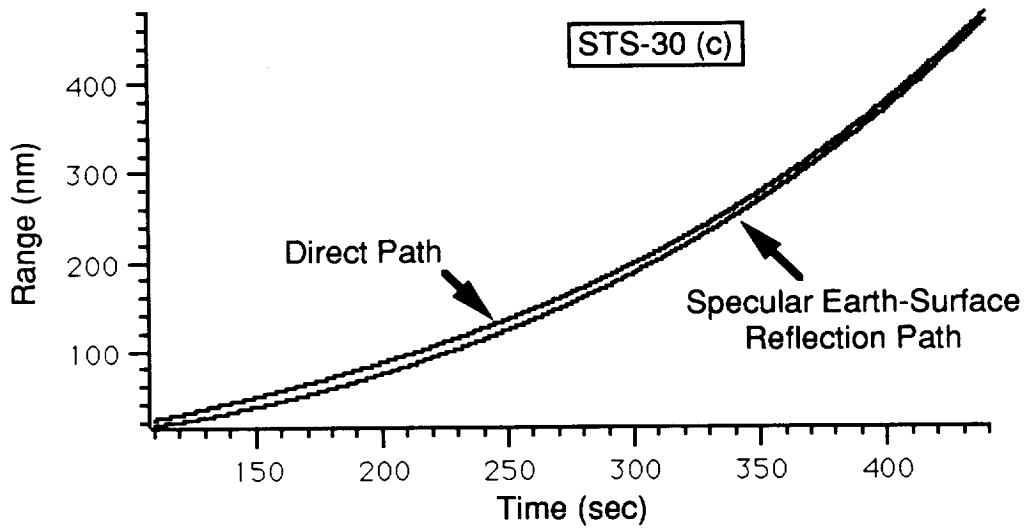


b. Longitude vs. Time

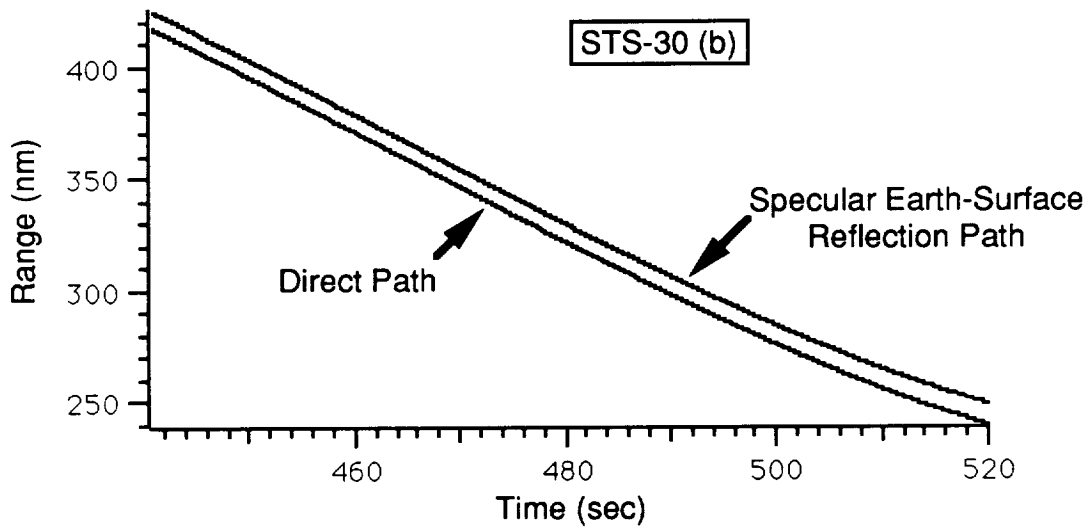
**Plots of Latitude (a.) and Longitude (b.) vs. Time After Launch**



**Ground Trace of Shuttle Trajectory**

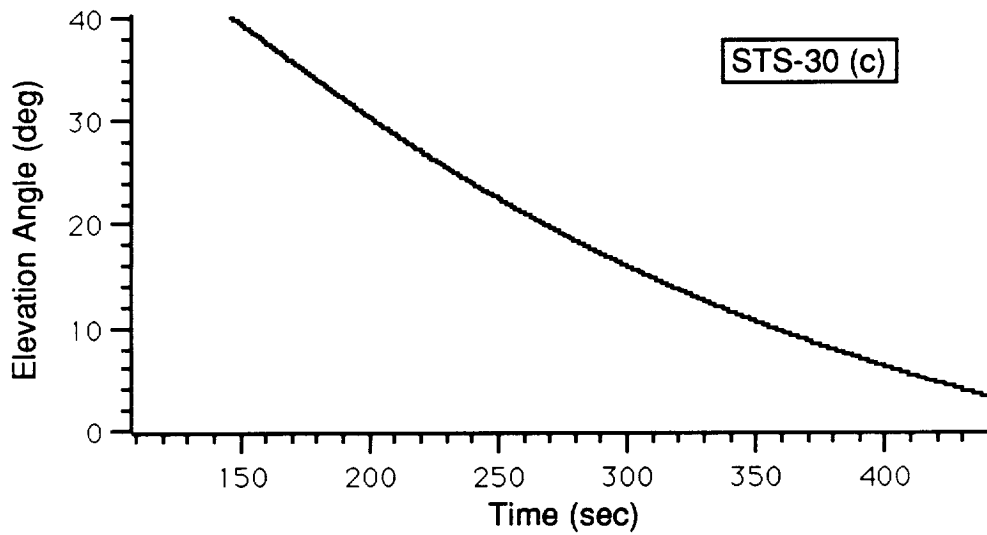


a. Transmission From Cape Canaveral

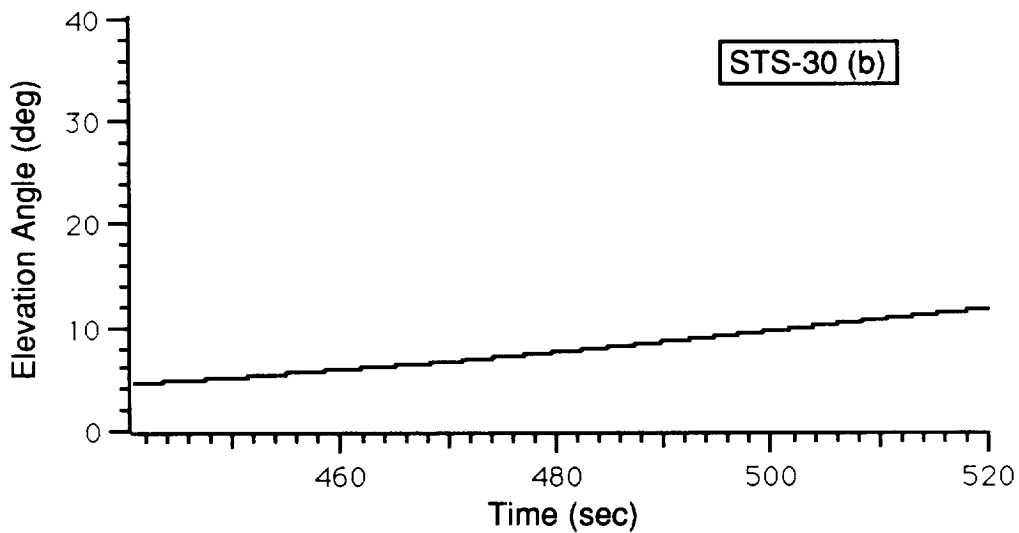


b. Transmission From Bermuda

**Range From Transmitter Site to Shuttle vs. Time After Launch**

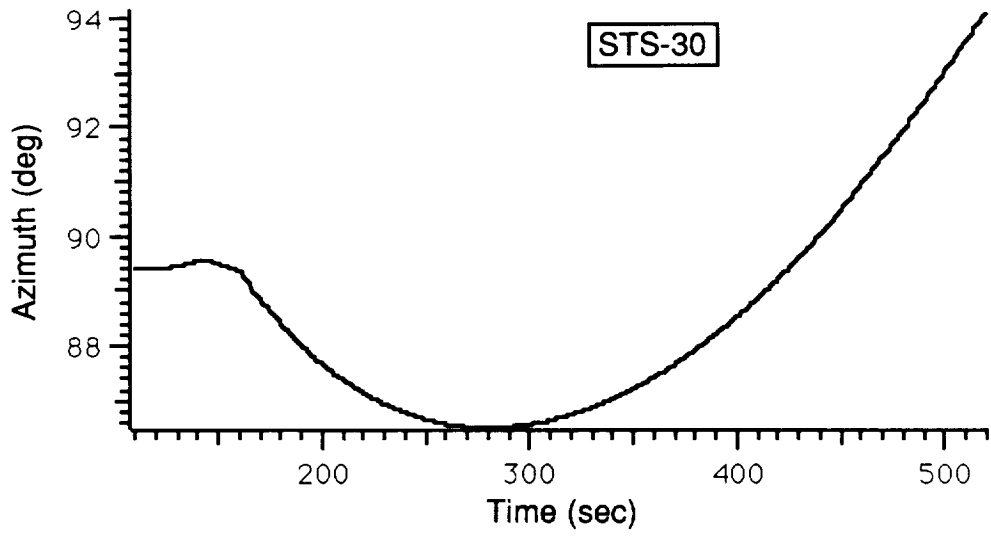


a. Transmission From Cape Canaveral

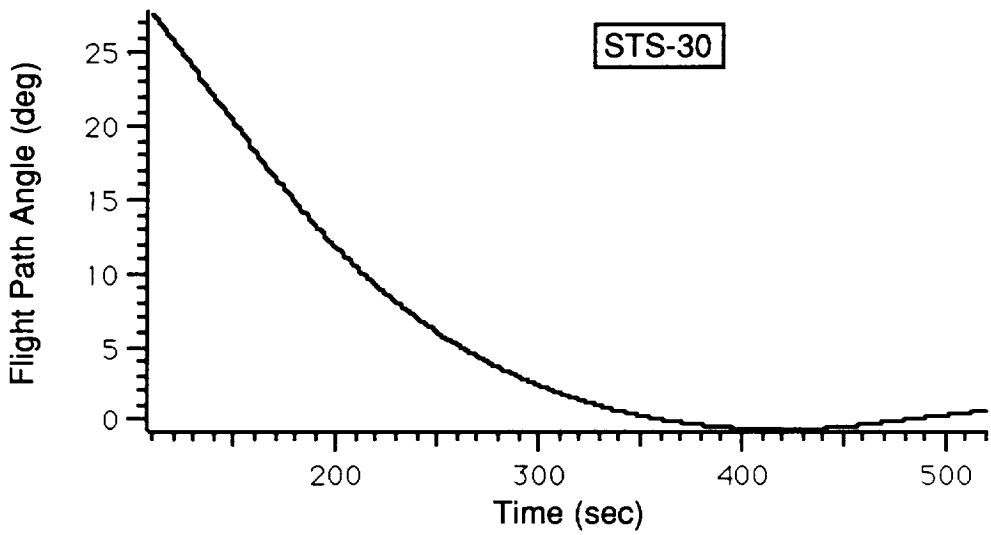


b. Transmission From Bermuda

**Elevation Angle (Transmitting Site to Shuttle) vs. Time After Launch**

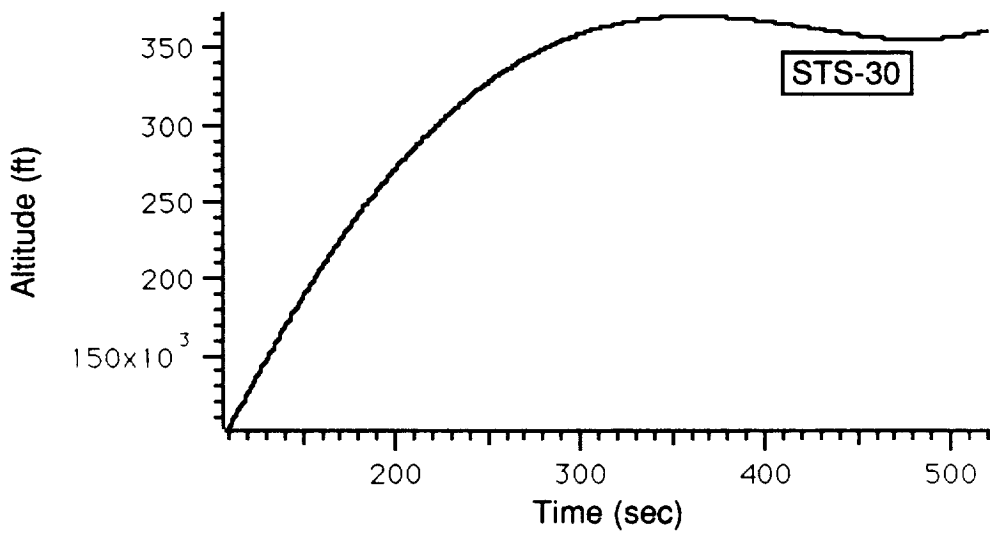


a. Horizontal

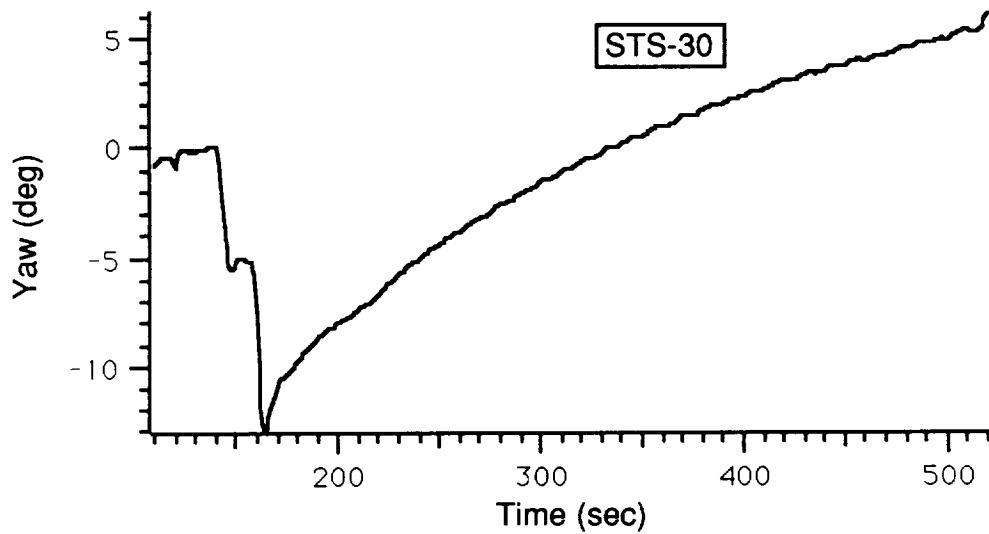


b. Vertical

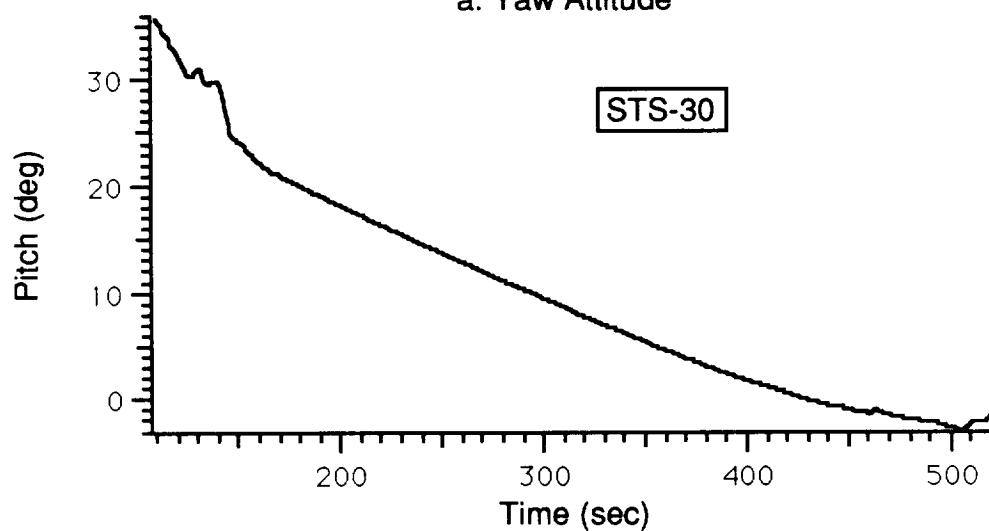
**Shuttle Flight Path Angles vs. Time After Launch**



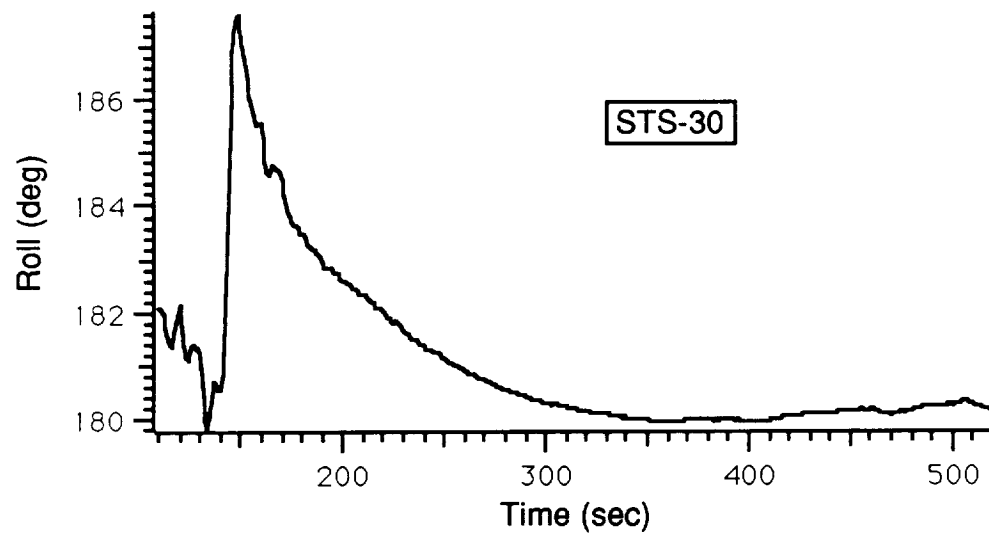
**Shuttle Altitude vs. Time After Launch**



a. Yaw Attitude

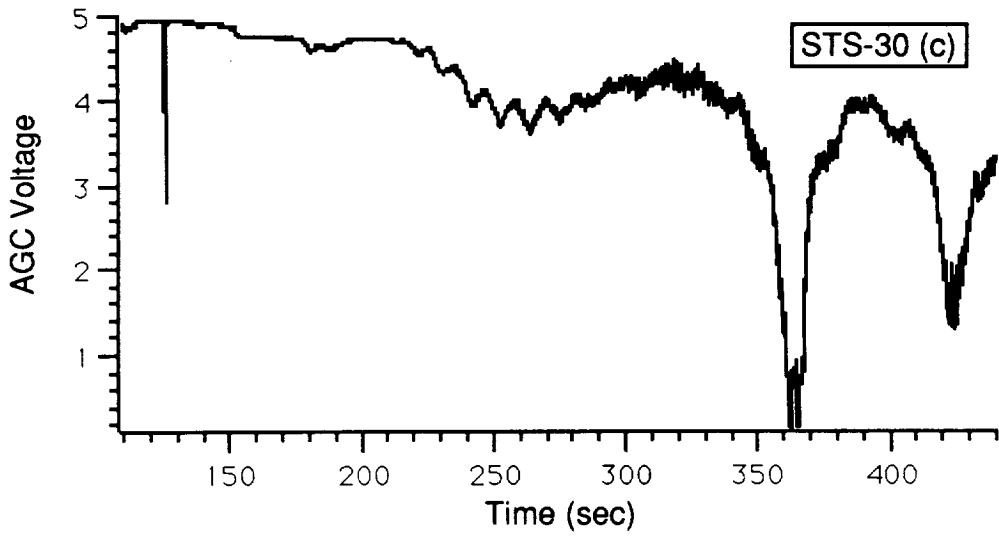


b. Pitch Attitude

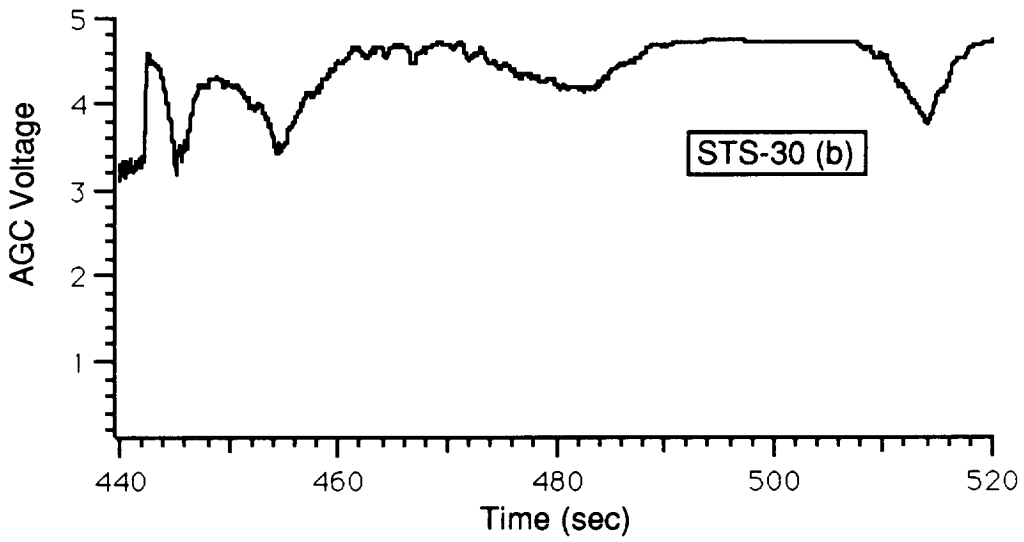


c. Roll Attitude

**Shuttle Attitude Angles (With Respect to Velocity Vector) vs. Time After Launch**

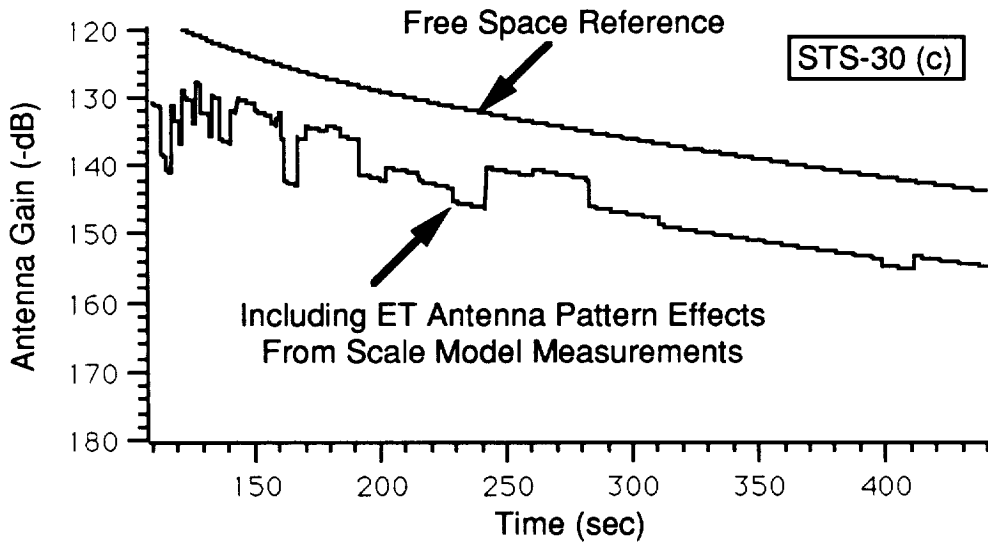


a. Transmission From Cape Canaveral

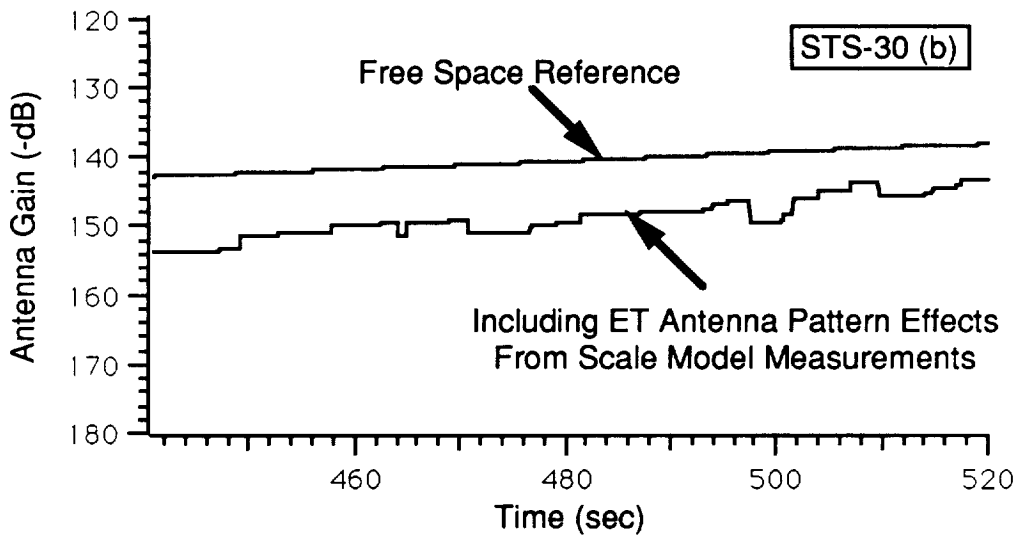


b. Transmission From Bermuda

**Record of ET Receiver AGC Voltage vs. Time After Launch**

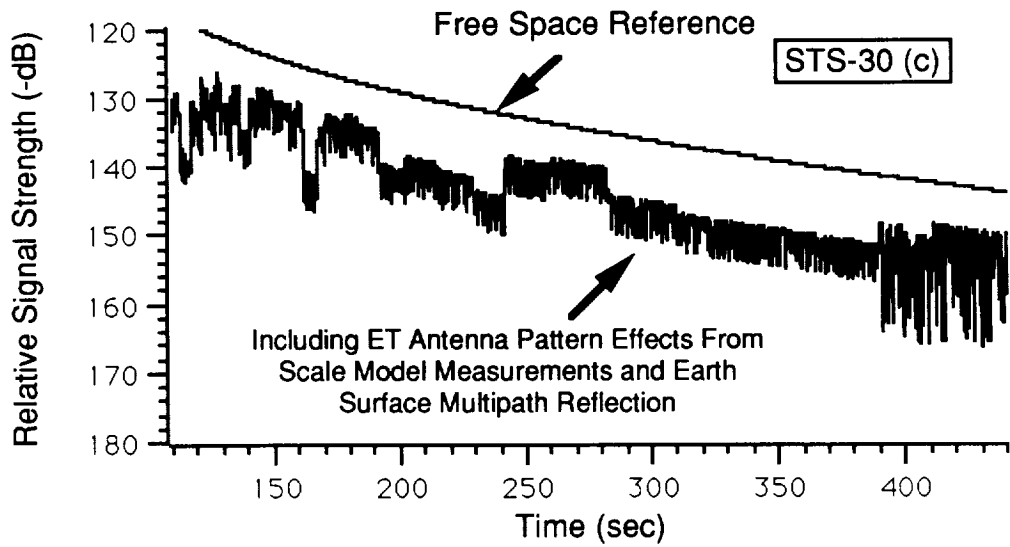


a. Transmission From Cape Canaveral

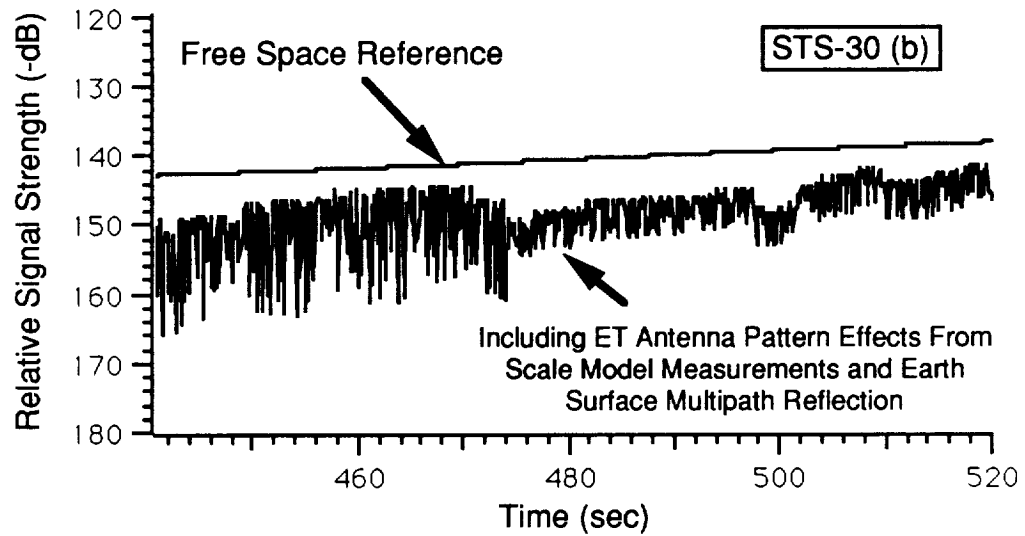


b. Transmission From Bermuda

**Computer Simulation of Relative Signal Strength at ET Receiver vs. Time After Launch  
(Without Earth-Surface Multipath Reflection)**



a. Transmission From Cape Canaveral



b. Transmission From Bermuda

**Computer Simulation of Relative Signal Strength at ET Receiver vs. Time After Launch  
(Including Earth-Surface Multipath Reflection)**



Yaw Degrees

20

40

60

80

100

120

140

160

20

60

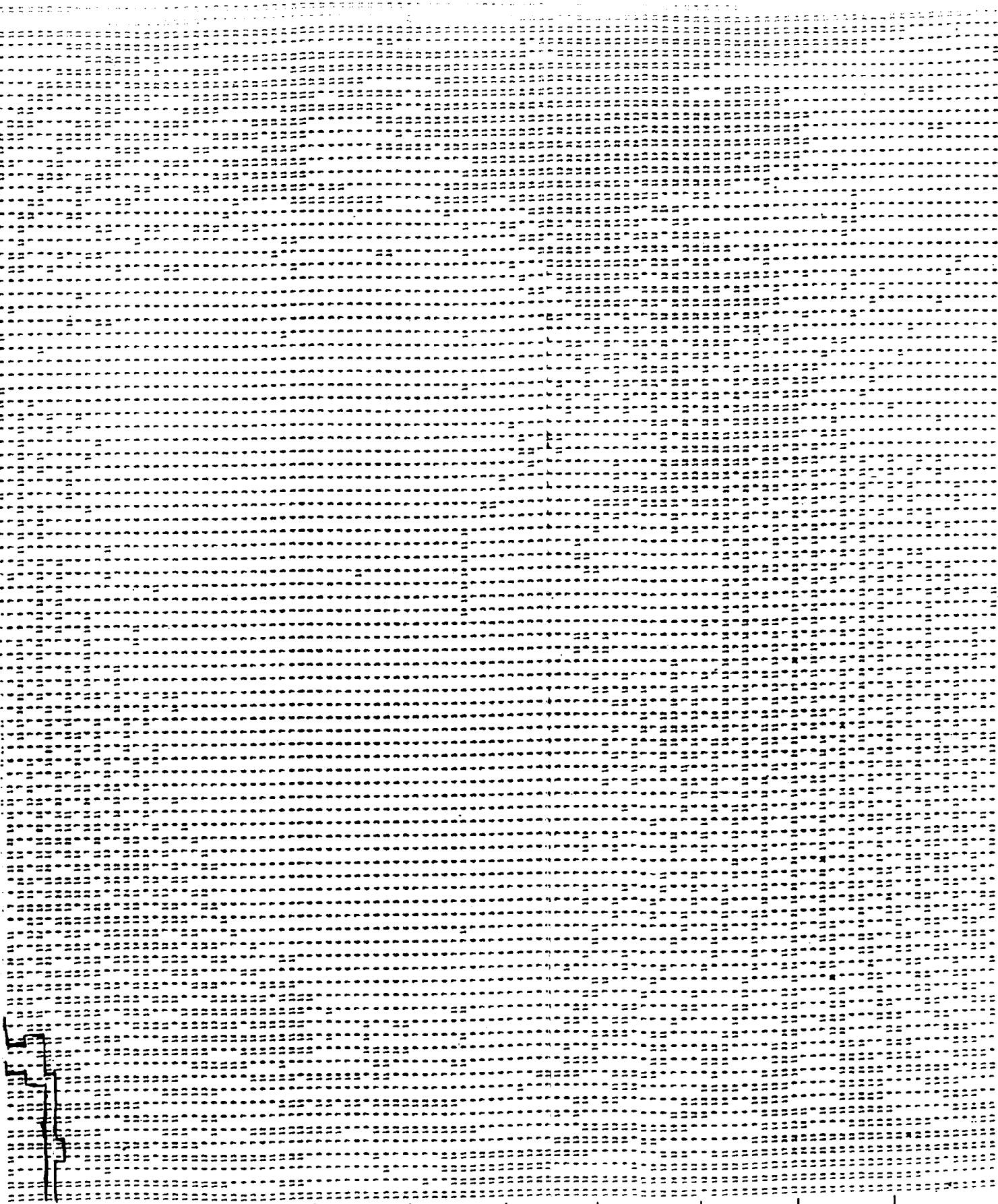
100

140

FOLDOUT FRAME 1

C-2

Locus of An



180

140

100

60

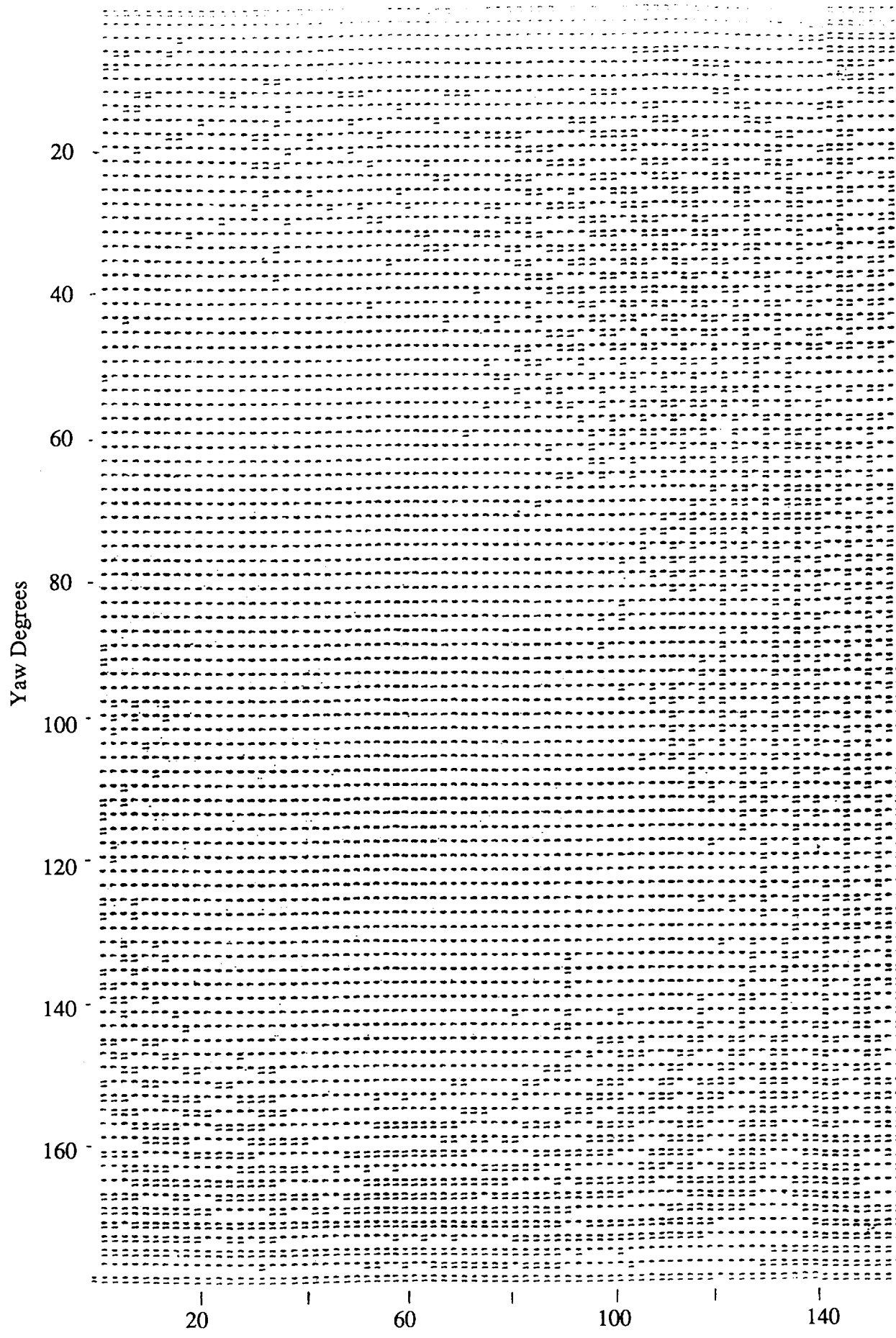
20

Roll Degrees

STS-30 (Cape Canaveral)

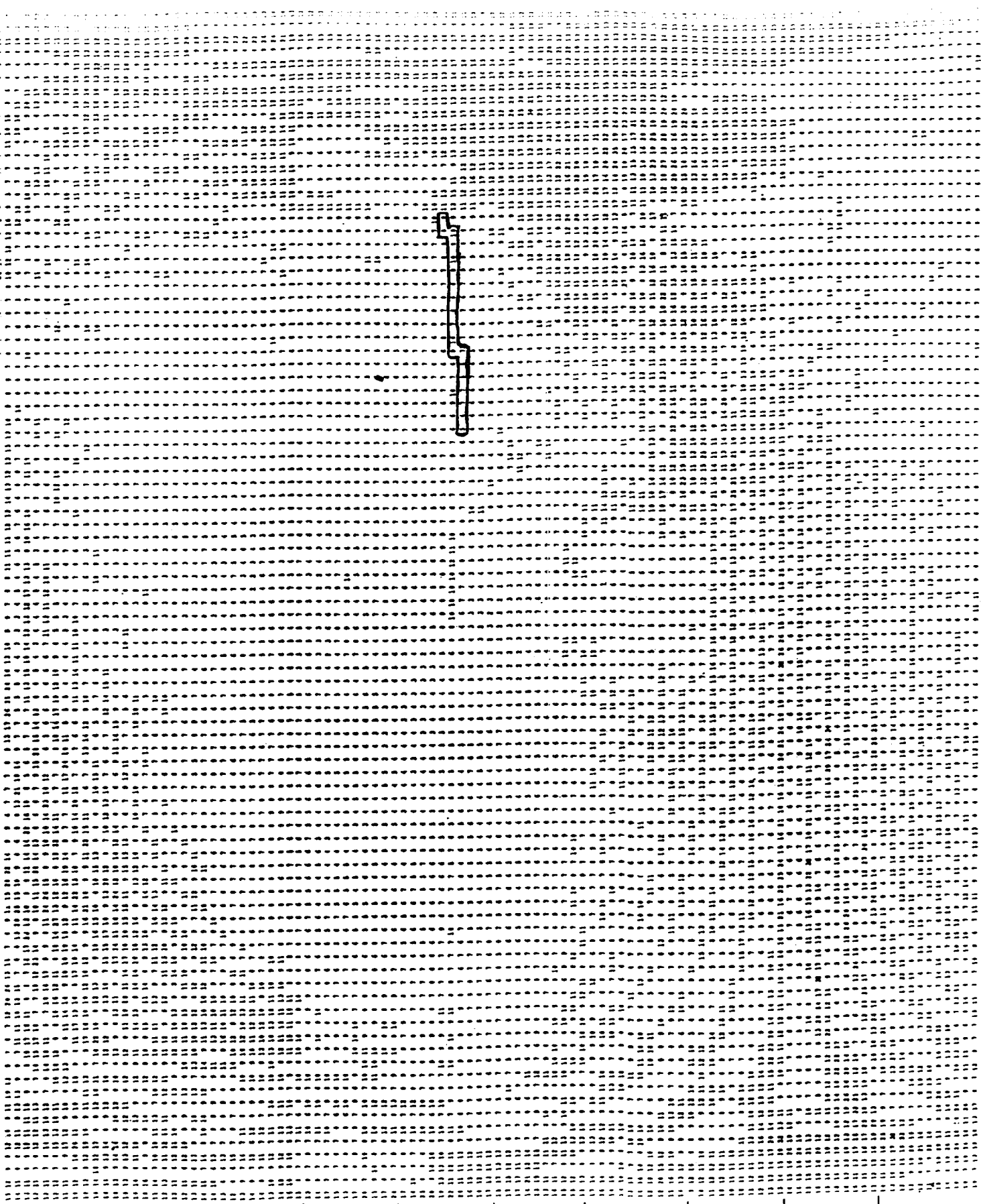
es of Arrival on ET Antenna Pattern

FOLDOUT PAGE 2



FOLDOUT FRAME /

Locus of Angl



Roll Degrees

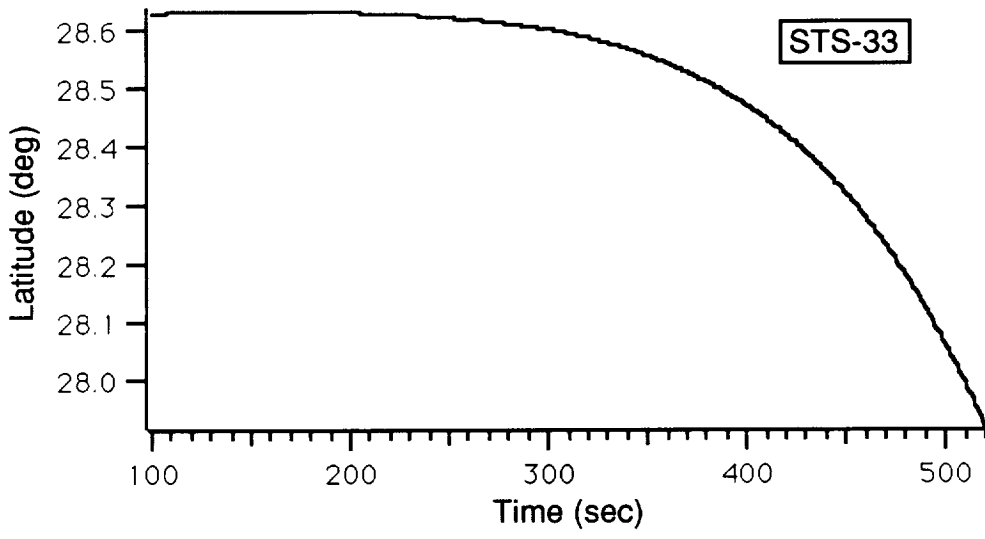
STS-30 (Bermuda)

of Arrival on ET Antenna Pattern

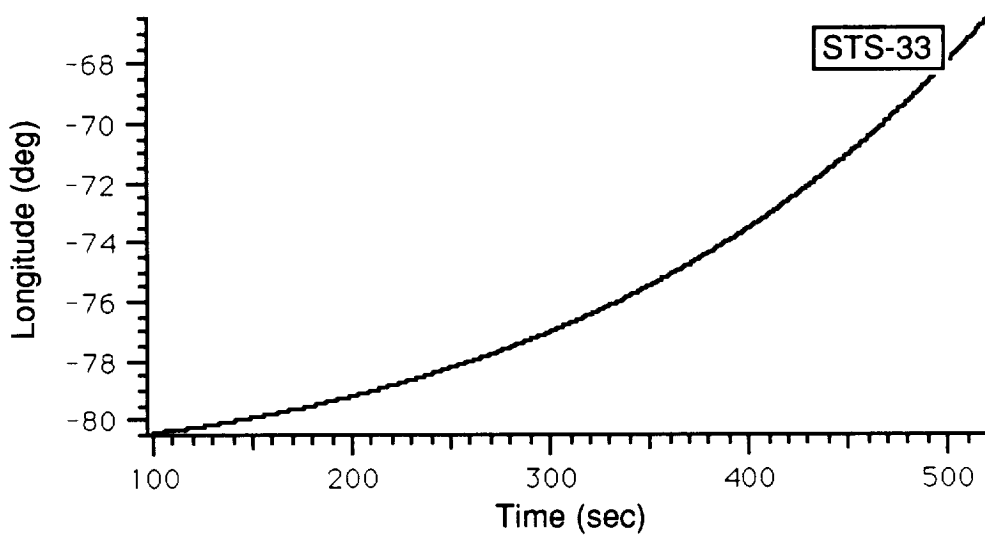
FOLDOUT FOR 2.

STS-33  
Appendix

The STS-33 flight was launched to the east. The Cape low power transmitter was used on this flight to approximately 150 seconds. There is a deep signal fade which lasts for approximately 150 seconds on this flight. The fade occurs when the aspect angle is between  $2^{\circ}$  and  $4.5^{\circ}$  away from directly aft.

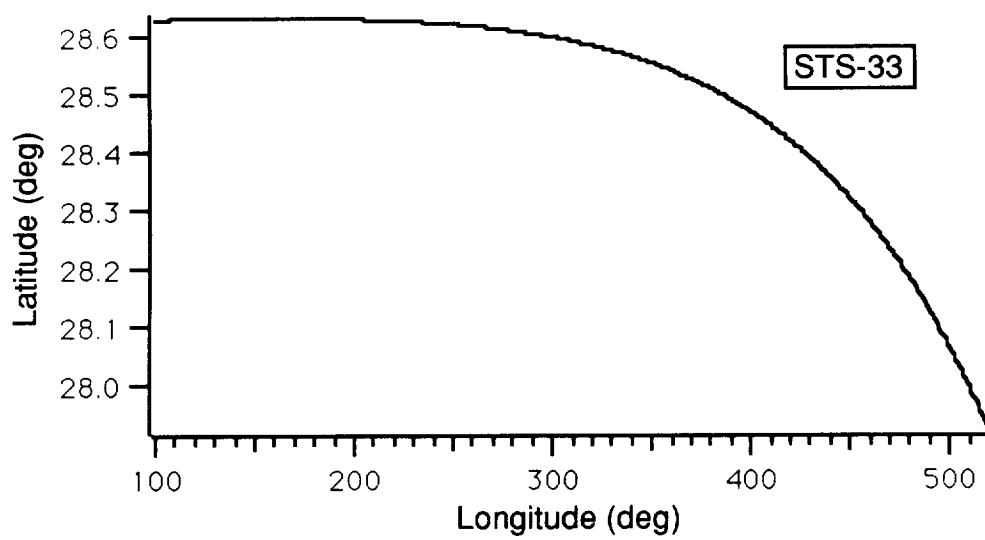


a. Latitude vs. Time

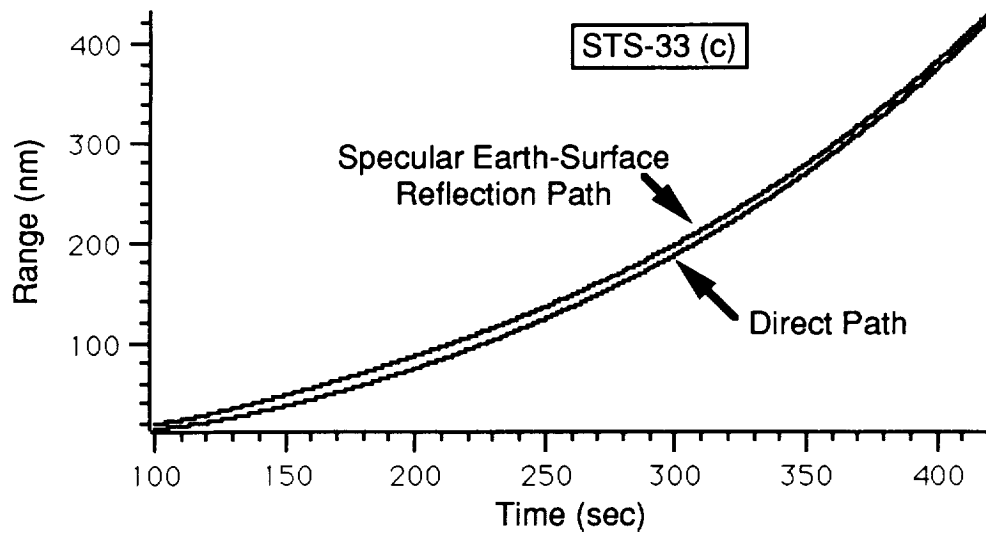


b. Longitude vs. Time

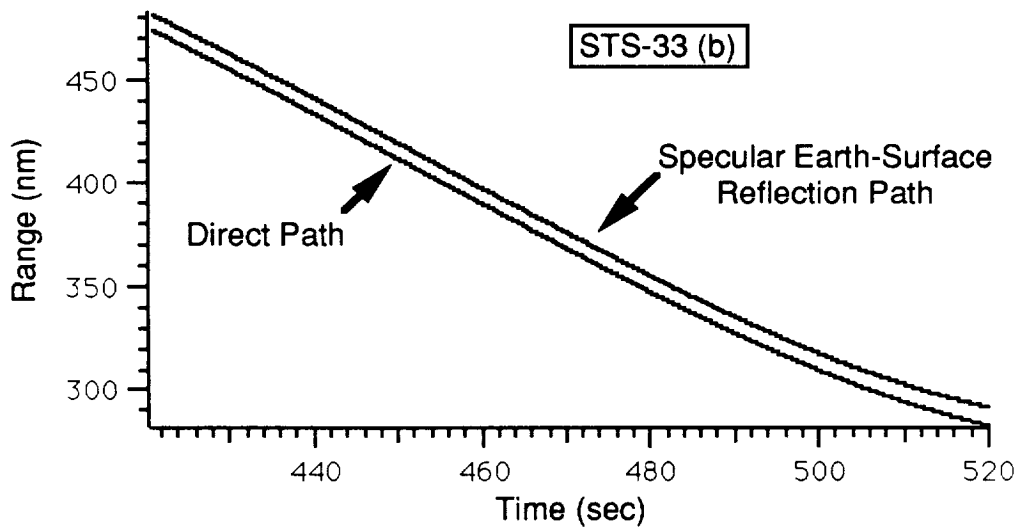
**Plots of Latitude (a.) and Longitude (b.) vs. Time After Launch**



**Ground Trace of Shuttle Trajectory**

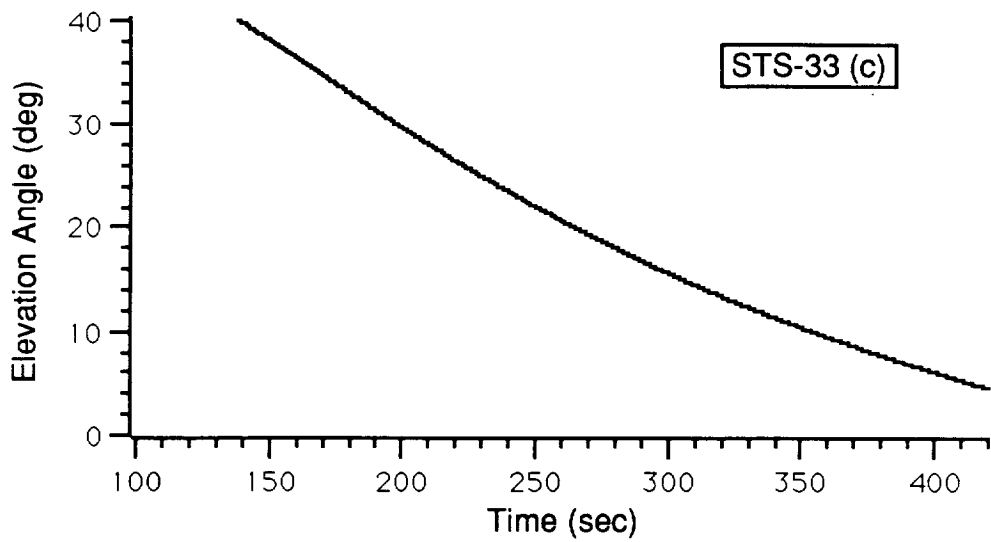


a. Transmission From Cape Canaveral

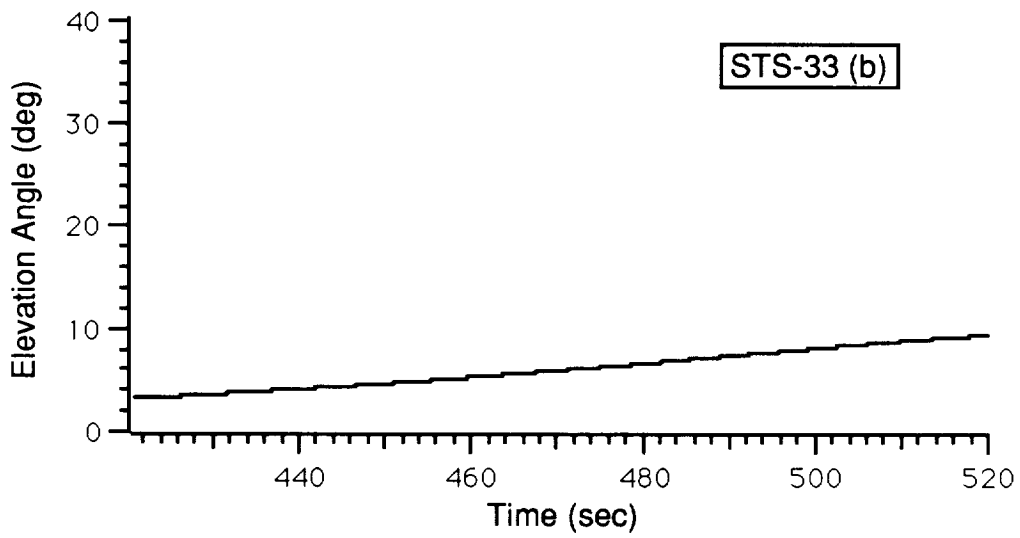


b. Transmission From Bermuda

**Range From Transmitter Site to Shuttle vs. Time After Launch**



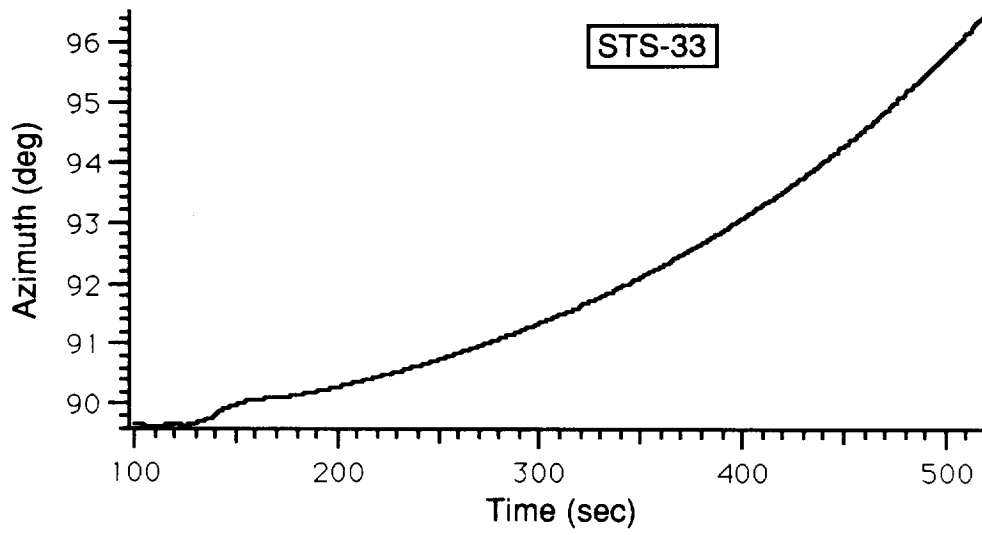
a. Transmission From Cape Canaveral



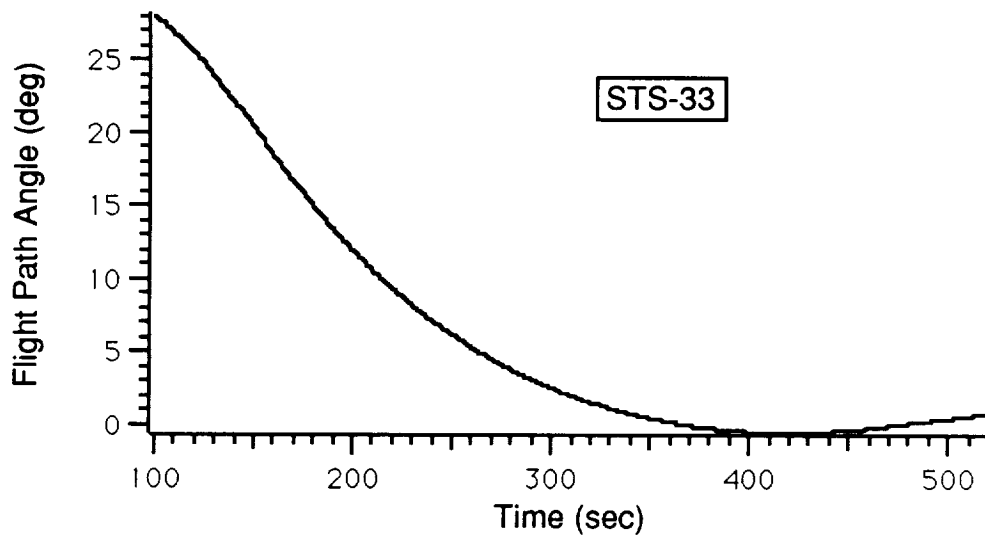
b. Transmission From Bermuda

**Elevation Angle (Transmitting Site to Shuttle) vs. Time After Launch**



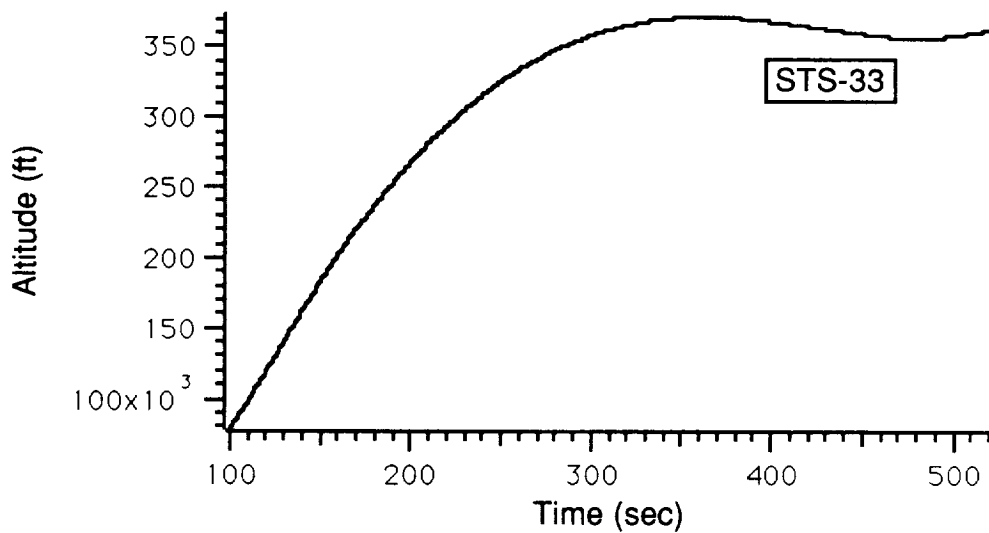


a. Horizontal

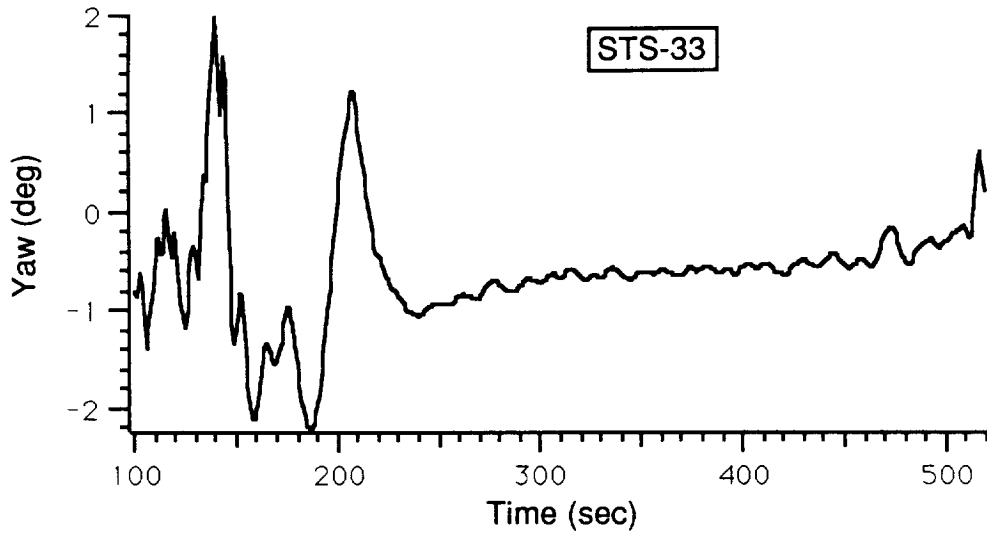


b. Vertical

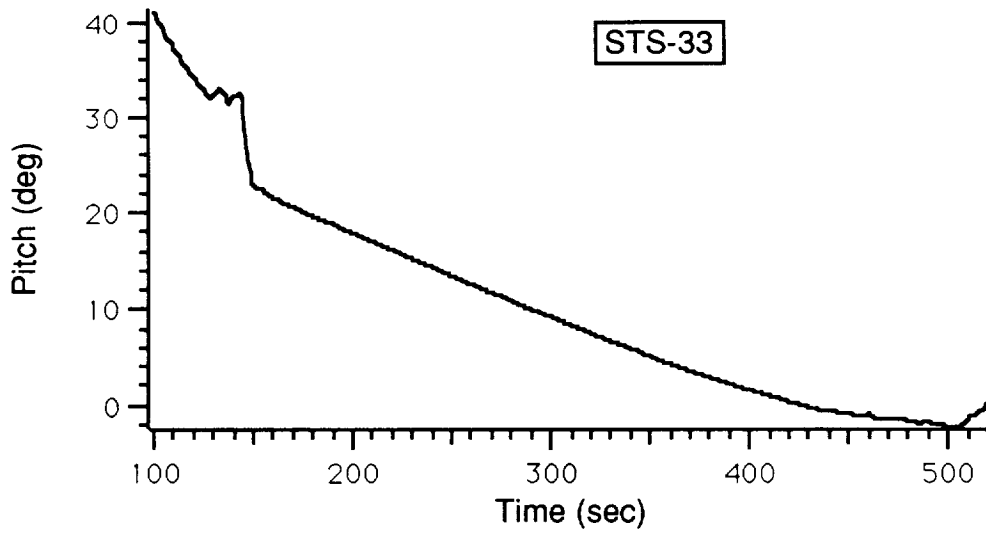
**Shuttle Flight Path Angles vs. Time After Launch**



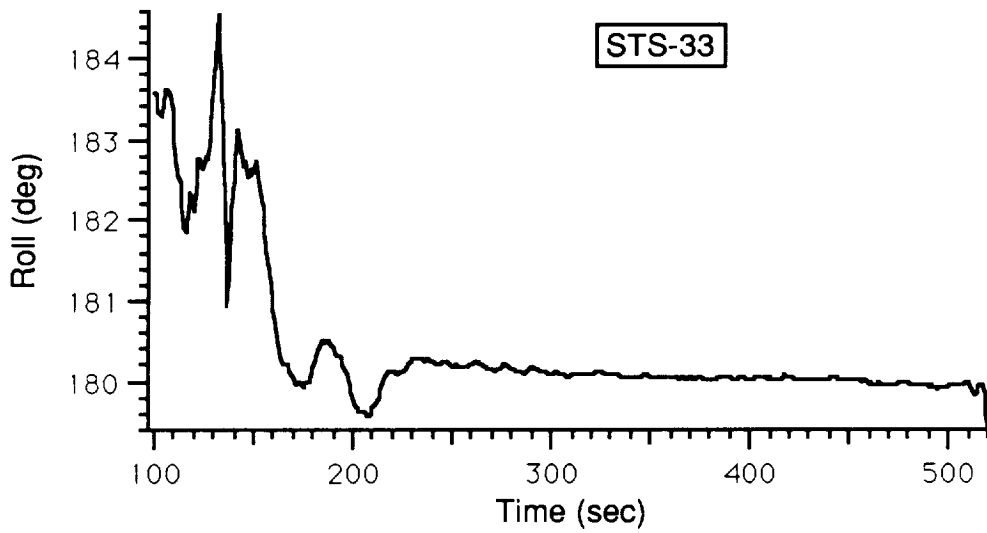
**Shuttle Altitude vs. Time After Launch**



a. Yaw Attitude

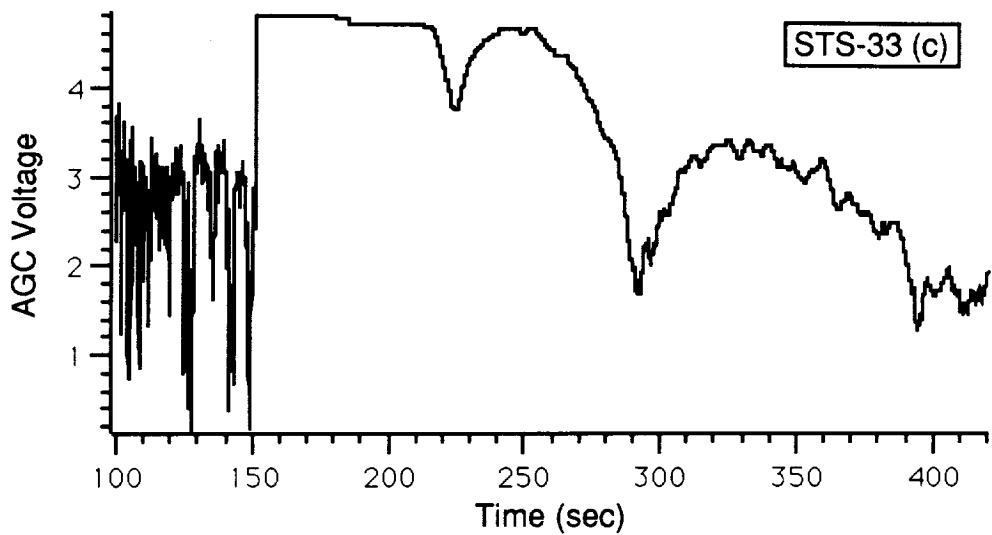


b. Pitch Attitude

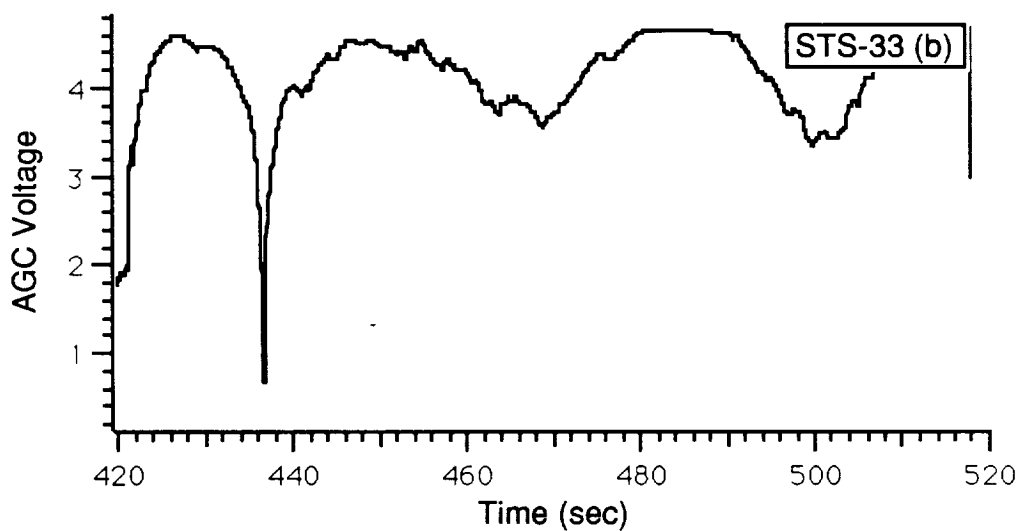


c. Roll Attitude

**Shuttle Attitude Angles (With Respect to Velocity Vector) vs. Time After Launch**

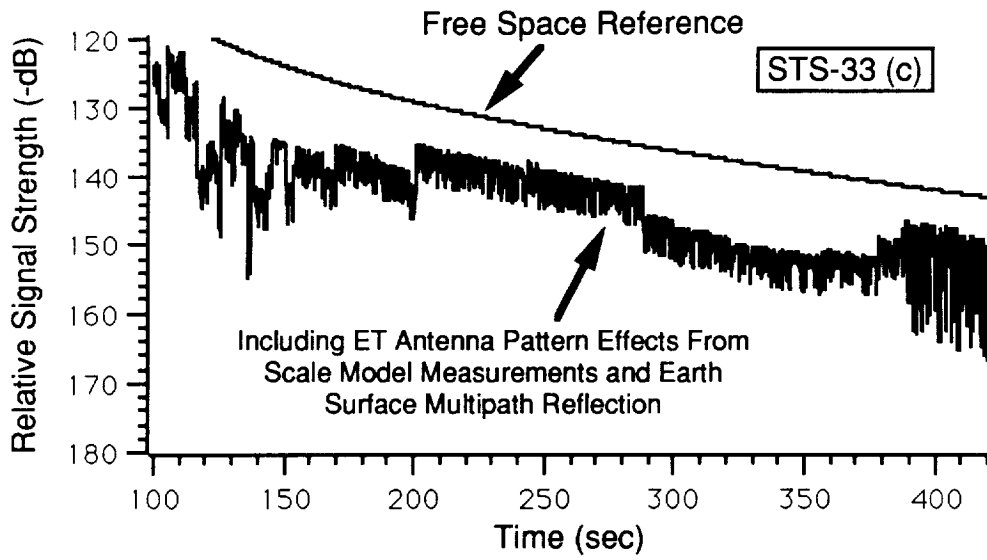


a. Transmission From Cape Canaveral

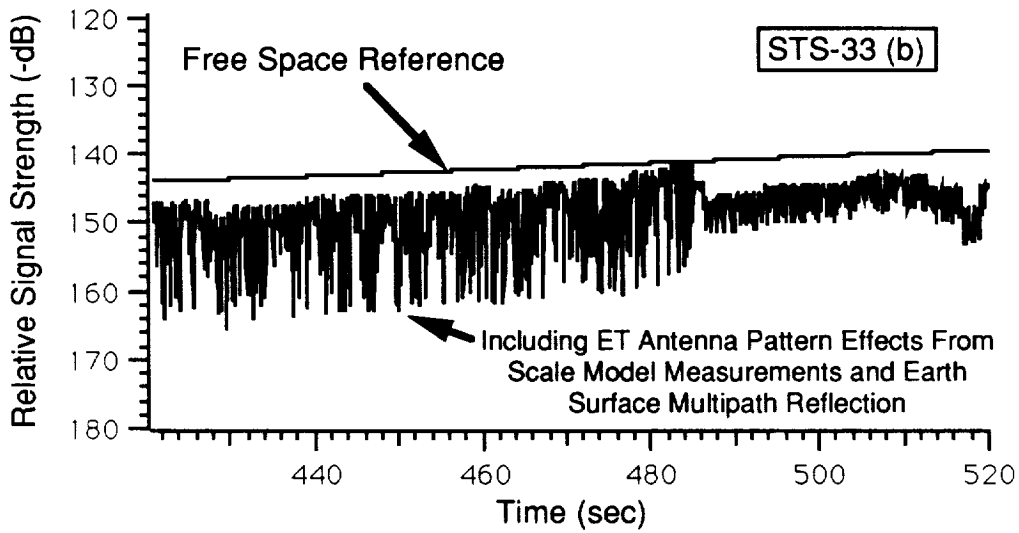


b. Transmission From Bermuda

**Record of ET Receiver AGC Voltage vs. Time After Launch**

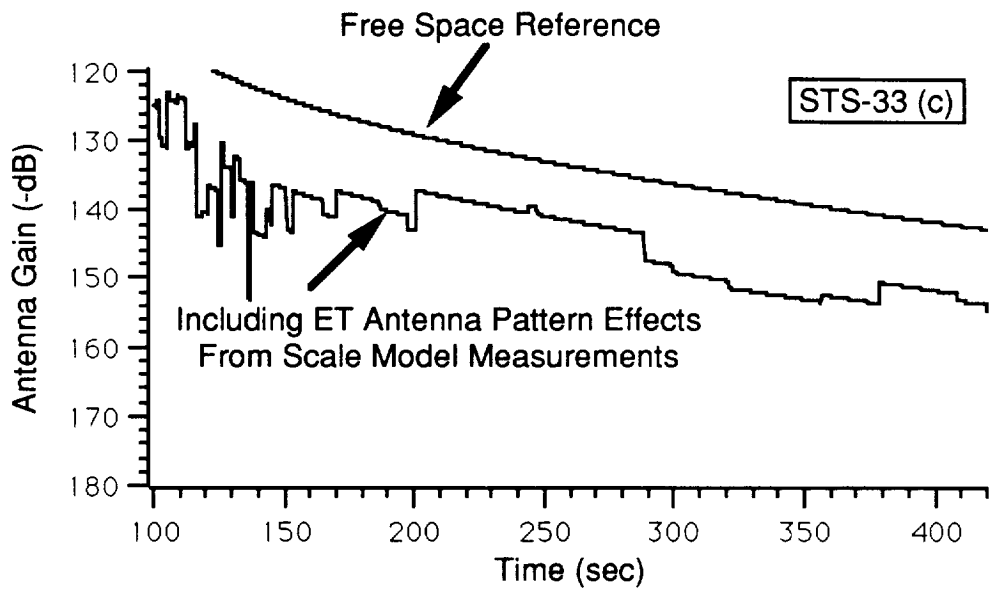


a. Transmission From Cape Canaveral

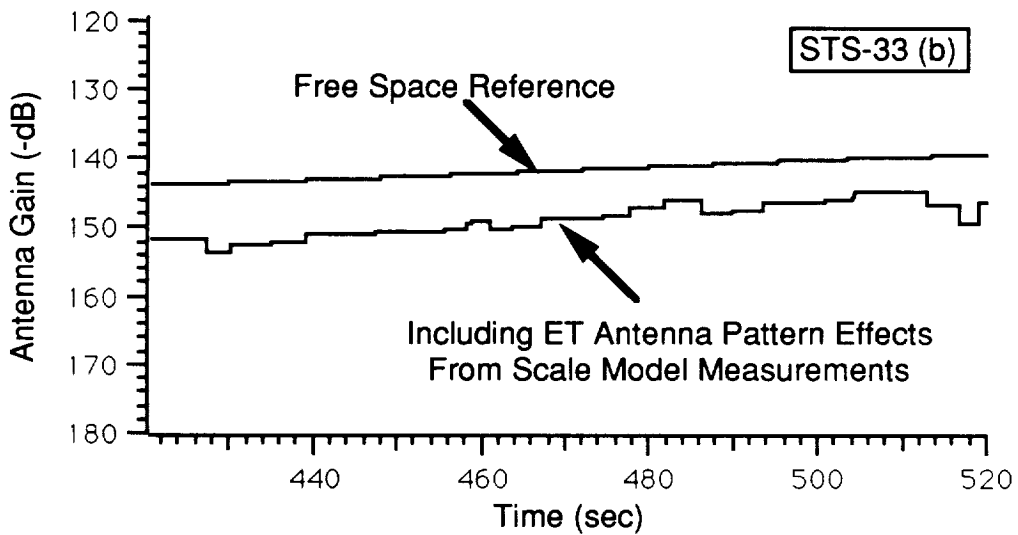


b. Transmission From Bermuda

**Computer Simulation of Relative Signal Strength at ET Receiver vs. Time After Launch (Including Earth-Surface Multipath Reflection)**



a. Transmission From Cape Canaveral



b. Transmission From Bermuda

**Computer Simulation of Relative Signal Strength at ET Receiver vs. Time After Launch  
(Without Earth-Surface Multipath Reflection)**

Yaw Degrees

20

40

60

80

100

120

140

160

20

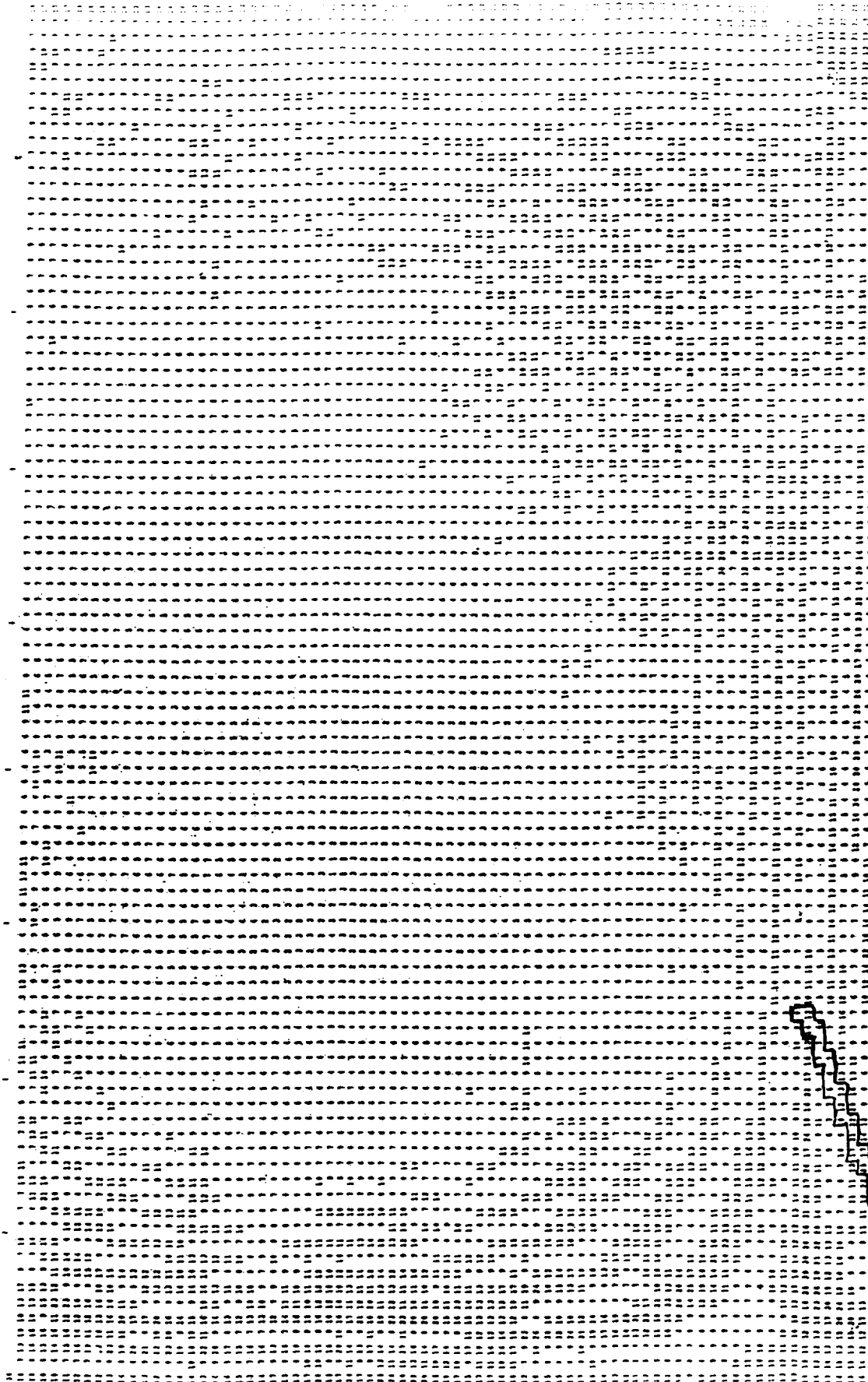
60

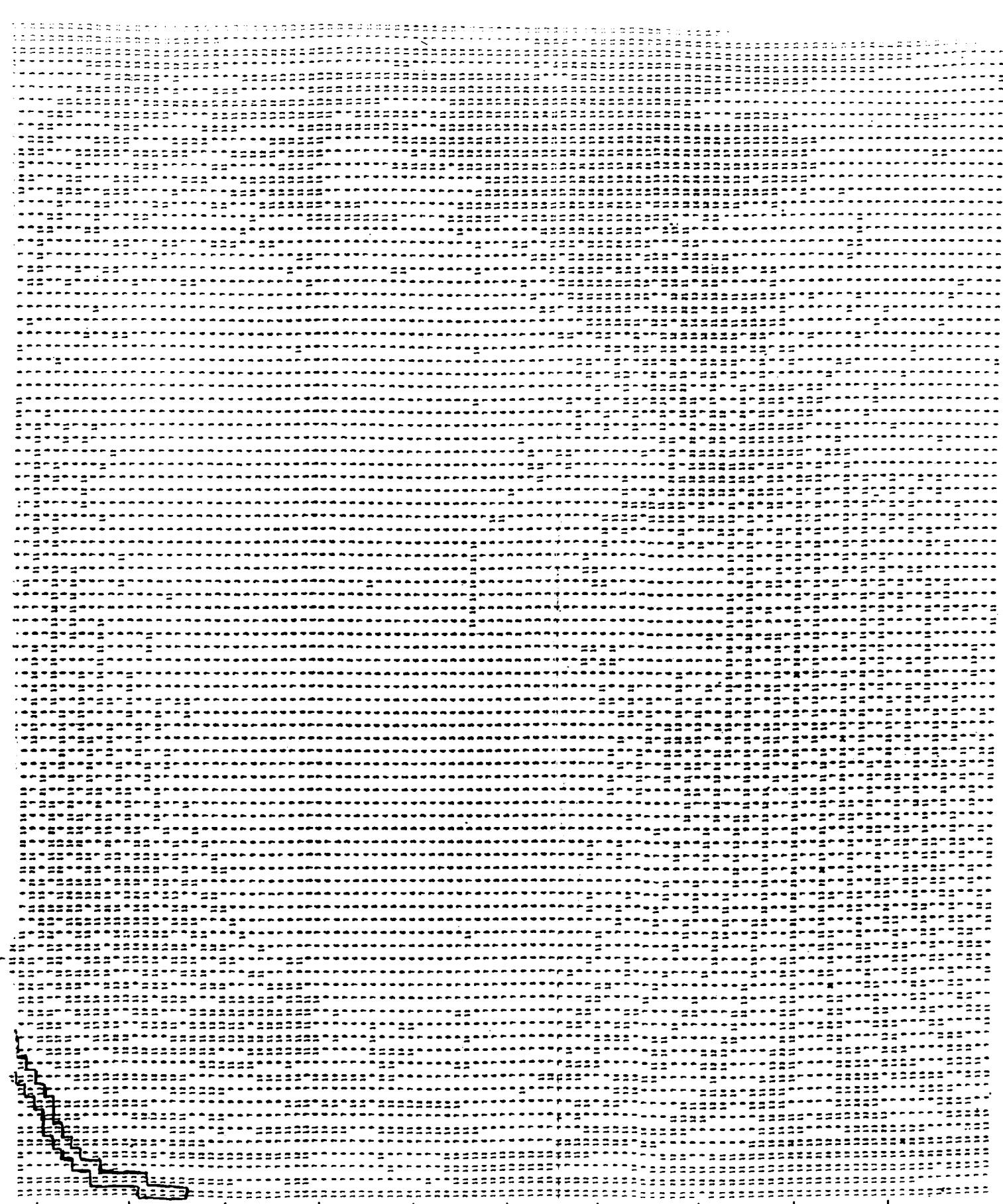
100

140

FOLDOUT FRAME

Locus of Ang





180  
140  
100  
60  
20  
Roll Degrees

STS-33 (Cape Canaveral)

es of Arrival on ET Antenna Pattern

FOLDOUT FRAME 2

Yaw Degrees

20

40

60

80

100

120

140

160

20

60

100

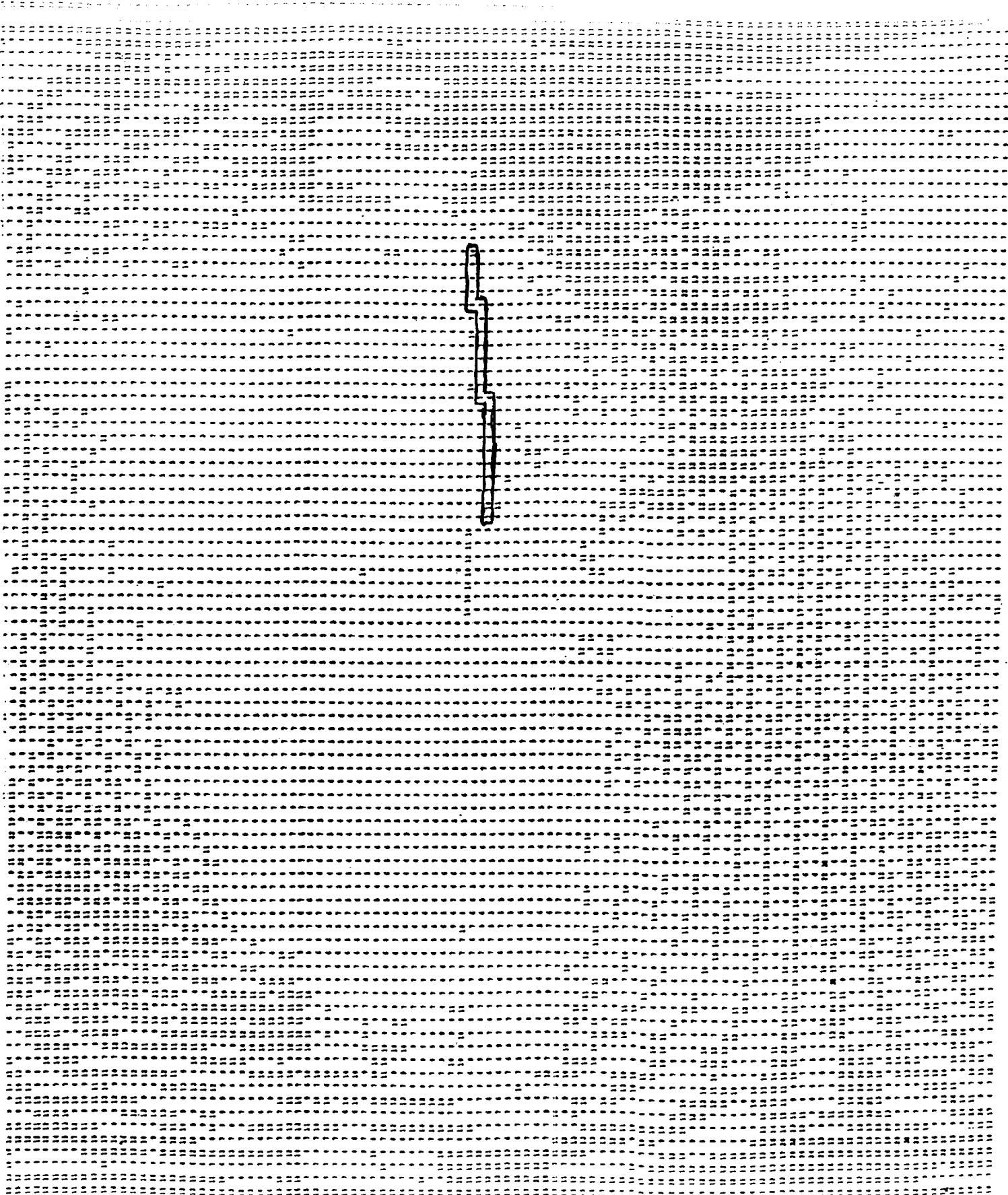
140

FOLDOUT

/

Locus of Ang





180  
140  
100  
60  
20  
Roll Degrees

STS-33 (Bermuda)

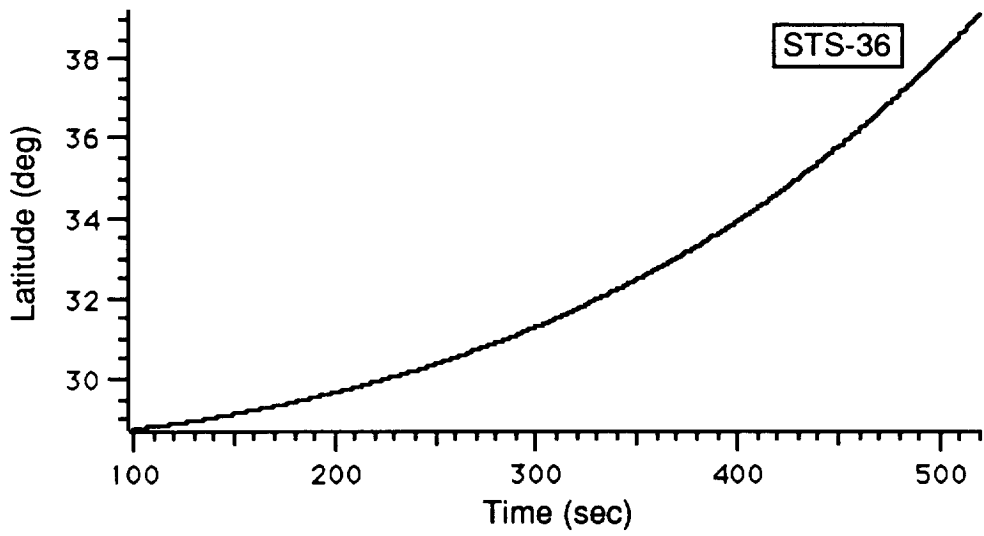
Time of Arrival on ET Antenna Pattern

FOLLOW

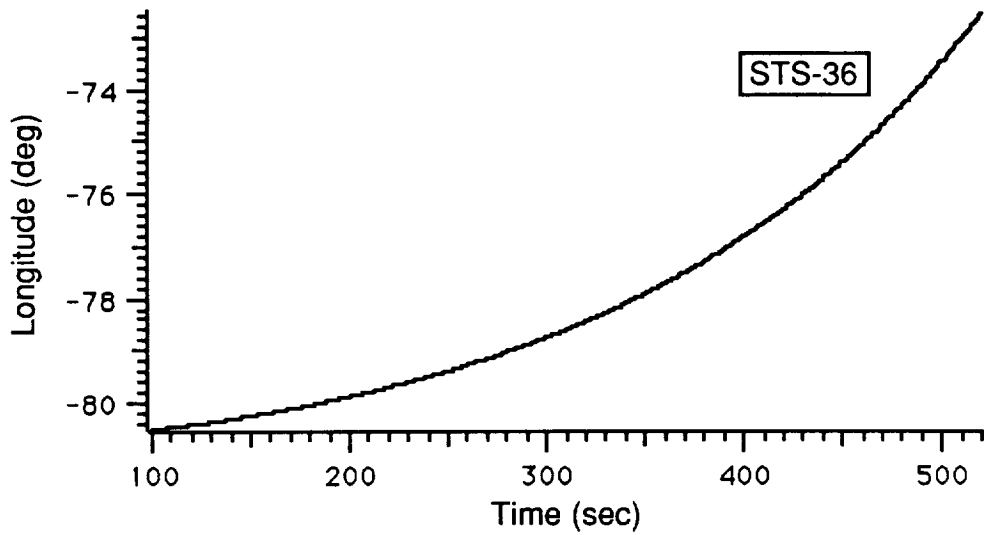
2

STS-36  
Appendix

The STS-36 flight was launched to the northeast. It did not experience deep fades. Some signal degradation did occur at approximately 380 seconds in flight for some duration but the magnitude of the losses were not severe.

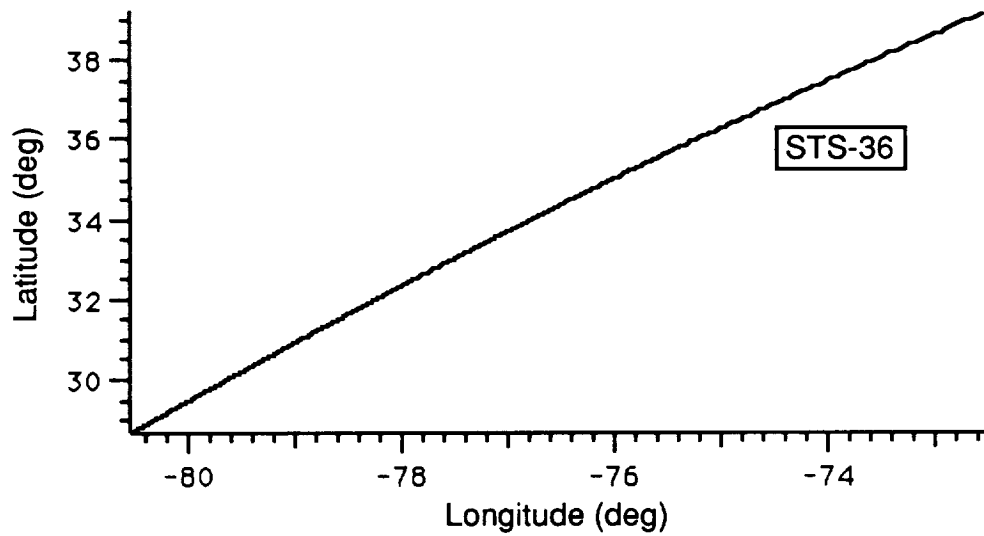


a. Latitude vs. Time

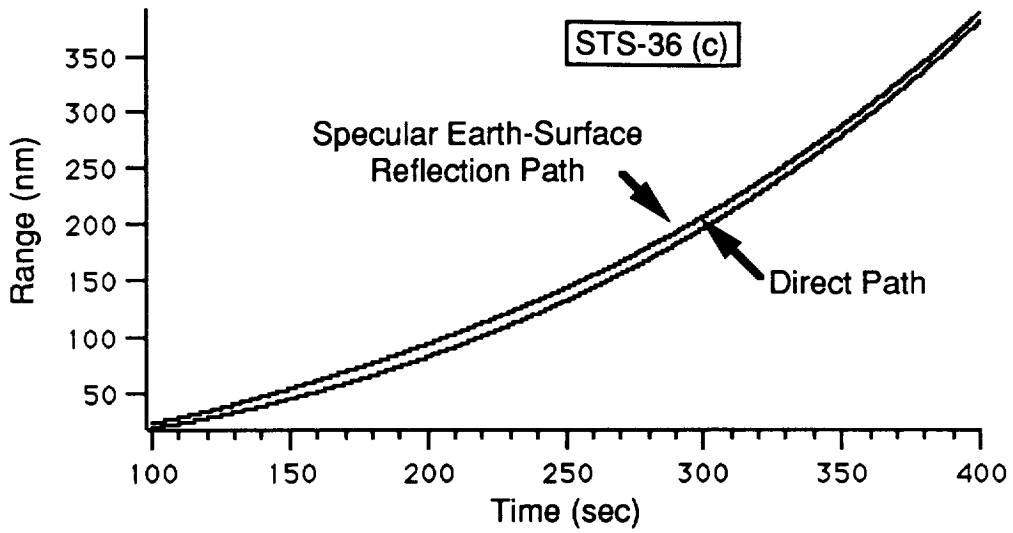


b. Longitude vs. Time

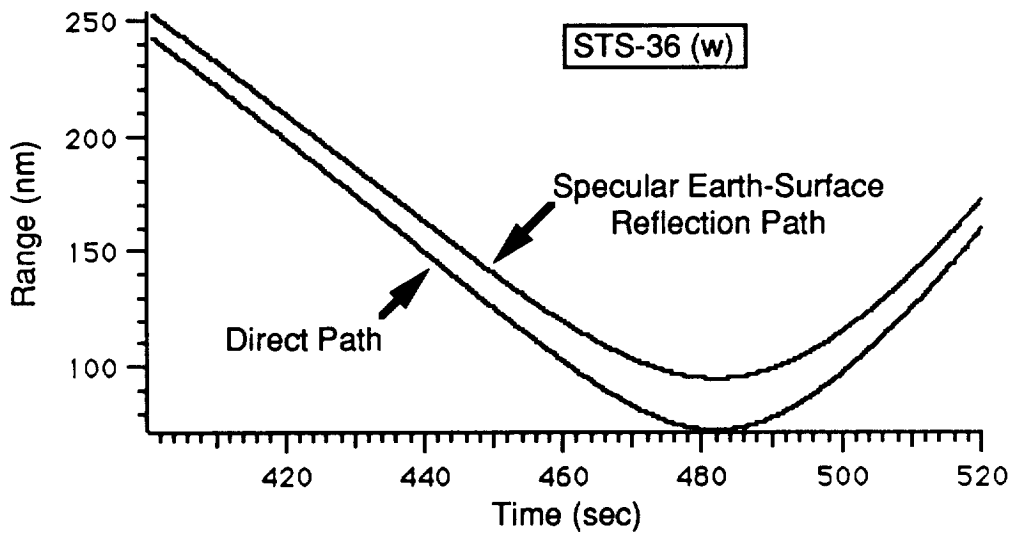
**Plots of Latitude (a.) and Longitude (b.) vs. Time After Launch**



**Ground Trace of Shuttle Trajectory**

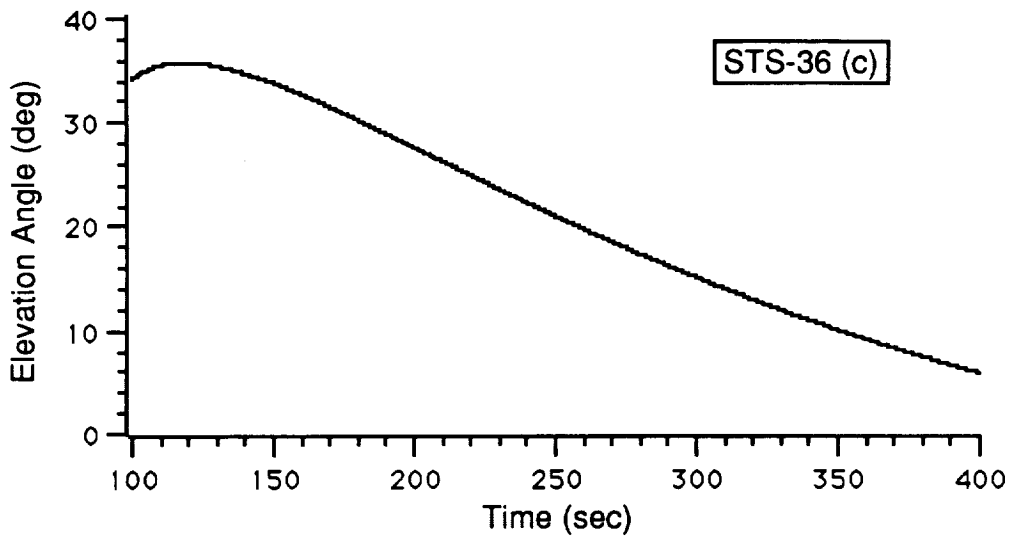


a. Transmission From Cape Canaveral

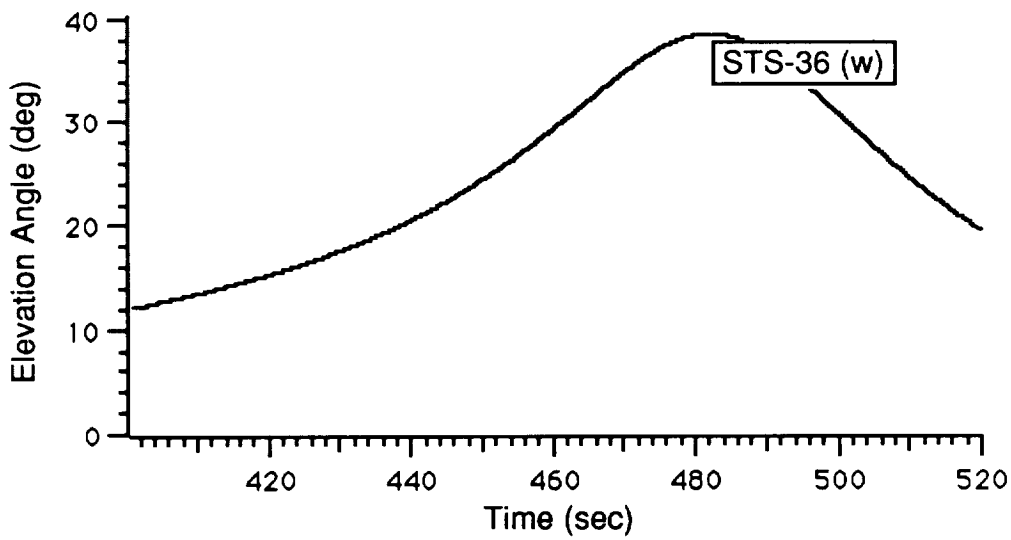


b. Transmission From Bermuda

**Range From Transmitter Site to Shuttle vs. Time After Launch**

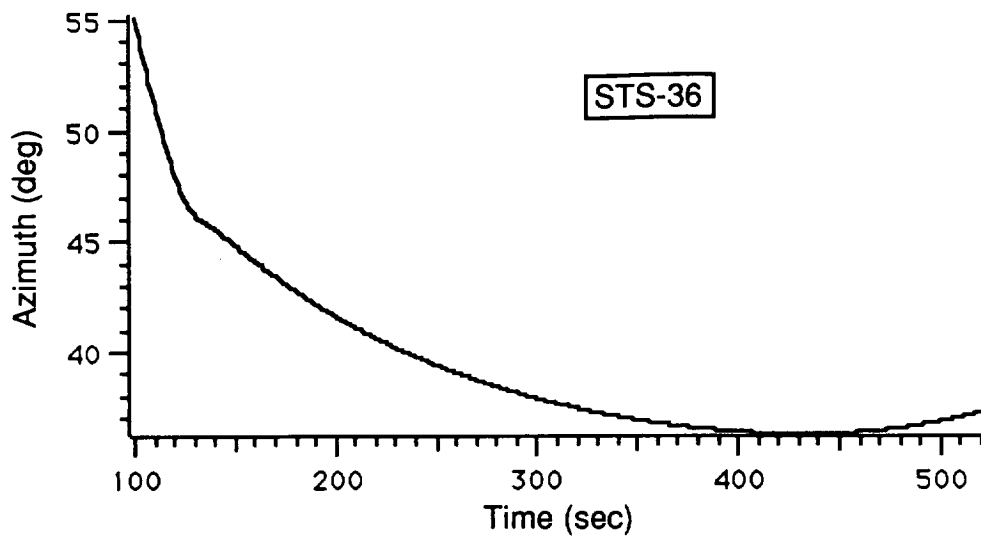


a. Transmission From Cape Canaveral

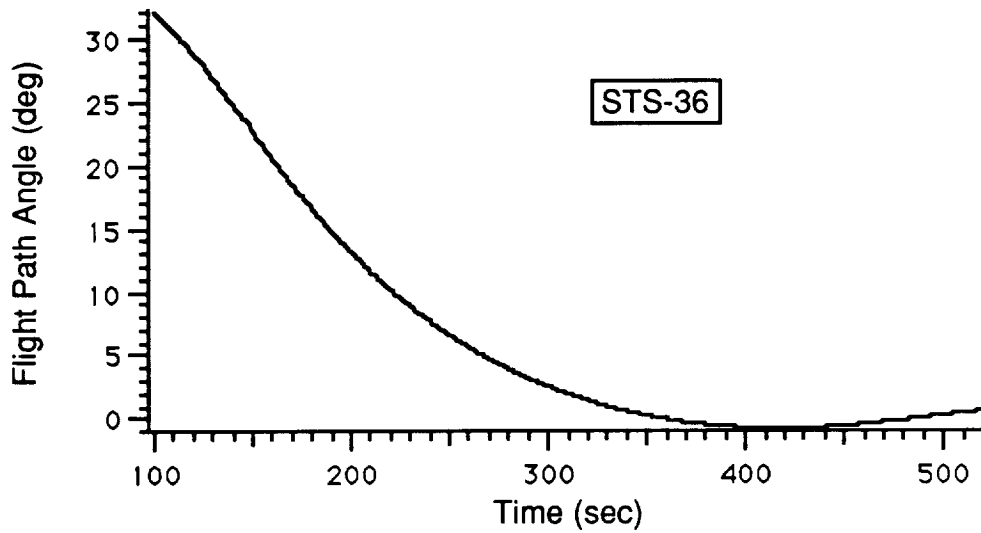


b. Transmission From Bermuda

**Elevation Angle (Transmitting Site to Shuttle) vs. Time After Launch**

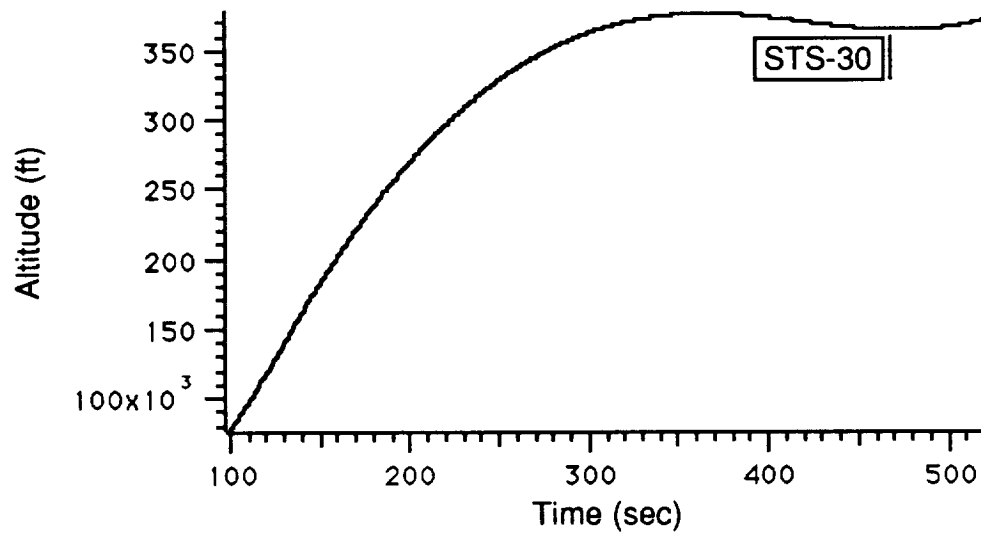


a. Horizontal

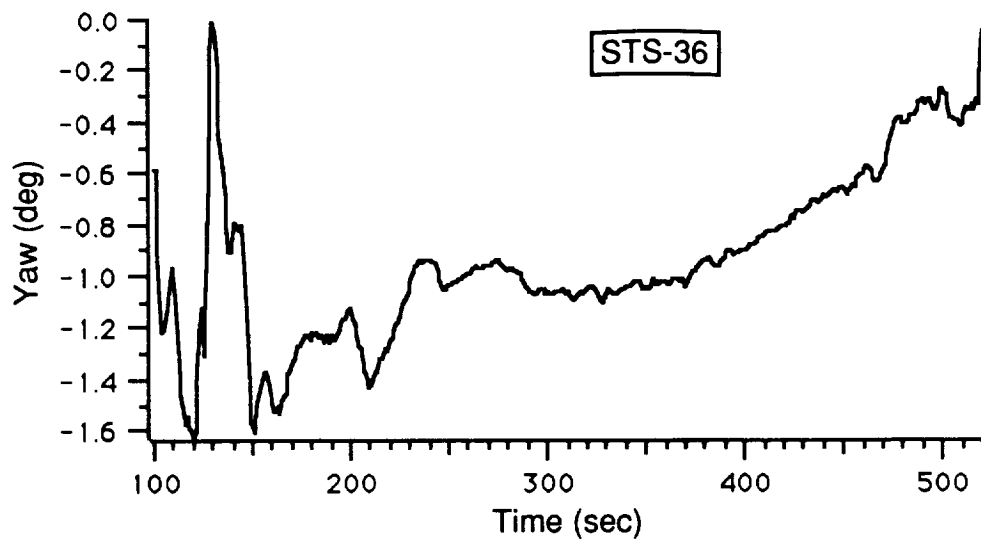


b. Vertical

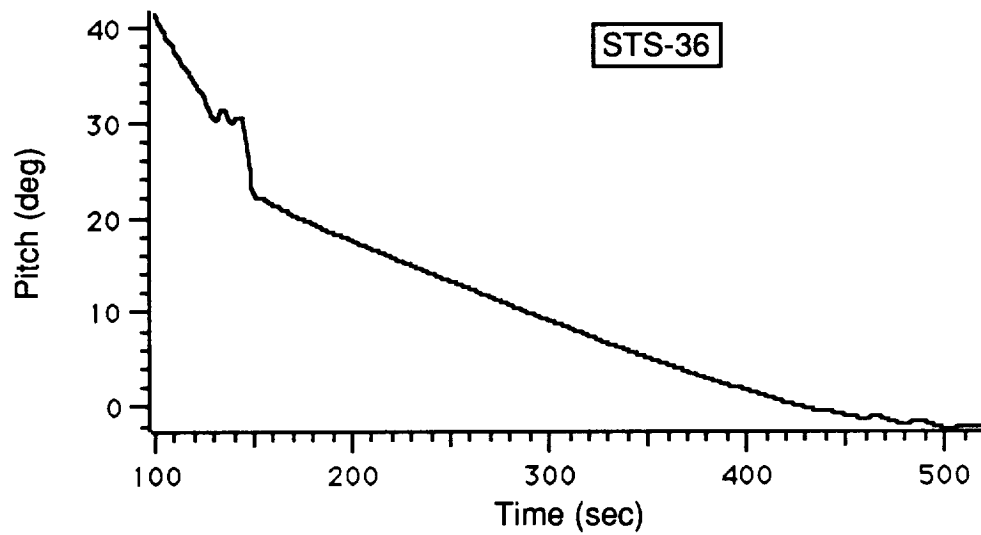
**Shuttle Flight Path Angles vs. Time After Launch**



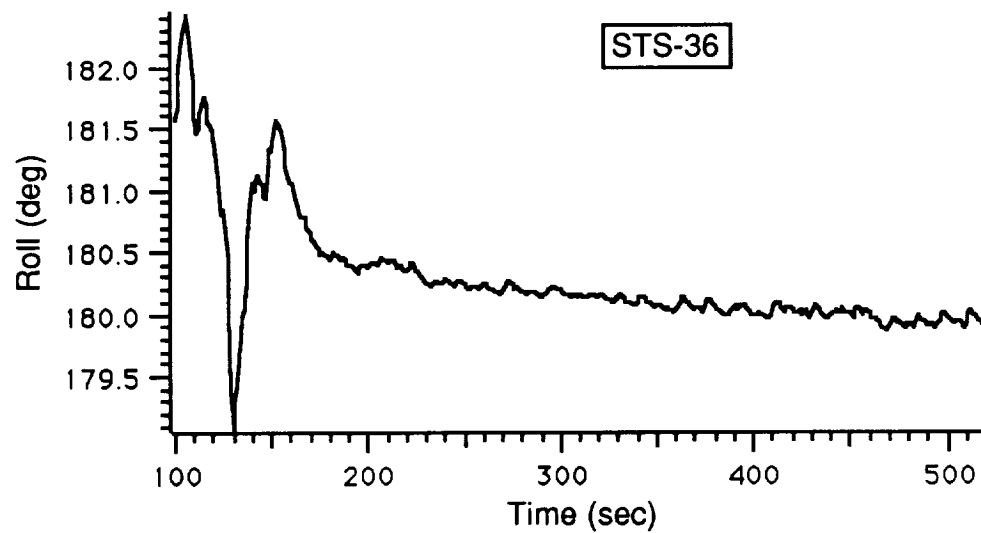
**Shuttle Altitude vs. Time After Launch**



a. Yaw Attitude

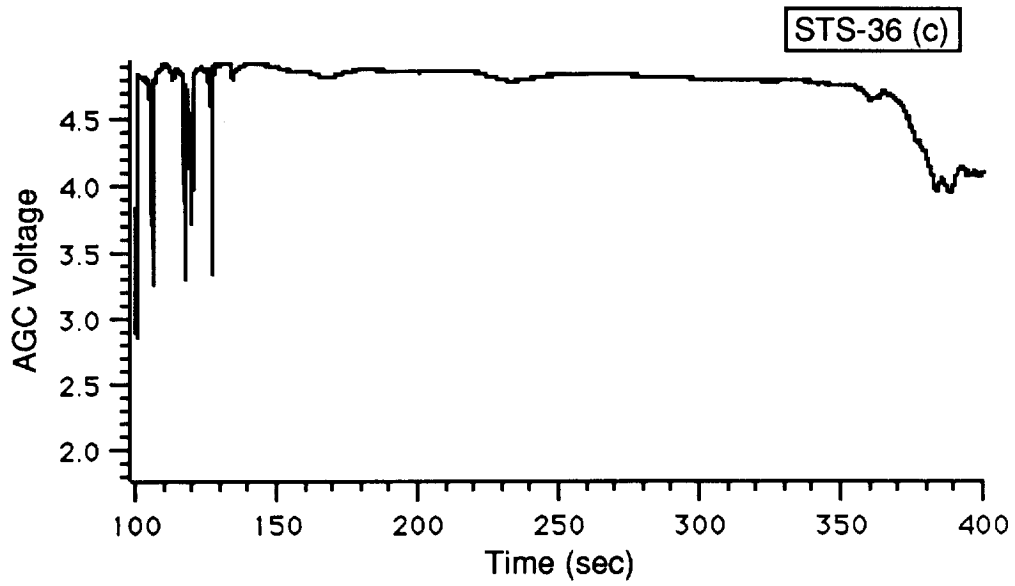


b. Pitch Attitude

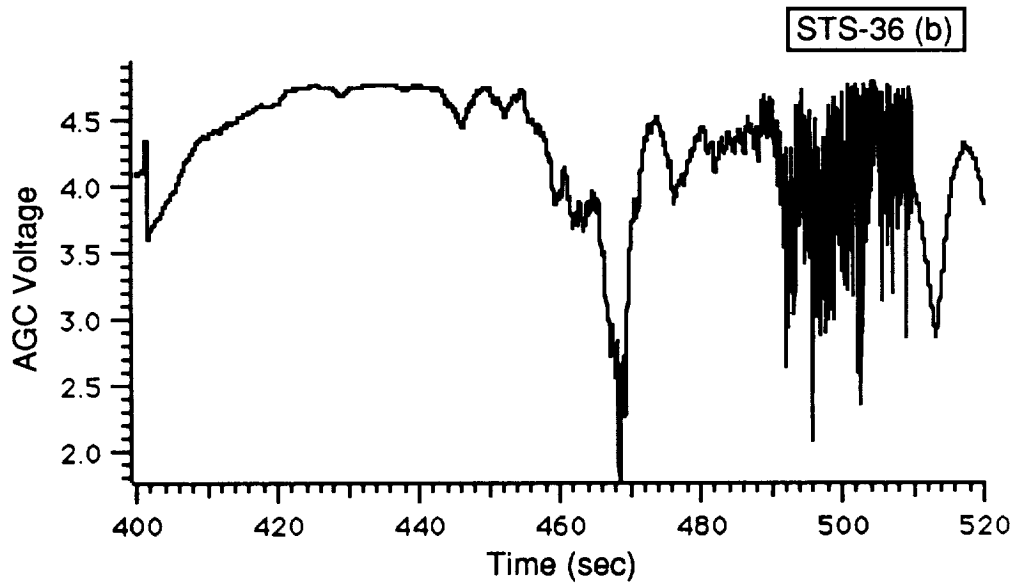


c. Roll Attitude

**Shuttle Attitude Angles (With Respect to Velocity Vector) vs. Time After Launch**



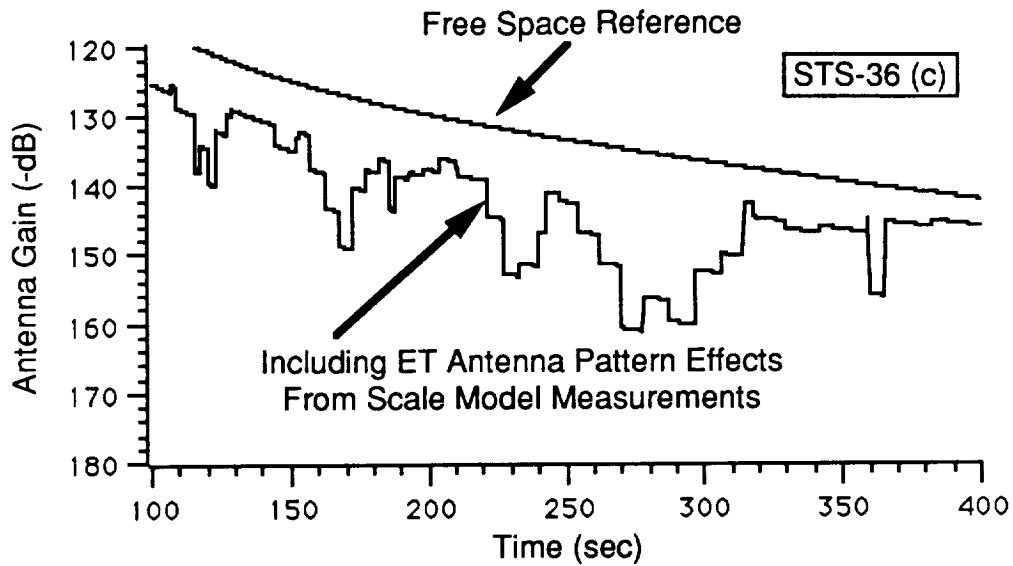
a. Transmission From Cape Canaveral



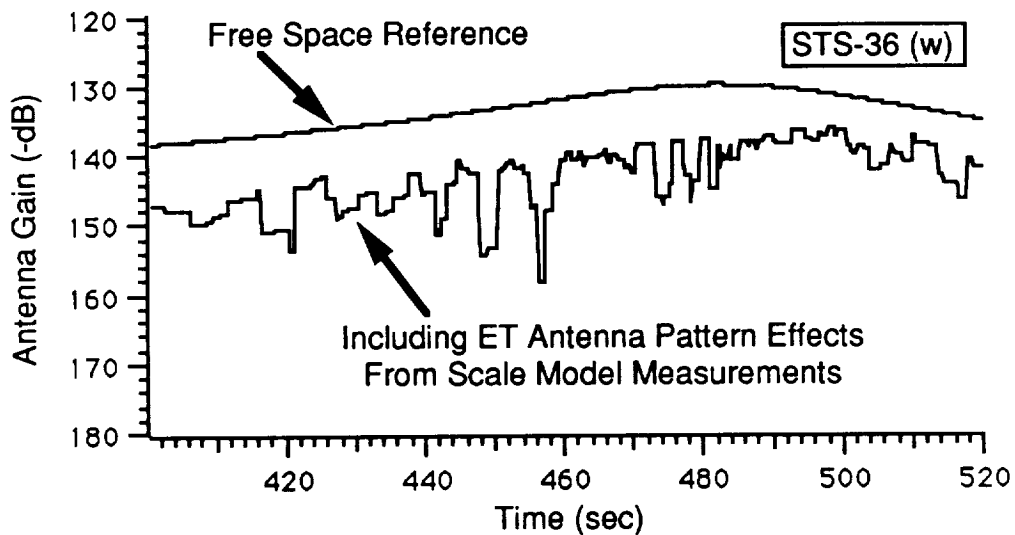
b. Transmission From Bermuda

**Record of ET Receiver AGC Voltage vs. Time After Launch**



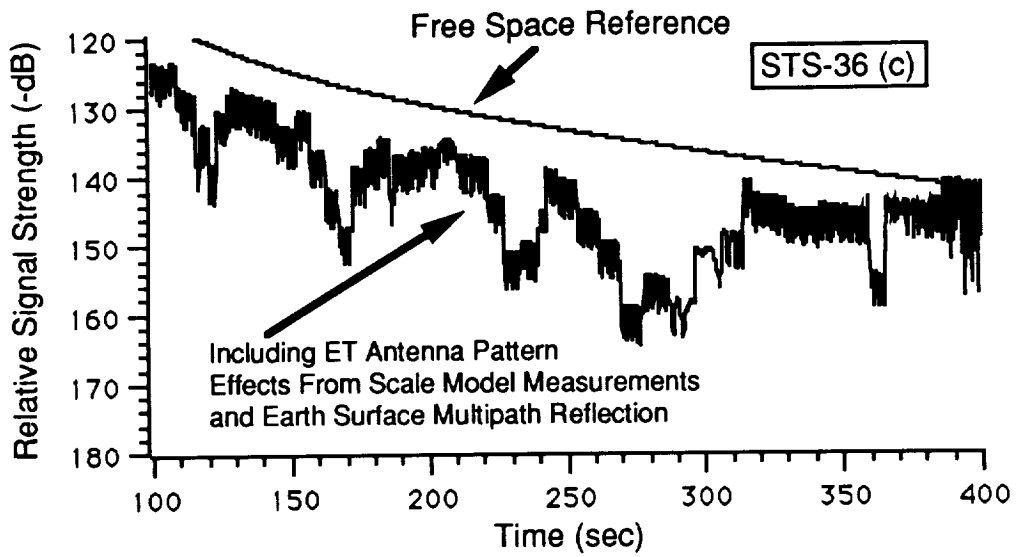


a. Transmission From Cape Canaveral

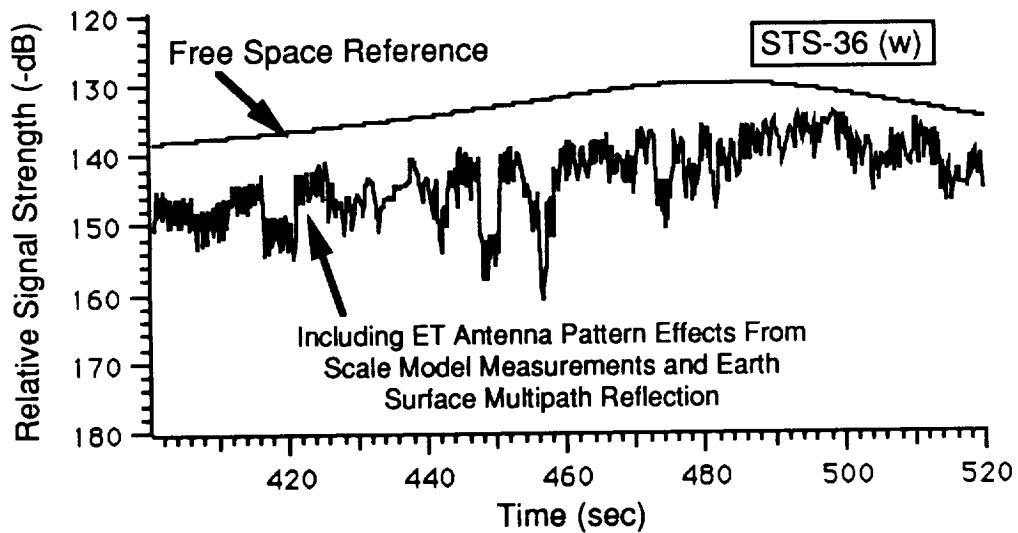


b. Transmission From Bermuda

**Computer Simulation of Relative Signal Strength at ET Receiver vs. Time After Launch  
(Without Earth-Surface Multipath Reflection)**



a. Transmission From Cape Canaveral



b. Transmission From Wallops Island

**Computer Simulation of Relative Signal Strength at ET Receiver vs. Time After Launch  
(Including Earth-Surface Multipath Reflection)**

Yaw Degrees

20

40

60

80

100

120

140

160

20

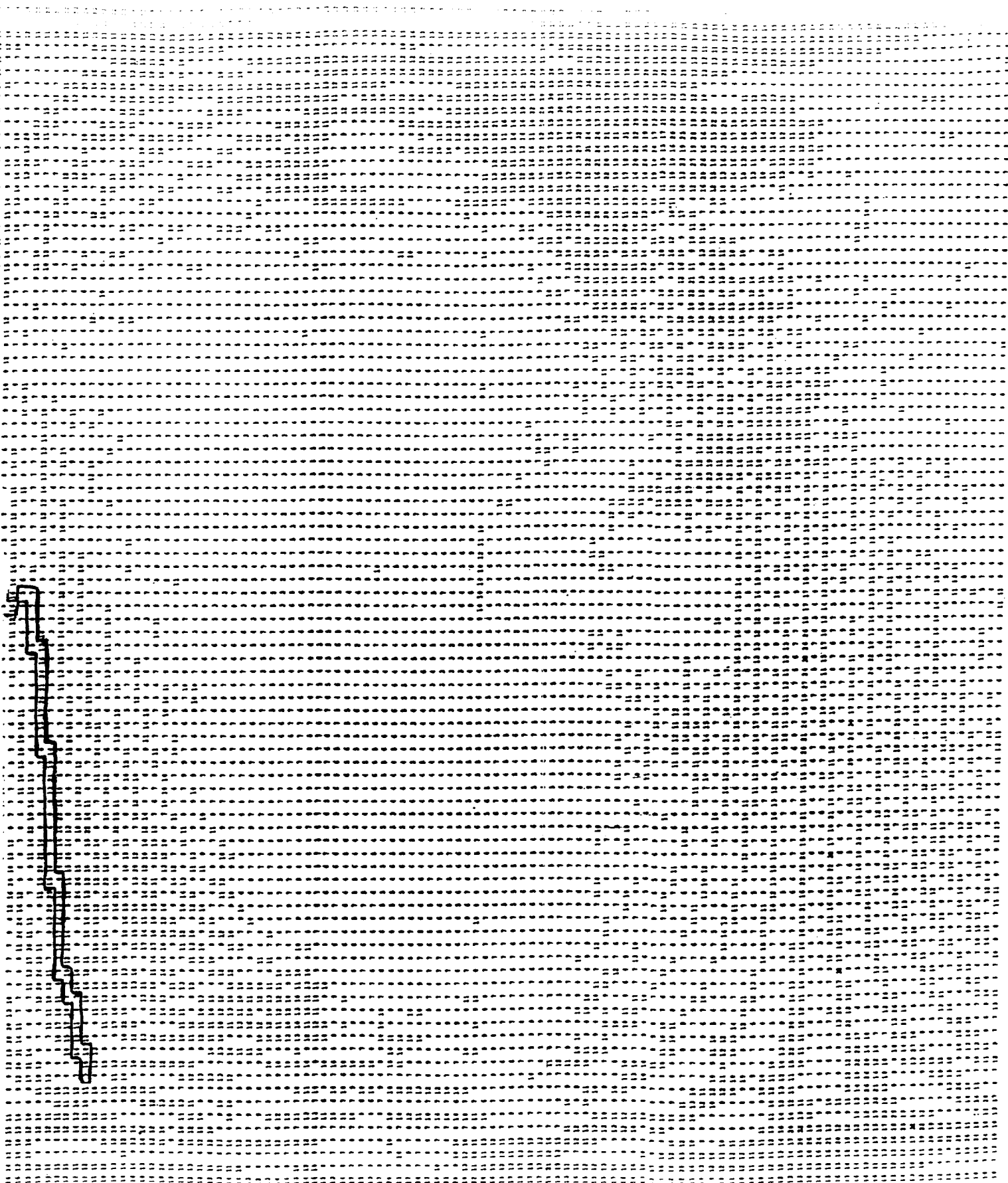
60

100

140

FOLDOUT FRAME

Locus of A



180

140

100

60

20

Roll Degrees

STS-36 (Cape Canaveral)

Angles of Arrival on ET Antenna Pattern

FOLDOUT DRAWING 2

Yaw Degrees

20

40

60

80

100

120

140

160

20

60

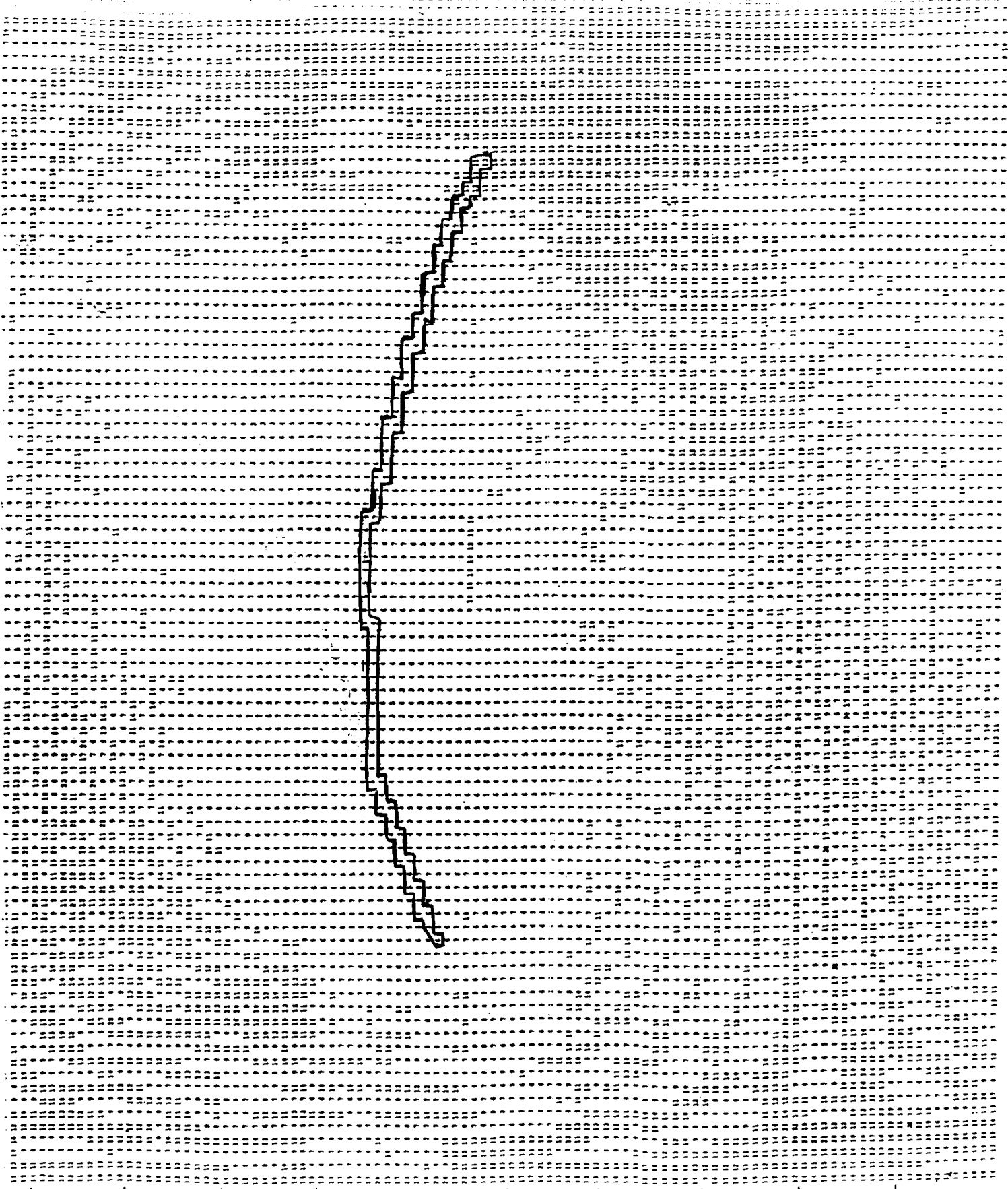
100

140

Locus of An

FOLLOW

1-



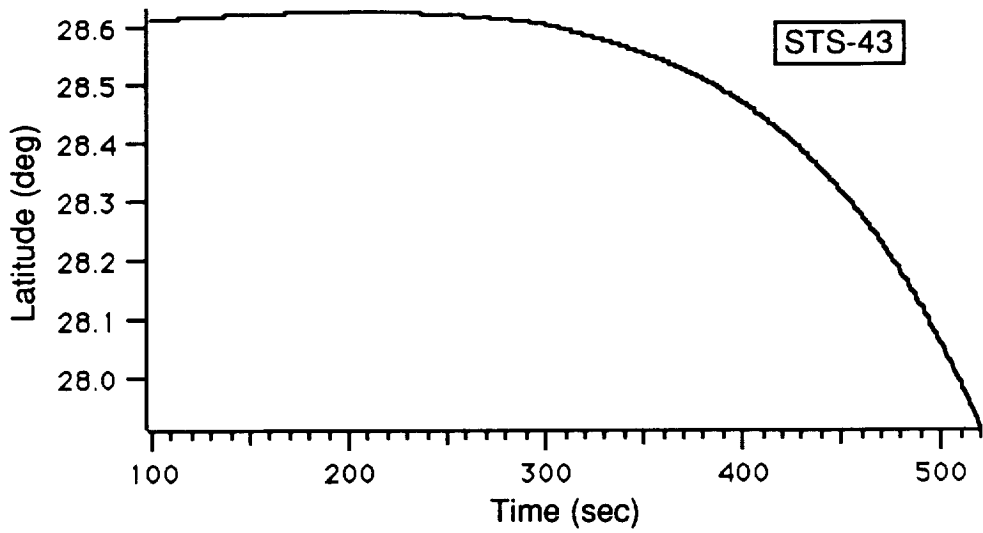
180  
140  
100  
60  
20  
Roll Degrees

STS-36 (Wallops Island)

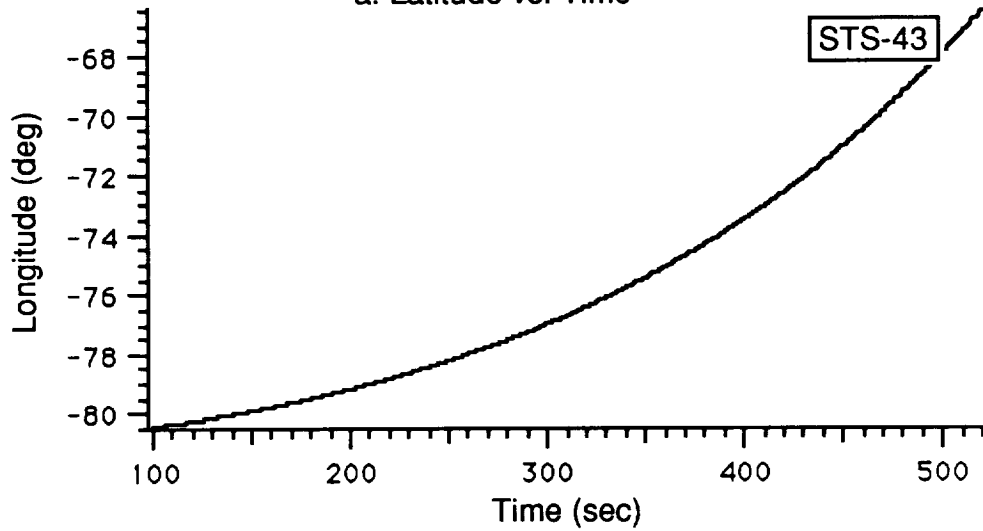
es of Arrival on ET Antenna Pattern

STS-43  
Appendix

The STS-43 flight was launched on an easterly trajectory. Moderate signal fading was observed during the 370 to 420 second period, when handover to Bermuda took place.

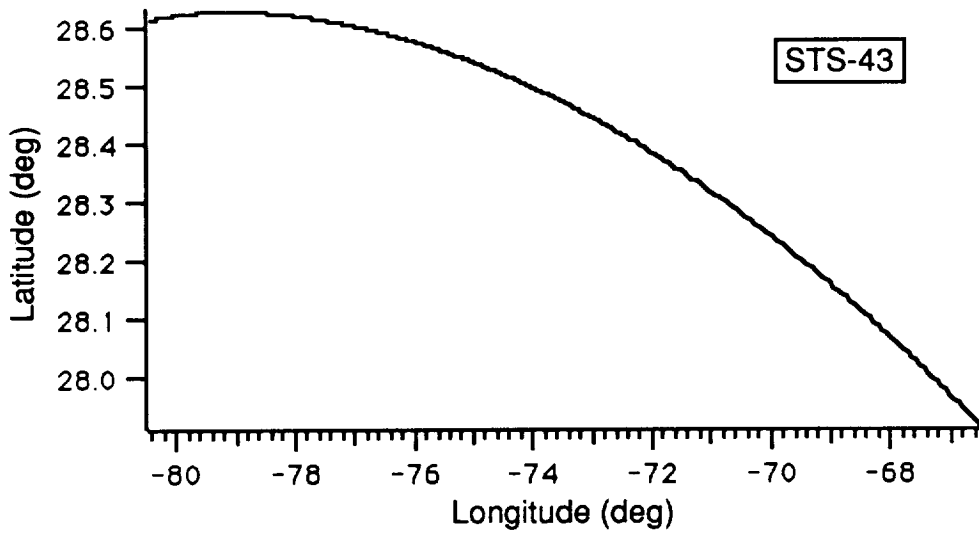


a. Latitude vs. Time



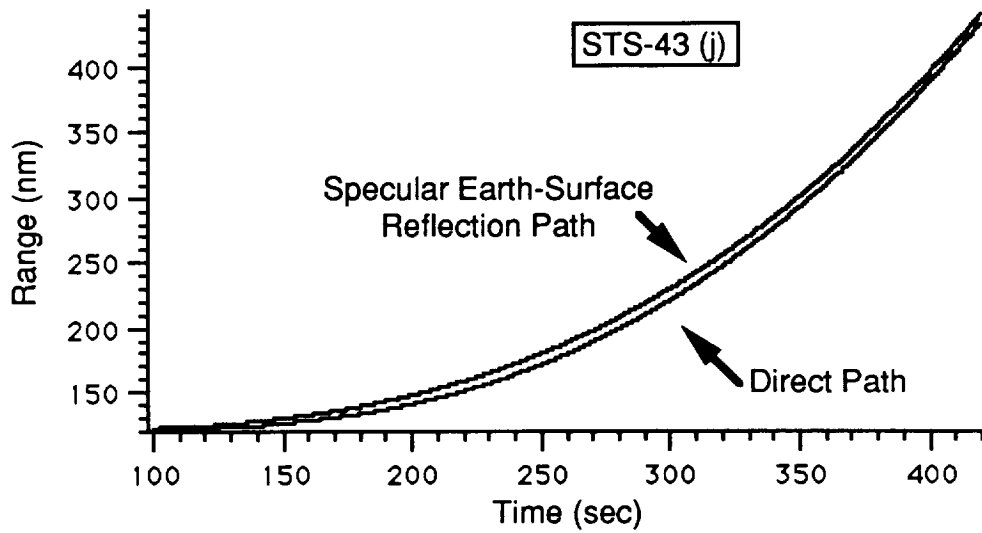
b. Longitude vs. Time

**Plots of Latitude (a.) and Longitude (b.) vs. Time After Launch**

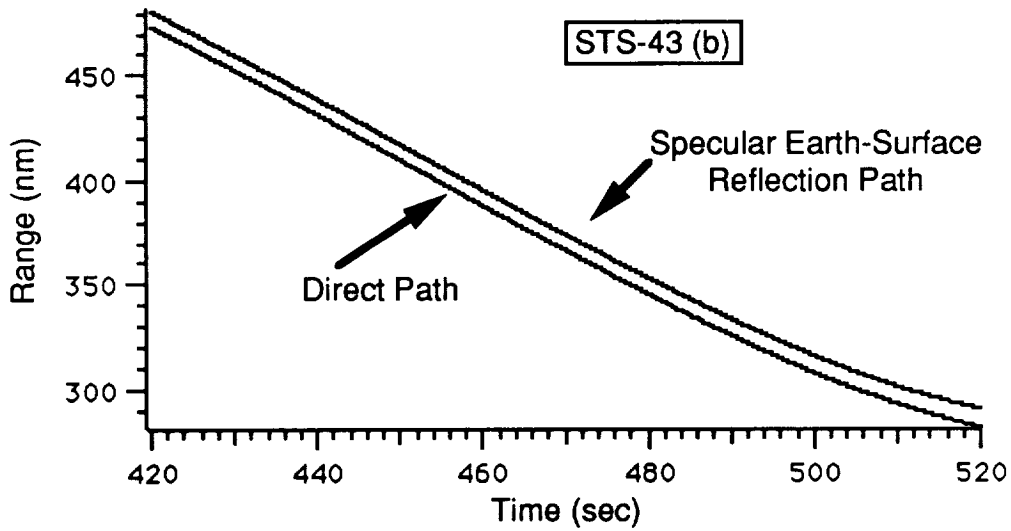


**Ground Trace of Shuttle Trajectory**



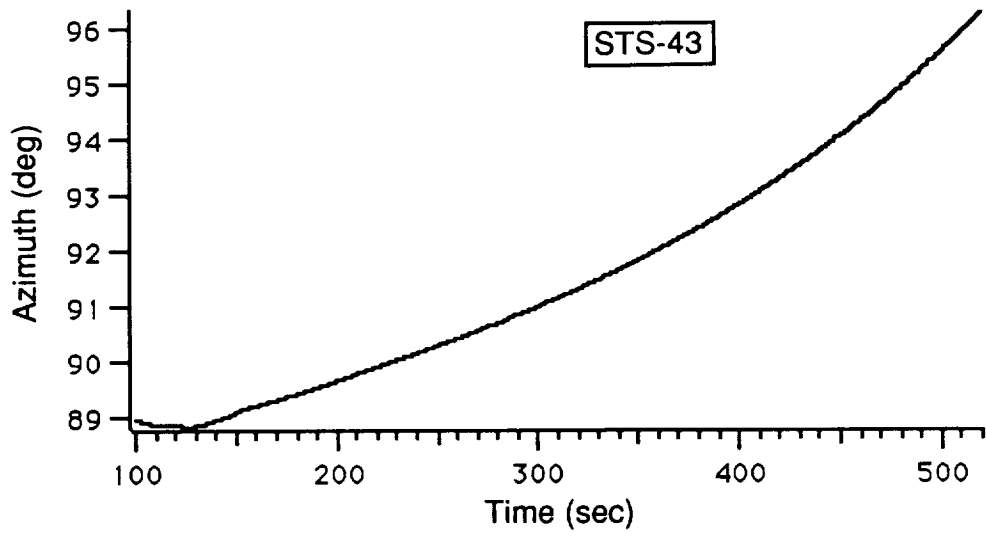


a. Transmission From Cape Canaveral

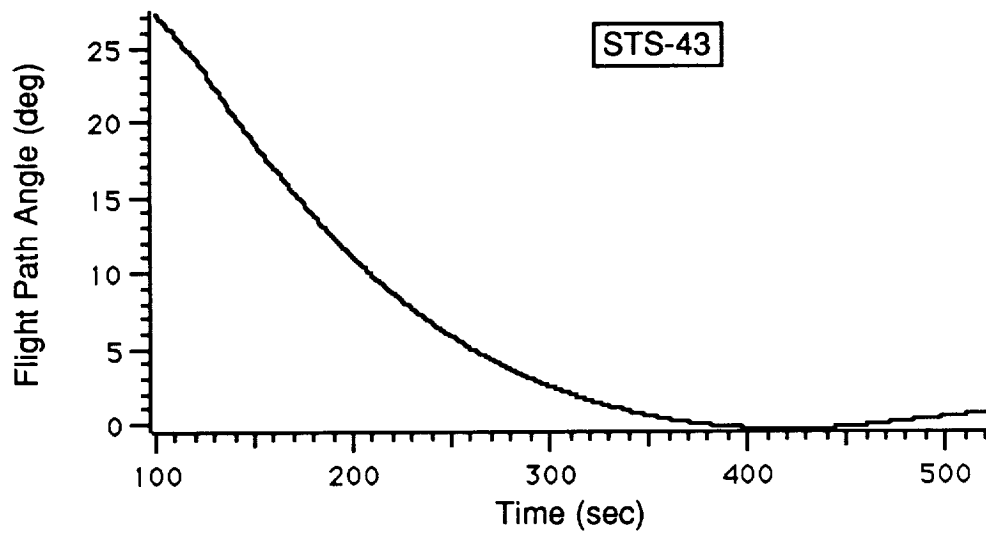


b. Transmission From Bermuda

**Range From Transmitter Site to Shuttle vs. Time After Launch**

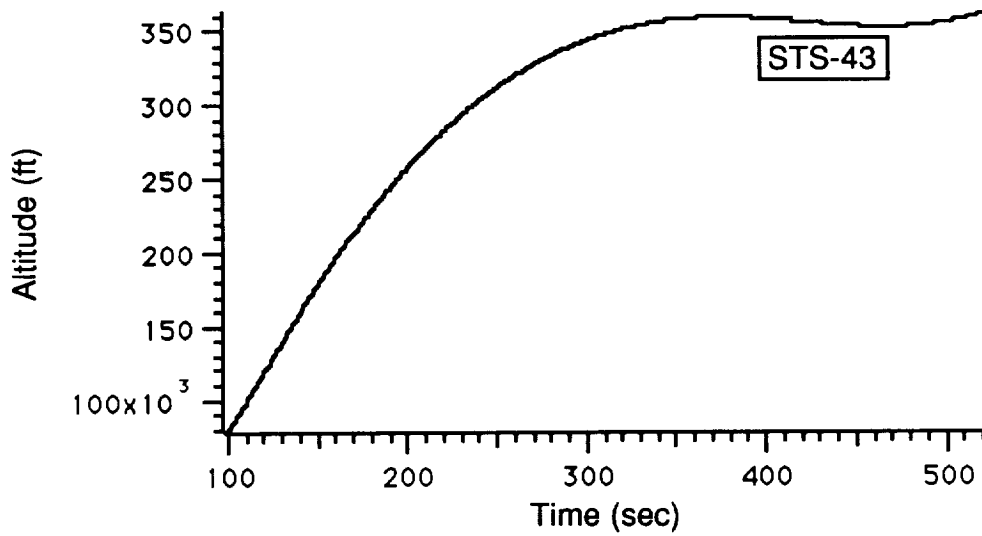


a. Horizontal

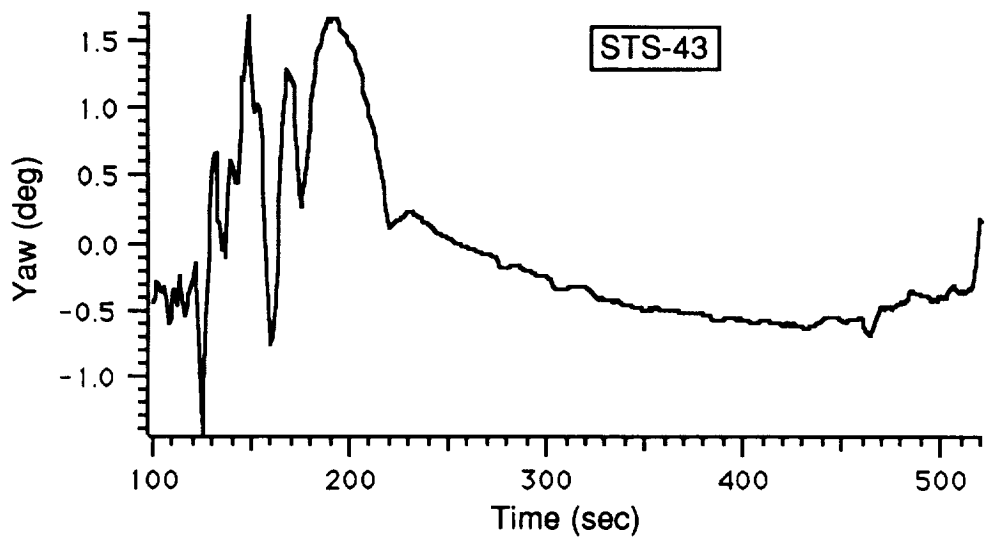


b. Vertical

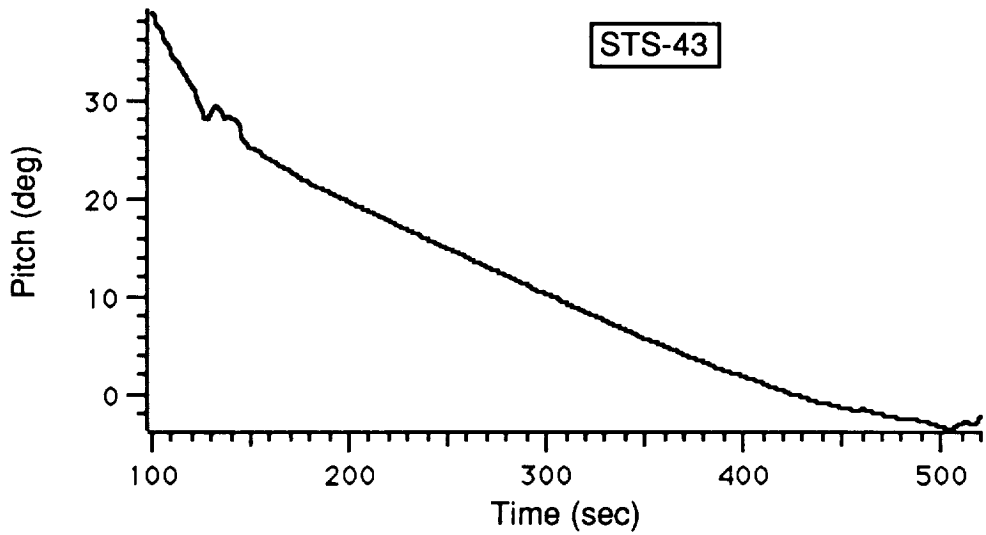
**Shuttle Flight Path Angles vs. Time After Launch**



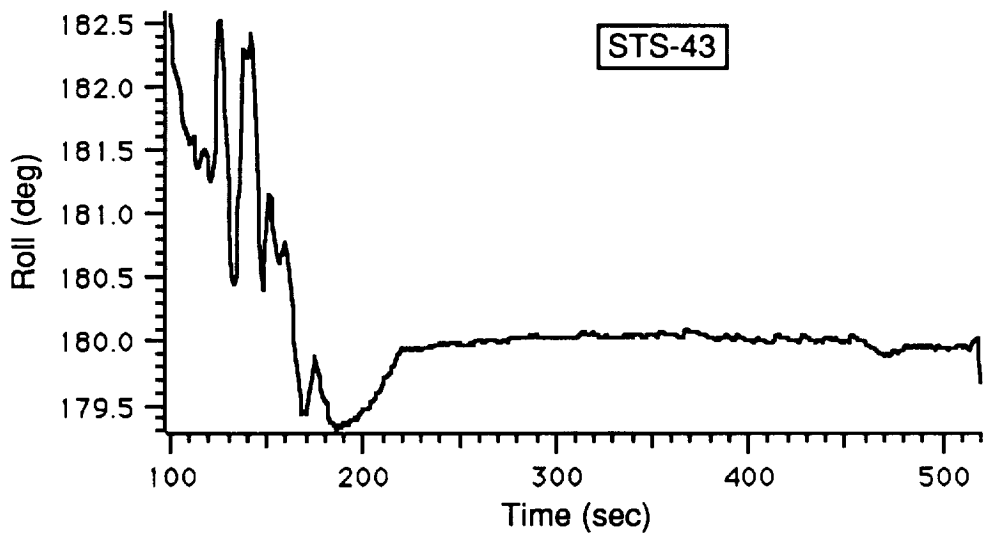
**Shuttle Altitude vs. Time After Launch**



a. Yaw Attitude

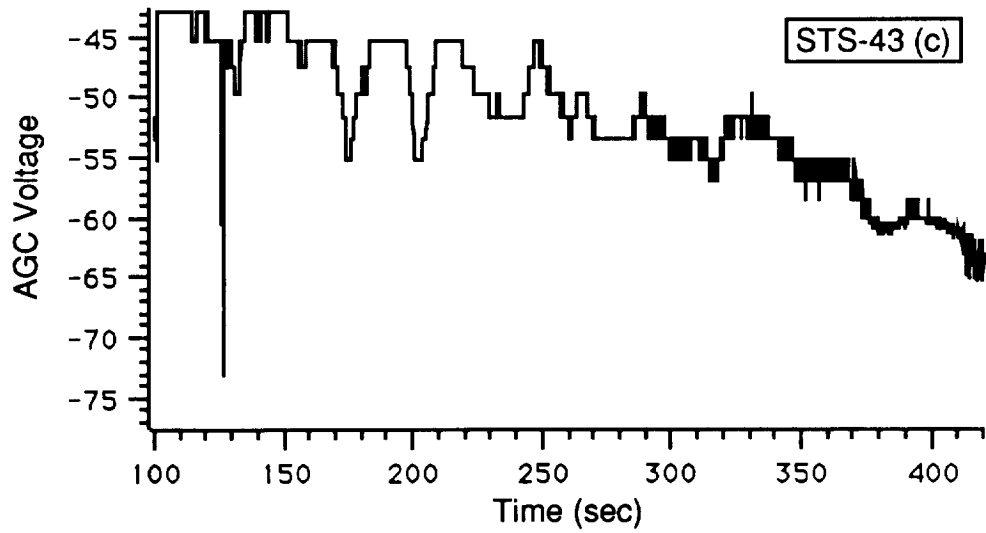


b. Pitch Attitude

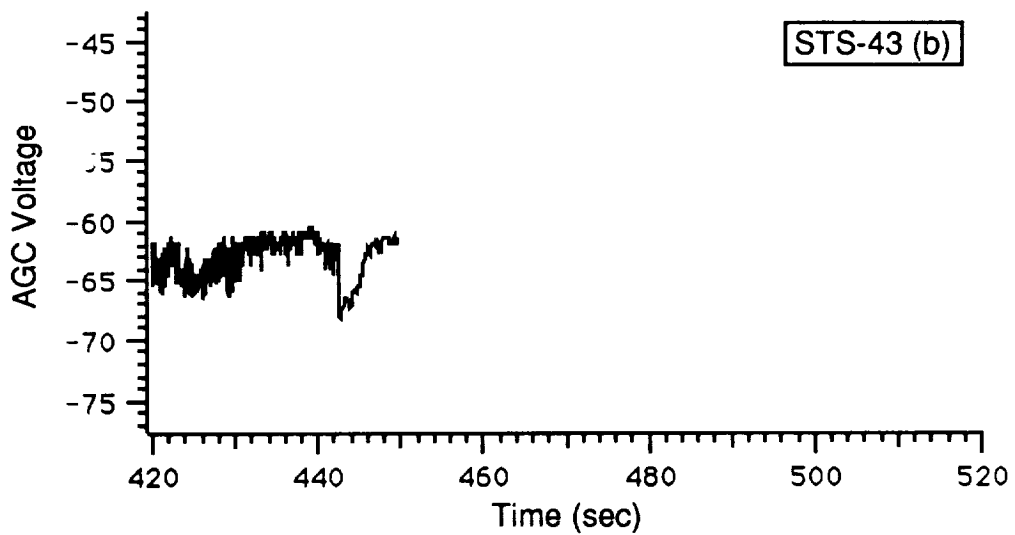


c. Roll Attitude

**Shuttle Attitude Angles (With Respect to Velocity Vector) vs. Time After Launch**

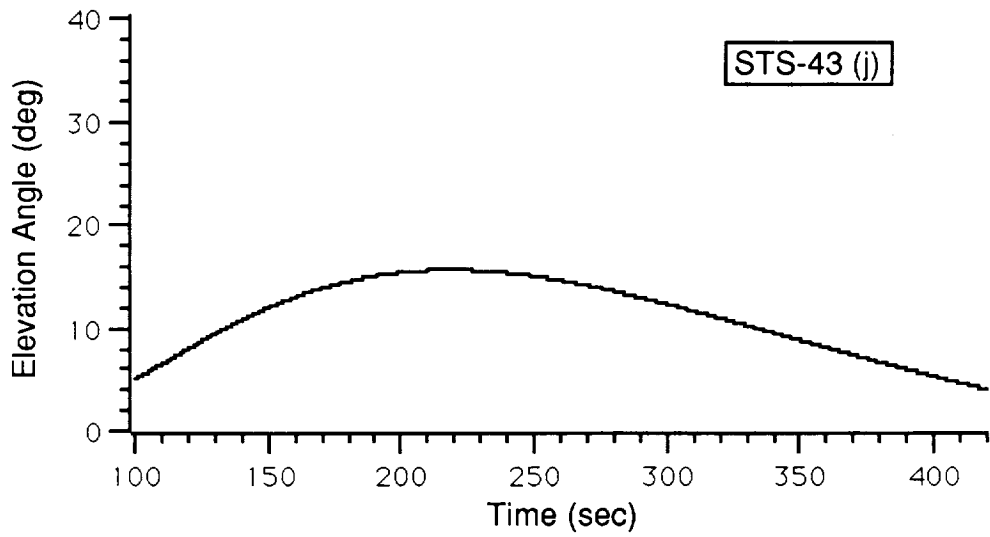


a. Transmission From Cape Canaveral

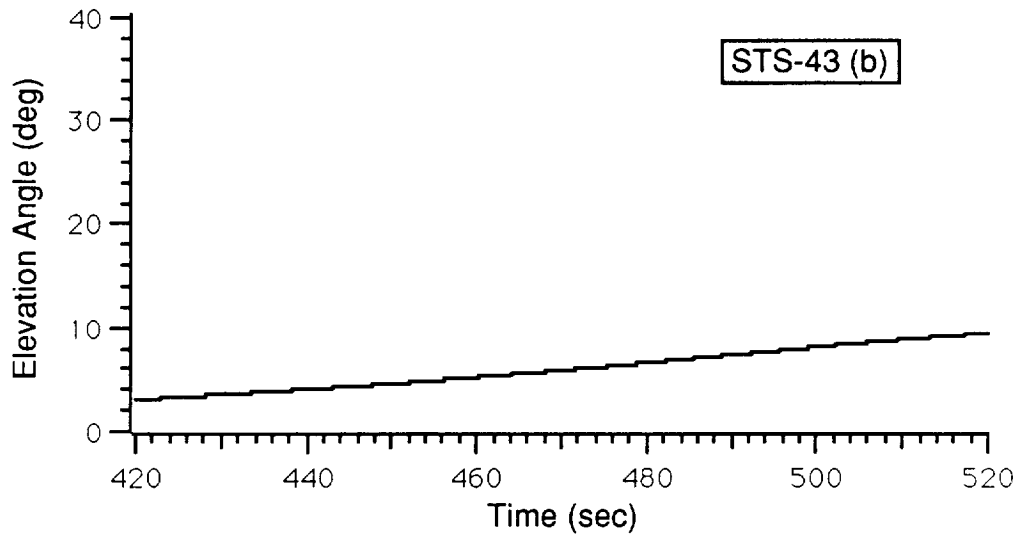


b. Transmission From Bermuda

**Record of ET Receiver AGC Voltage vs. Time After Launch**

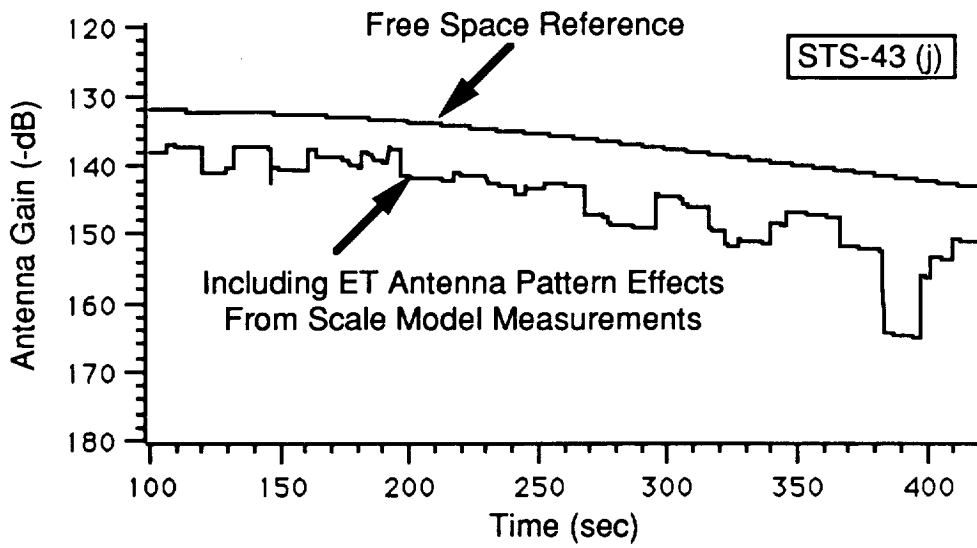


a. Transmission From Cape Canaveral

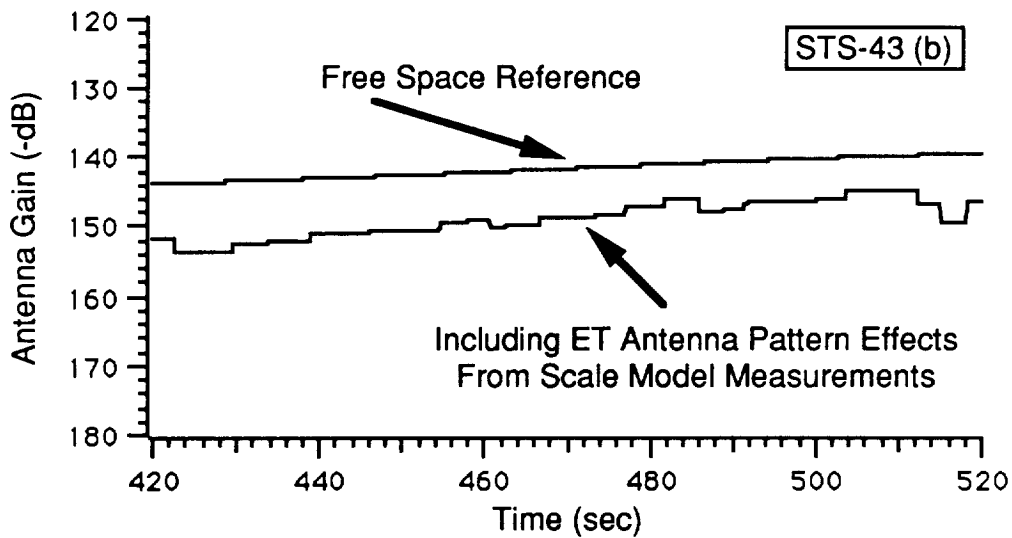


b. Transmission From Bermuda

**Elevation Angle (Transmitting Site to Shuttle) vs. Time After Launch**

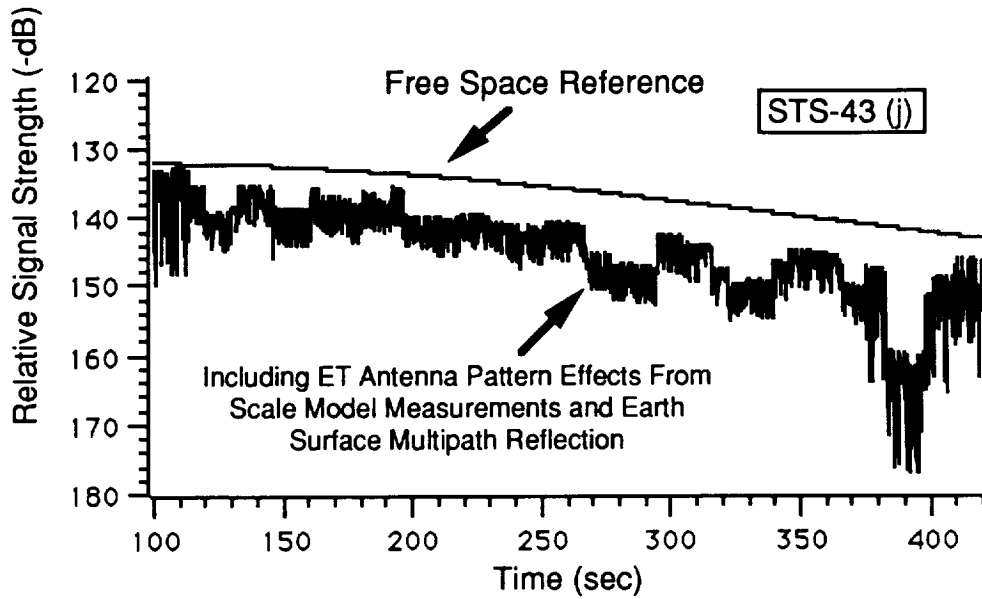


a. Transmission From Cape Canaveral

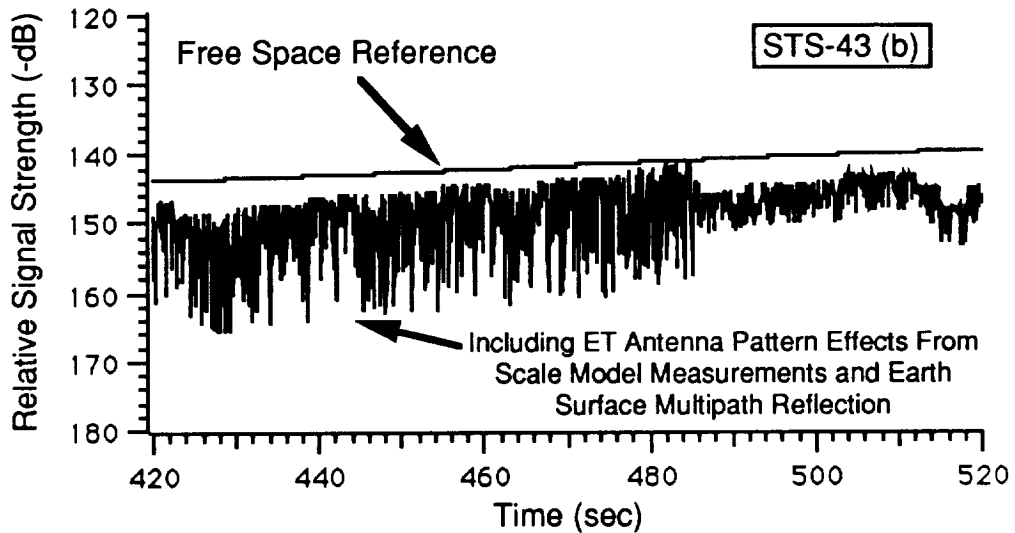


b. Transmission From Bermuda

**Computer Simulation of Relative Signal Strength at ET Receiver vs. Time After Launch  
(Without Earth-Surface Multipath Reflection)**



a. Transmission From Jonathan Dickinson



b. Transmission From Bermuda

**Computer Simulation of Relative Signal Strength at ET Receiver vs. Time After Launch (Including Earth-Surface Multipath Reflection)**

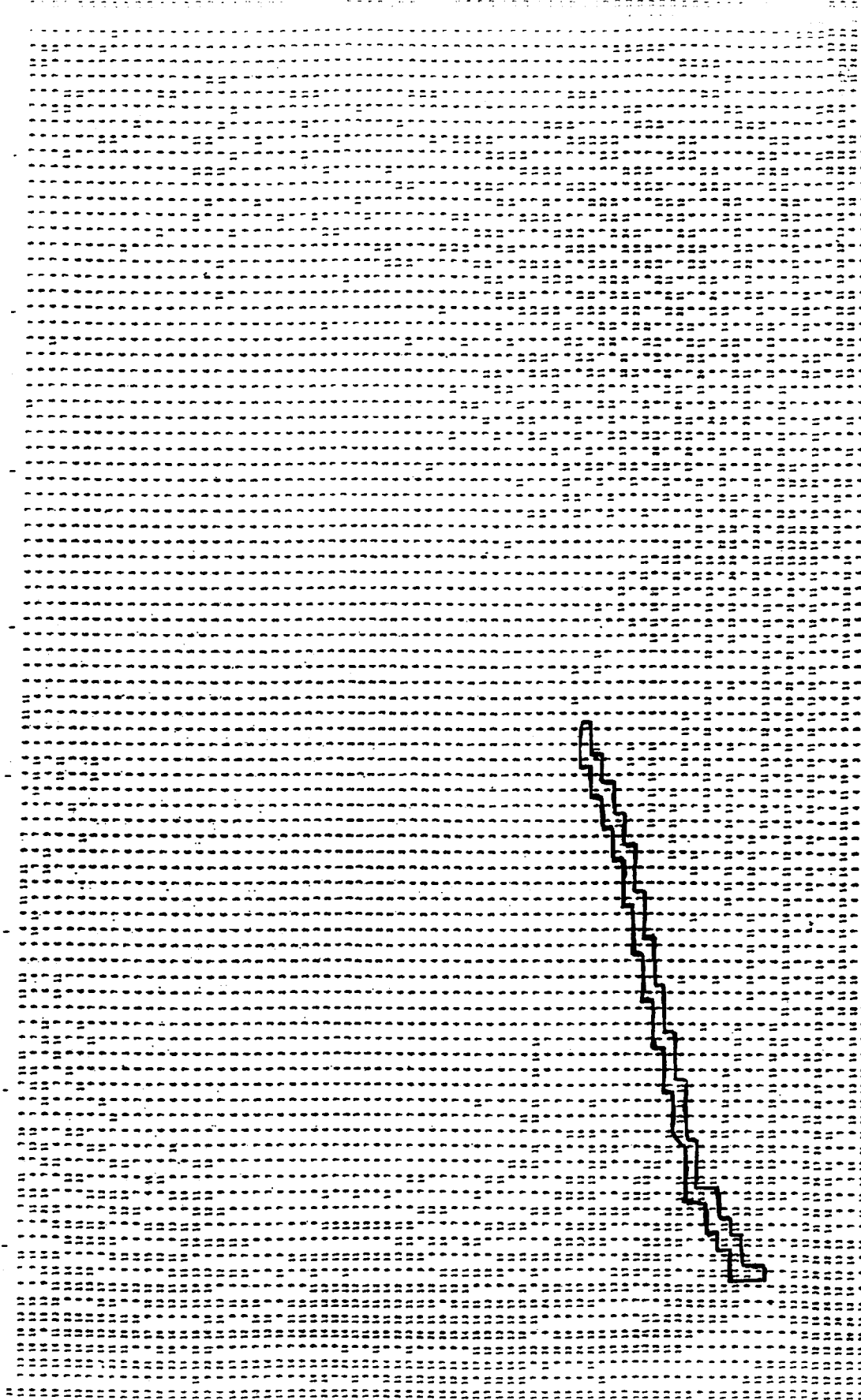
Yaw Degrees

20  
40  
60  
80  
100  
120  
140  
160

20 60 100 140

FOLDOUT FRAME /

Locus of A





180

140

100

60

20

Roll Degrees

TS-43 (Jonathan Dickinson)

Angles of Arrival on ET Antenna Pattern

FOLDOUT FRAME

2.

Yaw Degrees

20

40

60

80

100

120

140

160

20

60

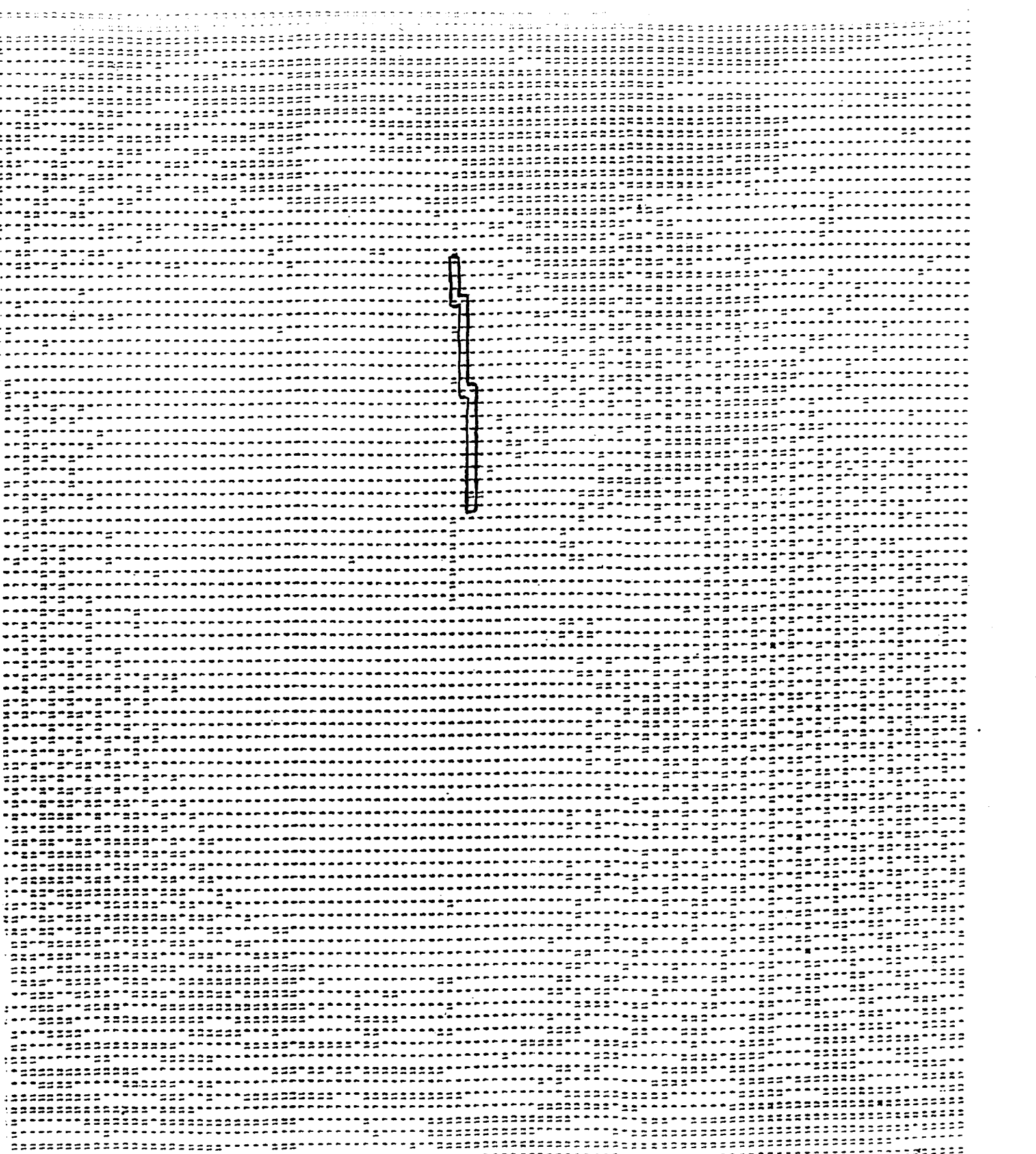
100

140

FOLDOUT FRAME /

F:

Locus of An



180

140

100

60

20

Roll Degrees

STS-43 (Bermuda)

es of Arrival on ET Antenna Pattern

OLDOUT FRAME

2